Engineering rock mass characterization - An integrated approach through Rock Mass Classification and Seismic Refraction - A case of TAMS Hydroelectric Power Dam Project in Gambella, Ethiopia

Daniel Gebremichael

A Thesis Submitted to

School of Earth Sciences

Presented in Partial Fullfillment of the requirements for the Degree of Masters of Science (Engineering Geology)

ADDIS ABABA UNIVERSITY

Addis Ababa, Ethiopia

May, 2017

Engineering rock mass characterization - An integrated approach through Rock Mass Classification and Seismic Refraction, A case of TAMS Hydroelectric Power Dam Project in Gambella, Ethiopia

Daniel Gebremichael

A Thesis Submitted to

School of Earth Sciences

Presented in Partial Fullfillment of the requirements for the Degree of Masters of Science (Engineering Geology)

ADDIS ABABA UNIVERSITY

Addis Ababa, Ethiopia

May, 2017

DECLARATION

I, the undersigned, declare that this thesis is my original work and has not been presented for a degree on any other university and all sources of materials used for the thesis have duly acknowledged.

DANIEL GEBREMICHAEL

Signature_____

Place and data of submission:
School of Graduate Studies, Addis Ababa University.
May, 2017

Addis Ababa University
School of Graduate Studies

This is to certify that the thesis prepared by **Daniel Gebremichael** entitled: *Engineering rock mass characterization – An integrated approach through Rock Mass Classification and Seismic Refraction a case of TAMS Hydroelectric power Dam Project in Gambella, Ethiopia* and submitted in partial fulfillment of the requirements for the Degree of Master of Science (Engineering Geology) complies with the regulations of the University and meets the accepted standards with respect to originality and quality.

Signed by the Examining Committee:

Examiner _____ Signature _____ Date _____

Examiner _____ Signature _____ Date _____

Advisor _____ Signature _____ Date _____

Co-Advisor _____ Signature _____ Date _____

_____
Chair of School or Graduate Program Coordinator

ABSTRACT

Engineering rock mass characterization – An integrated approach through Rock Mass Classification and Seismic Refraction; a case of TAMS Hydroelectric power Dam Project in Gambella, Ethiopia.

Daniel Gebremichael
Addis Ababa University, 2017

In the present study, an integrated geotechnical and geophysical approach was followed to characterize the dam foundation of TAMS Hydropower dam, situated in South-western Ethiopia, in Gambella National Regional State, Gambella Woreda, 721 km south-west of Addis Ababa. The dam is being constructed for the purpose of hydropower generation and will have a height of 265 m. A systematic methodology was followed for the present study. This includes review of secondary reports on investigations and design and collection of primary data from surface on geological and geotechnical parameters at the dam site. The investigations carried out in this regard includes; surface mapping, Rock mass rating (RMR) data collection, insitu testing on rock properties, and laboratory testing on representative samples. Besides, secondary raw data on drill hole logs, water pressure test and Seismic refraction survey data was also utilized to analyze and characterize the rock mass at the dam foundation.

Surface rock mass classification at exposed rocks have been conducted to characterize the rock mass at the dam foundation, accordingly, 50% of the foundation rock mass falls in RMR class 66 – 70, 40% falls in 61 – 65 and the rest 10% falls in class 70 – 80. The data analysis from the geological logs and the seismic refraction survey suggests that the bedrock in the dam foundation is fresh granite, granodiorite, metagranite and schist of different types which can be characterized as fresh, massive, strong, slightly fractured to unfractured rocks of high quality, represented by very high seismic velocities (>4500m/sec) from seismic refraction survey. With the exception of some very soft rocks and heavily jointed media, the majority of the rock mass can be classified as an excellent foundation material. Further, the permeability results from water pressure tests conducted in boreholes at both the abutments indicate very low to medium permeability. The permeability value on right abutment, in BH-3 borehole, demonstrated high to very high permeability in the top part of the dam foundation. The permeability in the intermediate reach on the right abutments is again high as the Lugeon value is more than 65. Therefore, the most effective means of checking seepage through the abutments and the river section would be a provision of a grout curtain.
Finally, on the basis of findings of the present research, recommendations are forwarded to be adopted as solutions against geotechnical problems identified at the proposed dam site.

Key Words: *Rock Mass Rating, Seismic refraction, Lugeon, Permeability, Rock Quality Designation.*

*****

ACKNOWLEDGMENT

First and for most, God must be thankful for being with me all the time in my life and putting those spectacular people around me who had played magnificent role in diverse ways to the success of this work.

I deeply thank Dr. Tarun K. Raghuvanshi, Associate Professor, School of Earth Sciences, College of Natural Science, Addis Ababa University who advised the present research work. He often went beyond the call of duty in encouraging, participation and supporting the goals of the research and providing his expertise. His devotion for guidance and constant encouragement strongly supported me to complete the present research work in this manner.

I would like also to express my gratitude to my Co-advisor Prof. Tilahun Mamo, School of Earth Sciences, College of Natural Science, Addis Ababa University for providing timely advice and comments that require time and patience.

I am thankful to Head and staff of School of Earth Sciences, College of Natural Science, and Addis Ababa University for providing a nice working environment and its entire supportive staff who helped me by providing support what I needed on time.

I would like to present my deepest gratitude to Ewnetu Tessema (Engineering Geologist) for his valuable comment, encouragement and cooperation which gave me enough strength to carry out the present research study and the Ethiopian Construction Design and Supervision Works Corporation for funding the research, letting me free access to inquired data, encouraging me and willingly putting their technical support for the fertility of the work. Special thanks are due to Dr. Tesfaye Kebede (Geotechnical Investigation Sub-process Manager) and Ato Getinet Asfaw (Senior Engineering Geologist and Project Manager).

Special thanks are due to all my wonderful workmates, my friends and my family. In particular, I am grateful to my parents for their support and encouragement throughout my life, to my wife, mother, father, brother and sister, whose constant challenge always made me work harder.

TABLE OF CONTENT

List of Tables

List of Figures

List of Plates

List of Annexes

ABBREVATIONS

a.s.l	Above sea level
ASTM	American Society for Testing and Materials
BH	Borehole
C	Cohesion (Kpa)
D	Disturbance factor
EAO	East African Orogeny
EIGS	Ethiopian Institute of Geological Survey
E-W	East-West
E_d	Deformation modulus (Gpa)
FAO	Food and Agriculture Organization
GPS	Global positioning system
GSI	Geological strength index
ISRM	International Society For Rock Mechanics
Lu	Lugeon Value
m_b	Material Constant
MER	Main Ethiopian Rift
MW	Mega watt
Mpa	Mega Pascal
MoWIE	Ministry of Water, Irrigation and Energy
mm	Millimeter
NATM	New Australian Tunneling Method
N-S	North-South
NNW	North-North-West
NE-SW	North east to south west
NGI	Norwegian Geotechnical Institute
NW-SE	North West to south east
R	Hammer Rebound
RMR	Rock mass rating
RSR	Rock Structure Rating
RMi	Rock Mass index
RQD	Rock quality designation
SMR	Slope Mass Rating
SRF	Stress Reduction Factor
SL	Seismic Line
TCR	Total core recovery
UCS	Unconfined Compressive Strength
U.S.A.C.E	United States Arms Corps Engineers
UTM	Universal Traverse Mercator
VES	Vertical Electrical Sounding
Xc	Critical Distance
Φ	Internal Friction Angle (°)
g	Density of the rock (N/m^3)
σ_1	Major principal stress
σ_3	Minor principal stress
σc	Uniaxial compressive strength (Mpa)
σv	Vertical stress (Mpa)
σ cm	Unconfined Compressive Strength Of Rock Mass
σ ci	Unconfined Compressive Strength Of Intact Rock

Chapter I INTRODUCTION

1.1 Overview

Physical properties of the rock mass such as strength and deformation parameters or permeability may differ substantially from those of the rock materials, as the properties of the rock mass is strongly influenced by the type of discontinuities (joints), their orientation, spacing, persistence, aperture and filling, roughness, waviness, etc. (Palmstrom, 1996).

Rock mass characterization is the process of collecting and analyzing qualitative and quantitative data that provide indices and descriptive terms of the geometrical and mechanical properties of a rock mass. A rock mass classification scheme is intended to classify the rock mass, which provides a basis for estimating deformation and strength properties, supply quantitative data for support estimation, and present a platform for communication between exploration, design and construction groups (Ocepec, 2006).

For arriving at appropriate results in rock engineering and design, Bieniawski (1989) advises application of at least two classification systems when applying such empirical tools. However, many users are practicing this recommendation by finding the value (quality) in one classification system from a value in another, using some sort of transition equation. (Bieniawski, 1989)

The geophysical survey is an important indirect method of investigation which enables acquisition of information in wider areal extent and in a relatively shorter period of time, and relatively at lower cost as well (Ajzebeokhai, 2010).Large hydropower projects need to conduct geophysical exploration intensively to maximize quality and the extent of information gathered for techno-economic studies of the project.

In general, the geophysical investigation has a role to:

(i) Obtain thickness of overburden/depth of bedrock;

(ii) The lateral and vertical variations of subsurface stratification;

(iii) Groundwater condition;

(iv) Indicate the presence and extent of seams (shear zones, fault zones, cavities, etc.); and

(v) To provide information for borehole locations, interpolation of data or addition of borehole between executed/drilled boreholes.(sjorgen, 1979)

Seismic refraction survey is the geophysical method most closely related to rock mass properties because the longitudinal seismic wave velocity varies with the main features, which characterizes the rock mass (rock properties, jointing, stresses etc.). Therefore, the results from such seismic measurements may assist in site selections and in rock engineering. The seismic survey methods utilize the propagation of compression or primary seismic waves. Particularly, when used in conjunction with the exploratory drill, significant information about the subsurface layers in terms of velocities, thickness, and water saturation as well as elastic properties can be obtained. Moreover, geoelectric resistivity imaging has also been used in many studies in site investigation for civil engineering (Ajzebeokhai, 2010; Andy, 2012).

To determine the characteristics of rock mass, the investigation and analysis are first undertaken in the main research phase. The purpose of the investigation and analysis is to determine the input parameters for a numerical analysis which are needed to specify supporting and retaining measures for the excavation of dam axis, underground structures, or for cutting slopes in front of tunnel portals, and other structures associated with the hydropower scheme (Robin et.al, 2005).

The present research work was carried out at the TAMS Hydropower rock fill concrete face dam which has a height of 265 m and a crest length of 1480 m with a reservoir capacity of 9 billion $m^3$and a reservoir area of 100 km^2, which is constructed for the purpose of generating hydropower.

1.2 Problem statement

The suitability of the dam foundation is governed by the engineering geological and geological properties of the dam foundation, as well as taking into consideration the seismicity of the area (U.S. ACE, 1994). Nowadays, identification and selection of the dam site for different purposes focus only on the economic importance and political perspective of the concerned authority. Even though the dam site falls relatively in geologically and topographically ideal terrain, proper investigation of rock mass characterization is crucial.

In practice the design of an efficient foundation system depends on appropriate characterization of the supporting soil and rock, and determining the proper geotechnical parameters (Robin et.al, 2005). In the case of hydropower schemes like Dam, power house and tunnels proper rock characterization is essential for the long life span of the project. For example the Unconfined Compressive Strength and elastic modulus of a rock specimen are

insufficient for proper design because of scale effect. Strength and deformability of rock mass is only a portion of those determined in laboratory specimens because of the presence of discontinuity within the rock mass (Cai, et.al 2009).

Because of Lack of integration of rock mass characterization including seismic and borehole, because of the prevailing vertical and horizontal fractures of the bedrock found on the right side of the study area could be the cause of instability and water tightness problem at the dam foundation and lack of integrated approach concerning geotechnical study at TAMS dam, this research was initiated.

1.3 Previous works

Two main studies have been carried out for assessing the dam foundation of the study area. The first study conducted by the MoWIE is Pre-Feasibility and Feasibility Study for the TAMS Hydropower Project (2014). The pre-feasibility study at the area concluded that, the geological and geomechanical investigations and laboratory tests at the dam site have been limited to the left bank due to the accessibility problems of the right bank. Nevertheless, the consultant deems that the partial geological investigations performed in this prefeasibility study phase gave a good picture of the overall geological conditions of the dam site, expecting that these good conditions will be confirmed in the next phase geotechnical investigations.

In the project area, and especially at sites of major structures, the bedrock corresponds to the crystalline basement (metamorphic and deformed intrusive rocks) of Western Ethiopian Shield, which has been described in Volume 3. The main rock types are: mildly deformed to non-deformed granite, foliated granitoids (mostly tonalite); gneisses (both ortho- and paragneisses); schists (various kinds of meta-sedimentary and metavolcanic schists); amphibolites.

The second study was the seismic refraction survey conducted by Geomatrix plc. (2016), and it's concluded that the project is underlain by igneous rocks including granitic gneiss, pre/syn-tectonic granites with quartz vein lets and stringers along local shear planes and faint foliations. The refraction seismic survey has clearly identified the subsurface units on the basis of their compressional wave velocities and determined their thicknesses to a depth over 100m. Accordingly, a maximum depth of over 120m is attained by the refraction seismic survey in the southern, southwestern and northern part of the project area.

The bedrock underlying the dam site is generally represented by fresh granite, granodiorite and metagranite, which are characterized by fresh, massive, strong, very slightly fractured to unfractured rocks, of high quality represented by very high velocities (>4500m/sec).

1.4 Research objectives

1.4.1 General

The primary objective of the present research is to use an integrated approach to characterize the rock mass found at the dam foundation through rock mass classification and geophysical method (seismic refraction) of the dam.

1.4.2 Specific

More specific objectives of the research will include the following:

- To classify rock mass through rock mass classification system (Bieniawski, 1989)
- Interpretation of the Geophysical Survey (seismic refraction survey) results in to determine the quality of the rock mass, especially its seismic velocity;
- To conduct the local Geological/Engineering Geological map of the dam site at a scale of 1:10,000.
- To determine foundation permeability, bearing capacity and deformability of the rock mass.
- Integration of borehole data with seismic velocity to improve the resolution of the foundation rock and reduce the associated uncertainty.
- To conduct laboratory tests on rock core samples (such as UCS and Unit weight)to assess whether reliable correlations can be established to relate geophysical measurement results to important geotechnical properties and parameters such as: bearing capacity, deformability characteristics, erodibility potentials, water tightness and differential settlement potentials of the project area.

Besides, the correlation developed may also be extended for other engineering perspectives; especially for basement rocks in Western Ethiopia.

1.5 Significance of the Research

Engineering geological investigation especially rock mass characterization plays a very important role in proper site selection, designing and construction planning of a dam project (Robin et.al, 2005).

A comprehensive and systematic investigation ensures safety and long span of the project. Identification of geological and geotechnical problems in the preliminary stage of the investigation helps in adopting proper corrective measures during construction stage. The physical parameters of the subsurface from the site investigation are important for geoscientists and engineers to understand the geological and engineering parameters. As part of the second growth and transformation plan in Ethiopia, the country is engaged in study and construction of large hydropower dam projects like TAMS. Detailed rock mass characterization is vital, especially when combined with geophysical (seismic) and geotechnical (borehole) surveys.

The present research showed feasible methodology to make preliminary for characterizing of the dam foundation geological material for safe design and identifying any geological and engineering geological problem under the dam area. Furthermore, the present study forwarded the relative feasible and practical solutions for the sustainability of the foundation layers.

Furthermore, the results of present research could be used by the project Authority and the Enterprise as an additional input of the design. It may also be used as a source of information for later researchers who intend to work on the same subject or in the same study area.

1.6 Methodology

The findings of the current research were born through an organized and systematic methodology.

Broadly, four major activities briefed hereunder were addressed to fulfill the preset objectives of the research;

- Collecting and reviewing published and unpublished literature, scientific journals, reports and books pertaining to geophysical investigation and rock mass classification. It was intended to have overall background knowledge on the subject matter through systematic literature review. This was essential to develop conceptual framework which was further utilized in evolving the detailed methodology for the present study.
- Secondary data collection.
- Primary data collection and laboratory analysis.
- Data analysis and interpretation of results.

The literature survey has encompassed both published and unpublished reports of investigations, case studies, text books and Journals that were obtained from different sources for better understanding of aspects related to the current research topic such as: geological and geophysical works of the region. Further, geological mapping of the project area was undertaken to identify lithologic types and nature of lithological contacts, to obtain joint orientations, identify shear and fault zones, observe surface weathering, and to evaluate geologic hazards.

Secondary data collection incorporates all necessary data associated with the present research topic, such as; Geophysical (Seismic investigation) data, borehole core logging data, discontinuity logging data, in-situ permeability testing(packer) data, water level measurement at the installed boreholes and other related secondary data which is valuable for the specific research topic.

From field investigation lithological description, discontinuity data and in situ test (Schmidt hammer) data was collected. Representative samples from different locations (both from borehole core and surface outcrop samples) for laboratory analysis was also taken.

Rock mass classification is one of the approaches for estimating large-scale rock mass properties (Bieniawski, 1989). In this particular study RMR classification system was used to characterize the rock mass and seismic refraction survey was used as a tool in characterizing the rock mass in conjunction with the borehole data and surface discontinuity data.. Engineering properties of rock must account for the properties of the intact rock and for the properties of the rock mass as a whole, specifically considering the discontinuities within the rock mass. For the present study a combination of laboratory testing of samples of rock materials, empirical analysis, and field observations were employed to determine the requisite engineering properties of the foundation rock mass.

Software's such as AutoCAD, ArcGIS, CorelDraw, ERDAS, Global Mapper, Google Earth, PhotoScape and SPSS, Microsoft offices (word and excel) were used as an assisting tool in this research.

1.7 Limitations

The present research was focused only on the dam site and is based on limited number of samples because of time and financial limitations.

In this research, the major limitation that was faced was lack of sufficient surface outcrops at and near the dam site for the collection of RMR data. Besides, availability of appropriate literature on the specific subject matter and scarcity of documented data on integrated rock mass characterization were also major constraints in the present research work. However, maximum efforts were made to fulfill the gaps that were made due to these limitations. These efforts includes: by discussion with the site representative geologist, by review of detail literature review and etc.

1.8 Thesis Structure

The content of this research is categorized in to seven chapters.

Chapter 1 deals with the general introduction of the research, problem statement, objectives, General Methodology, significance of the research and the limitations.

Chapter 2 briefly describes the study area: including location and accessibility, salient features of the project, climate and hydrology, catchment characteristics, land use and land cover and etc... .

Chapter 3 discusses about literature review.

Chapter 4 presents the regional and local geological setting, structures, seismicity and hydrogeology of the area.

Chapter 5 demonstrates the general methodology employed and data collection.

RMR rock mass classification and failure criteria approach is reviewed in Chapter 6 followed by an assessment of the dam foundation, bearing capacity, deformability and permeability of the dam foundation, results and discussion from seismic survey, characterization of the rock mass and overall characterization is also included in this specific topic. Moreover, foundation treatment and excavation is also review in this specific chapter.

Chapter 7 briefly summarizes and gives conclusions on the thesis output. It also recommends some further necessary works on unattainable problems and matters in this thesis.

*****

Chapter II THE STUDY AREA

2.1 Location and Accessibility

The TAMS Hydropower Project site is situated in South-western Ethiopia, in Gambella National Regional State, Agnuwak Zone, Gambella Woreda; 43 km east of Gambella town and 721 km south-west of Addis Ababa (Fig. 2.1). The dam axis is located across the Baro River which is 9 km downstream of the confluence of Baro Kella and Birbir Rivers. Geographically the dam is located at a reference coordinate of 711087.2mE, 906849.6mN; in UTM WGS 84 Zone 36P, where the elevation of the river is about 495m.a.s.l.The project site is accessed by Addis Ababa-Gambella asphaltic road. The dam site is situated in the the steep-sided valley.

2.2 Salient features of the project

TAMS Dam and Reservoir (regulation)

- Type of dam- Concrete face rock fills.
- Dam Height-265 m
- Dam Crest Elevation-760 m
- Dam Crest Length-1480 m
- Max Pool Elevation-756 m
- Min Pool Elevation-625 m
- Total Storage Capacity-8471 Mm^3
- Live Storage-7410 Mm^3

The project also encompasses;

(i) The reservoir, with a total storage capacity of 9 billion m^3 and a reservoir area of 100 km^2, would reach approx. 24 km upstream to the Upper Baro and would flood Birbir canyon almost up to the confluence with Geba.

(ii) A gated cascade on the left bank. Spillway capacity is 7415 m^3/s.

(iii) A tailrace channel brings the water back to the river at the elevation of the downstream reservoir; i.e. 504 m a.s.l.

(iv) Have a potential to generate 1700 MW hydroelectric power in the second growth and transformation plan as per the plan to increase the percentage of population with access to electricity in the country.

Currently the project is under detailed design stage and verification of previous designs, specifically the Geological and Geotechnical components.

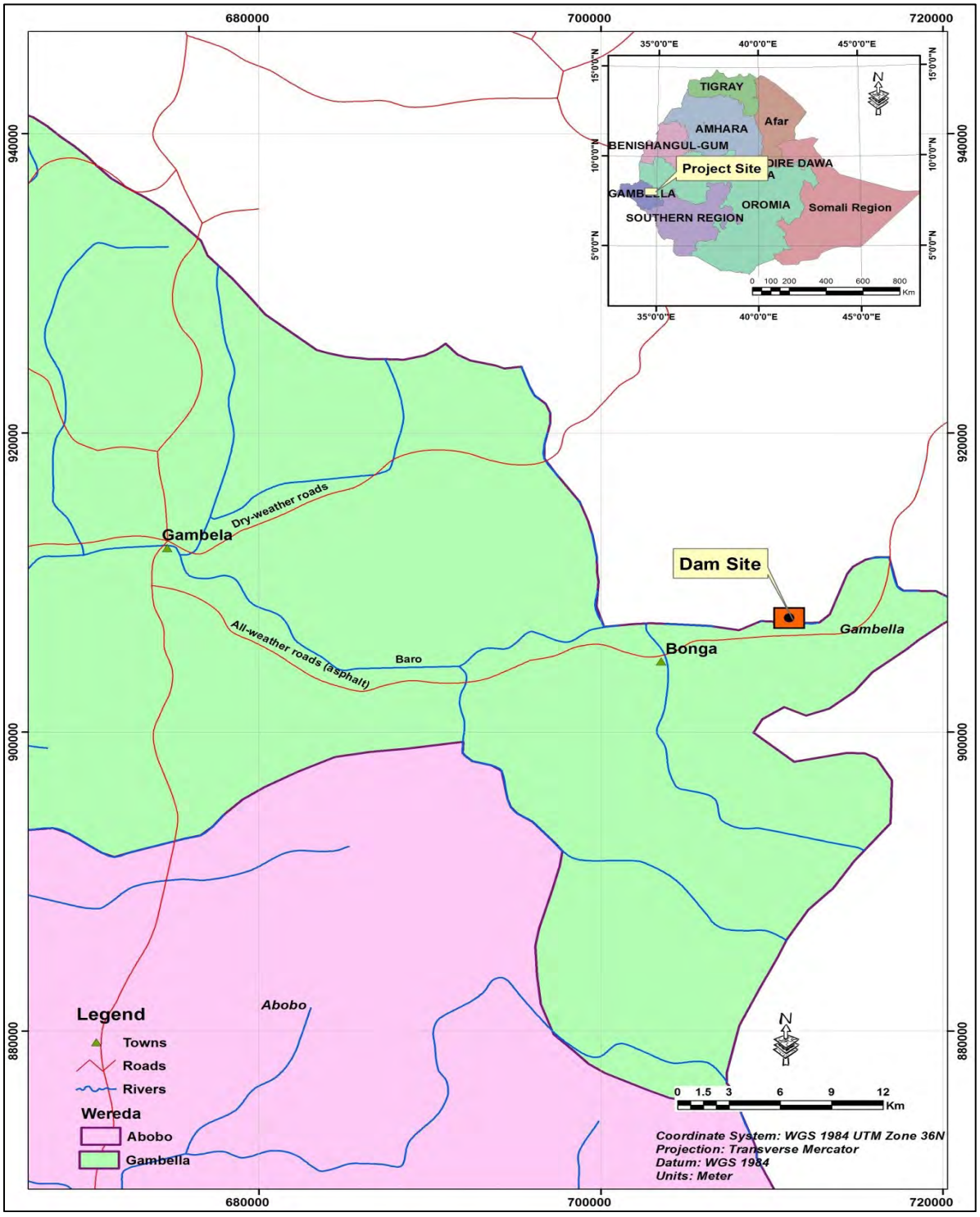

Fig. Error! No text of specified style in document.**.1 Location map of the study area**

2.3 Climate

According to MoWIE (2014), the Gambela Plain is formed under the influence of the tropical monsoons from the Indian ocean, which are characterized with abundant precipitations in the

wet season, which goes from May/early June to September/early October, and very low precipitations during the dry season.

The plain is protected with mountains from the east, north-east and south-east, and its elevations create favorable conditions for heat and precipitation accumulation. The region is characterized by a general increase of precipitation from the west to the east, with great influence by the orography of the area. Rainfall is highest at altitudes of 2,000 m a.s.l. and over, reaching around 2,000 mm per year in the region of the towns of Metu and Gore and locally maximum rainfall of around 2,300 mm per year in the region of Masha. Rainfall varies between 900 and 1,500 mm per year in the plain areas at altitudes of approx. 400 m a.s.l., with approx. 1,200 mm towards Gambela Plain. Mean annual air temperatures vary with altitude from 28° C in the plain area to 18° C in the mountains.

The flow regime of the rivers is closely linked to the monsoon climate with stream flows increasing through May to September, where they reach a maximum, mostly in the month of September. The stream flow increases unsteadily with periodic rises and falls especially in small rivers. When the wet season ceases, the river levels decline and the flows are the smallest from December through to April. The major rivers are perennial although some smaller courses dry out in most of the years.

2.3.1 Temperature

Mean annual air temperatures vary with altitude from 28°C in the plain area to 18°C in the mountains. July and August are usually the coldest months while March and April are the hottest, however the variability over the year is not large. Elevation, mean monthly temperature and mean annual temperature at various meteorological stations are shown in the Table 2.1 and Fig. 2.2. In the study area, temperatures at Gore and Gambela stations can be considered representative of average conditions in the mountains and in the plain, respectively.

2.3.2 Rainfall

According to MoWIE (2014), the rainfall in the project area is a season-dependable phenomenon and is greatly influenced by the orography of the area. Around 80 - 90% of the annual precipitation occurs during the wet season, from May/early June to September/early October, while December, January and February are the driest months. The annual precipitation increases significantly from the plain to the piedmont and then it smoothly increases with height in the highlands.

Table 2.1 Elevation and mean monthly and annual temperature at various meteorological stations

	Bedele	**Gore**	**Metu**	**Dembidolo**	**Bure**	**Gambella**	**Itang**
Elevation	2050	2002	1940	1800	1750	438	415
Period of Observation	1971-81	1971-86	1971-77, 81-82, 85-86	1973-78, 81-86	1977-86	1940-66, 75-87	1973-75, 77-85
Month	Air Temperature (^{O}C)						
	Bedele	**Gore**	**Metu**	**Dembidolo**	**Bure**	**Gambella**	**Itang**
September	17.6	19.3	18.6	19.3	23.5	28.2	27.5
October	19.0	20.2	20.0	19.9	24.2	29.6	28.5
November	17.7	20.4	21.0	19.8	24.2	30.7	29.0
December	19.8	20.1	21.0	19.7	24.1	30.2	29.8
January	19.0	18.4	20.0	18.7	21.4	28.3	25.5
February	18.3	17.2	18.9	18.0	19.8	26.9	24.9
March	16.9	16.5	17.7	17.2	19.0	26.1	24.5
April	16.6	16.7	18.5	17.3	19.6	26.1	24.9
May	17.2	17.1	18.6	17.6	20.2	26.7	24.8
June	17.2	18.0	18.9	18.1	21.3	27.2	25.3
July	17.2	18.2	18.5	18.3	22.1	27.6	25.6
August	16.5	18.8	18.3	18.7	23.0	27.9	26.1
Mean Annual	***17.9***	***18.4***	***19.2***	***18.6***	***21.9***	***27.9***	***26.4***

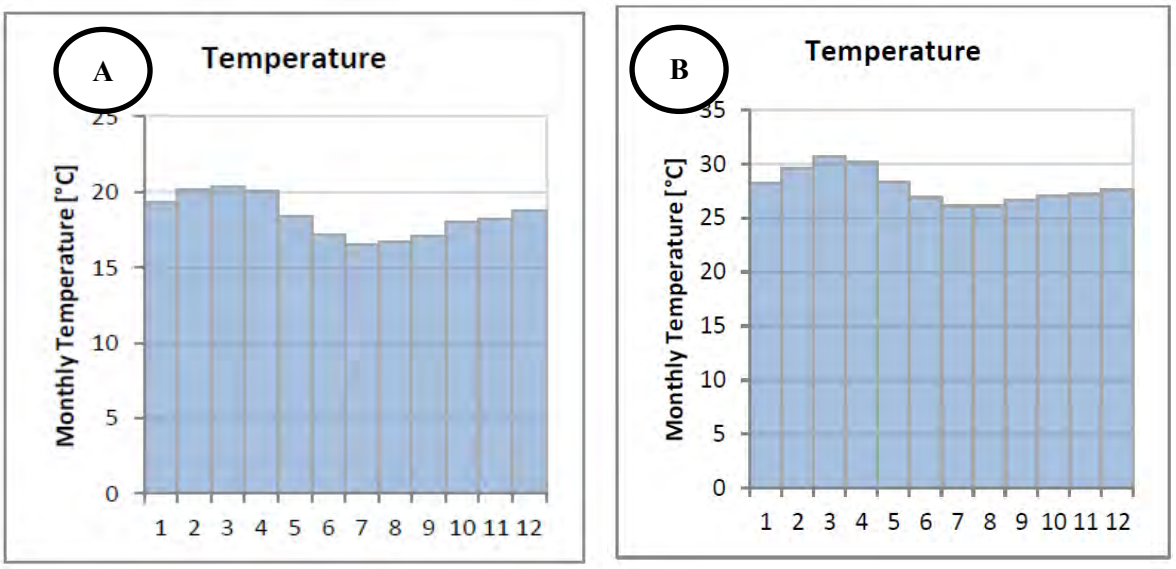

Fig. 2.2 Mean monthly temperature (A, Gore Station and B, Gambella Station)

Baro River basin presents an extensive network of meteorological stations. According to National Meteorological Agency, a number of 46 meteorological stations – ranging from class 1 to class 4 according to NMA classification - are located in the catchment area of the project. Furthermore, a class 1 meteorological station with a long term measurement period is present in Gambela town. Among the 47 stations, a number of 10 meteorological stations have been selected according to the available datasets, to the spatial distribution and to the station class (Fig.2.3).

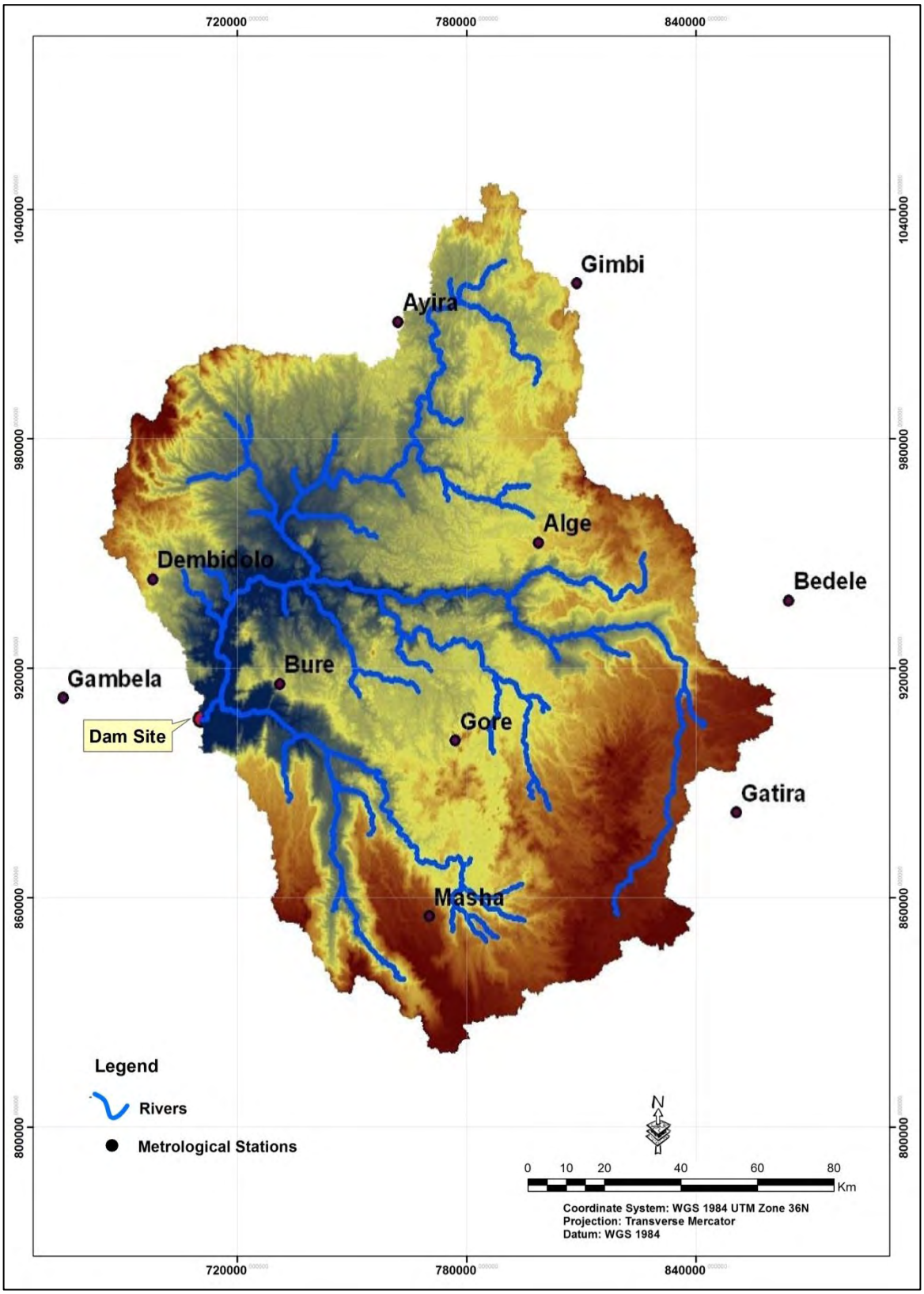

Fig. 2.2 Selected meteorological stations in the catchment area of the project and along Baro River

The elevation and mean annual rainfall at each station are summarized in Table 2.2. The calculated monthly rainfall patterns and statistics, as well as mean annual rainfall, are in

agreement with available data and calculations from previous studies. Fig. 2.3 shows rainfall measured at Gambella for 7 years (2006 - 2012).

Table 2.2 Elevation and mean annual rainfall at the selected meteorological stations (MoWIE, 2014)

Stations	Elevation (m)	Mean Annual Rainfall (mm)
Alge	1880	1889
Ayira	1555	1671
Bedele	2011	1910
Bure	1750	1333
Dembidolo	1850	1258
Gambella	500	1157
Gatira	2358	1890
Gimbi	1970	1840
Gore	2033	2090
Masha	2282	2315

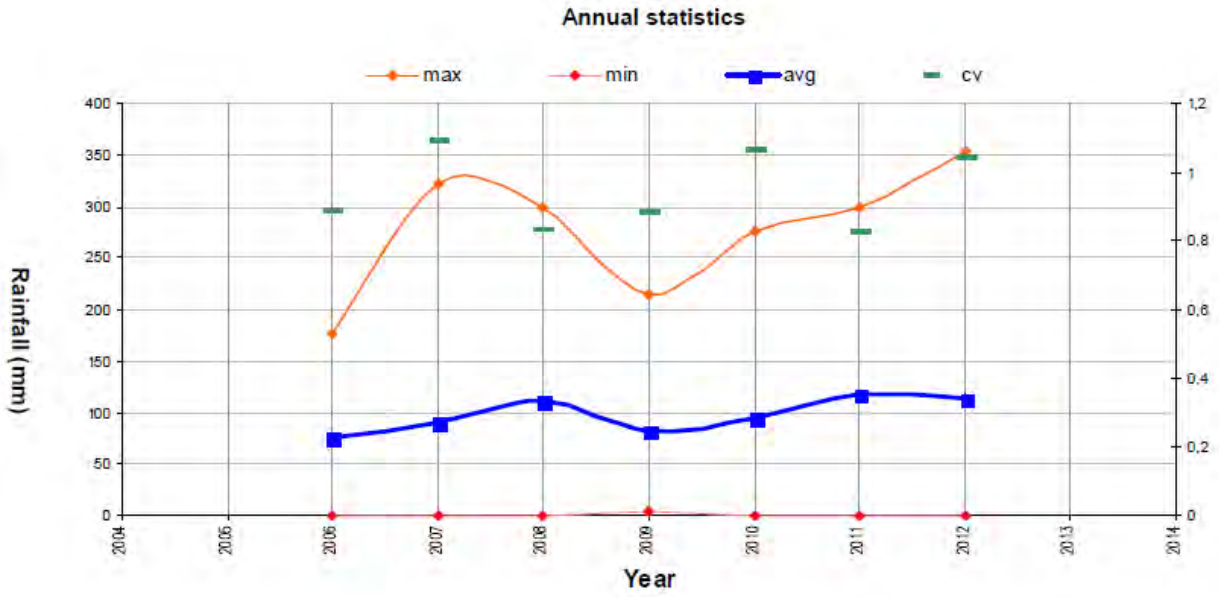

Fig. 2.4 Rainfall measured at Gambella for 7 years (2006 - 2012)

2.3.3 Evaporation and relative humidity

Monthly evaporation and annual evaporation were calculated starting from daily evaporation. The calculated monthly evaporation patterns and statistics, as well as mean annual evaporation, appear to be in agreement with available data and calculations from previous studies. Relevant graphs are shown in drawings relevant to the meteorology section at Gambella.

Mean monthly and total annual evaporation at Gambela station is shown in the following Table 2.3 and Fig. 2.5, according to previous study.

Table 2.3 Mean monthly and total annual evaporation at Gambela

Month	Water Surface Evaporation (mm) at Gambella (1976 – 85)
September	181.0
October	186.0
November	212.0
December	189.0
January	121.0
February	97.0
March	80.0
April	84.0
May	93.0
June	102.0
July	117.0
August	150.0
Total Annual	***1612.0***

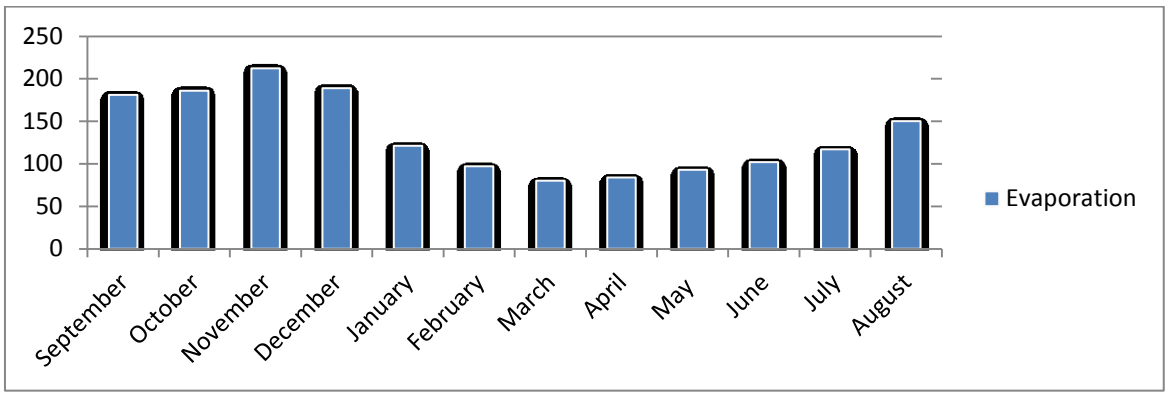

Fig. 2.5 Mean monthly annual evaporation at Gambela

2.4 Hydrology

2.4.1 Runoff data and observed river discharge

Discharge data was obtained from the Hydrology Department of the Ministry of Water, Irrigation and Energy (MoWIE, 2014). Daily discharge data and monthly discharge data were obtained for17 hydrometric stations located on the Baro River and major tributaries, as listed in Table 2.2. For these stations, with the exception of Baro at Itang and Kuni at Chanka, suspended sediment data were also obtained. From the distribution of the monthly flow of the average hydrologic year (Fig. 2.6) between the months July and October the river flow becomes in the range of 600m^3/s and 1000m^3/s, where the river usually reaches its peak flow in the month of September.

2.4.2 Catchment Characteristics

Baro River at potential dam section has a catchment area of 21,275 km^2. Baro River catchment area is formed by the two main tributaries, Upper Baro River and Birbir River. At the confluence

between Upper Baro and Birbir rivers, Upper Baro accounts for the 22% (4,743 km^2) of the basin at dam section, while Birbir river accounts for 77% (16,439 km^2) of the basin. The remaining portion of the catchment area (93 km^2) is located between the confluence of Upper Baro and Birbir and the dam section. Fig. 2.8 shows the catchment area up to dam site, distinguishing between the two main tributaries.

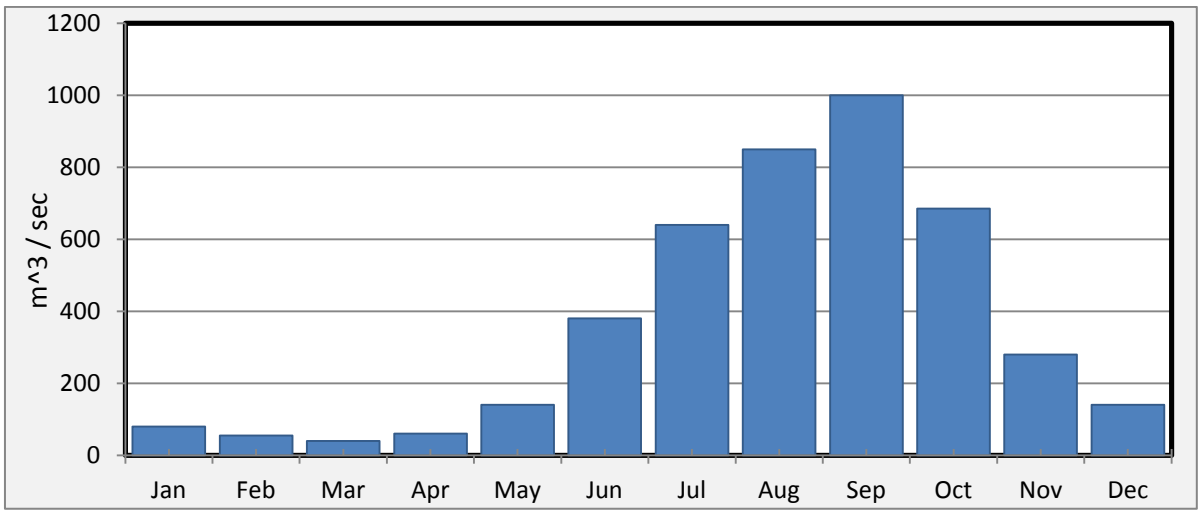

Fig.2.6 TAMS project area-average monthly flow (MoWIE, 2014)

Altitude in the catchment area varies between 495 m a.s.l. (dam location) and approximately 3,255 m a.s.l., with a weighted average of 1,755 m a.s.l. The area-elevation distribution curve of the catchment area is shown in Fig. 2.7. According to MoWIE (2014) the average annual precipitation on the watershed is variable between approx. 1,300 mm towards Gambela Plain and 2,000 mm towards the mountains, with rains mostly falling during the rainy periods, mainly from June to September.

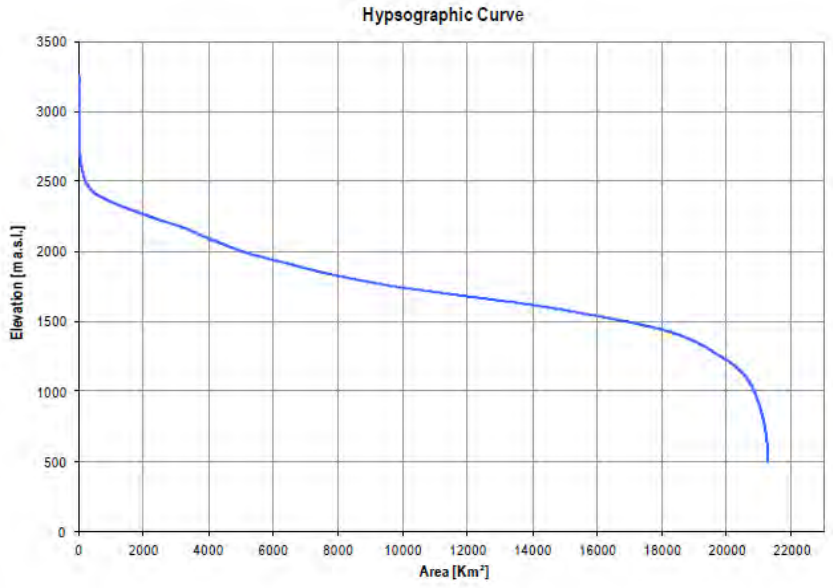

Fig. 2.7 Area-elevation distribution curve of catchment, obtained from SRTM digital elevation model

The Baro River is a part of the Baro-Akobo Basin, which is one of the largest basins in the country. The western, north western and south western side of the basin borders with Sudan, while in the north and north east it is bordered by the Abbay Basin and in the east and south east it is bordered by the Omo-Gibe Basin. Baro-Akobo River basin has an extension of around 76,000 km^2 and is a part of the White Nile Basin.

The major rivers within the Baro-Akobo Basin, together with Baro and its tributaries (Birbir, Geba, Sor and Baro), are Alwero, Gilo and Akobo. The general flow direction of the rivers is from east to west originating from the highlands and falling in the Gambela Plain.

The Akobo River joins the River Pibor which borders the south western part of the basin with South Sudan at Tirgol. The river Gilo joins the River Pibor at the border, just before a village called Madeng. The Baro River flows down to the west till it reaches Jikawo, a border town in South Sudan. It then keeps on flowing to the west till it joins the River Pibor at Burbey, a village near the border, which is the outlet of all the Baro-Akobo River basin.

2.5 Physiography

The TAMS Dam site is located in the western end of the lowering Ethiopian relieves, which make a gradual transition to the lowlands of Sudanese plain. The project area relief corresponds to a very mature morphology, which perfectly corresponds to a stable continental crust with just a very ancient deformation history (Fig. 2.9).

It lies in the junction zone between the progressively lowering highlands of Baro basin and the alluvial plain of lower Baro River, towards Gambela. The site lies within the last relieves which border the western alluvial plain of Baro-Akobo fluvial system and corresponds to the deeply dissected western margin of the Ethiopian Plateau. Due to tectono-metamorphic, volcanological and geomorphological evolution of Ethiopia, these relieves are made of ancient crystalline basement rocks, in this area lacking of the cover of Tertiary volcanic rocks (MoWIE, 2014).

The pattern of the drainage network shows the structural control along the two main trends: roughly E-W and roughly N-S. General pattern of both morphological relief and drainage network show frequent E-W and N-S linear trends (linked to geological structures). The geomorphic modelling in the project site was dominated by erosion processes which gave rise to a general slope denudation and a deep cutting of the drainage network.

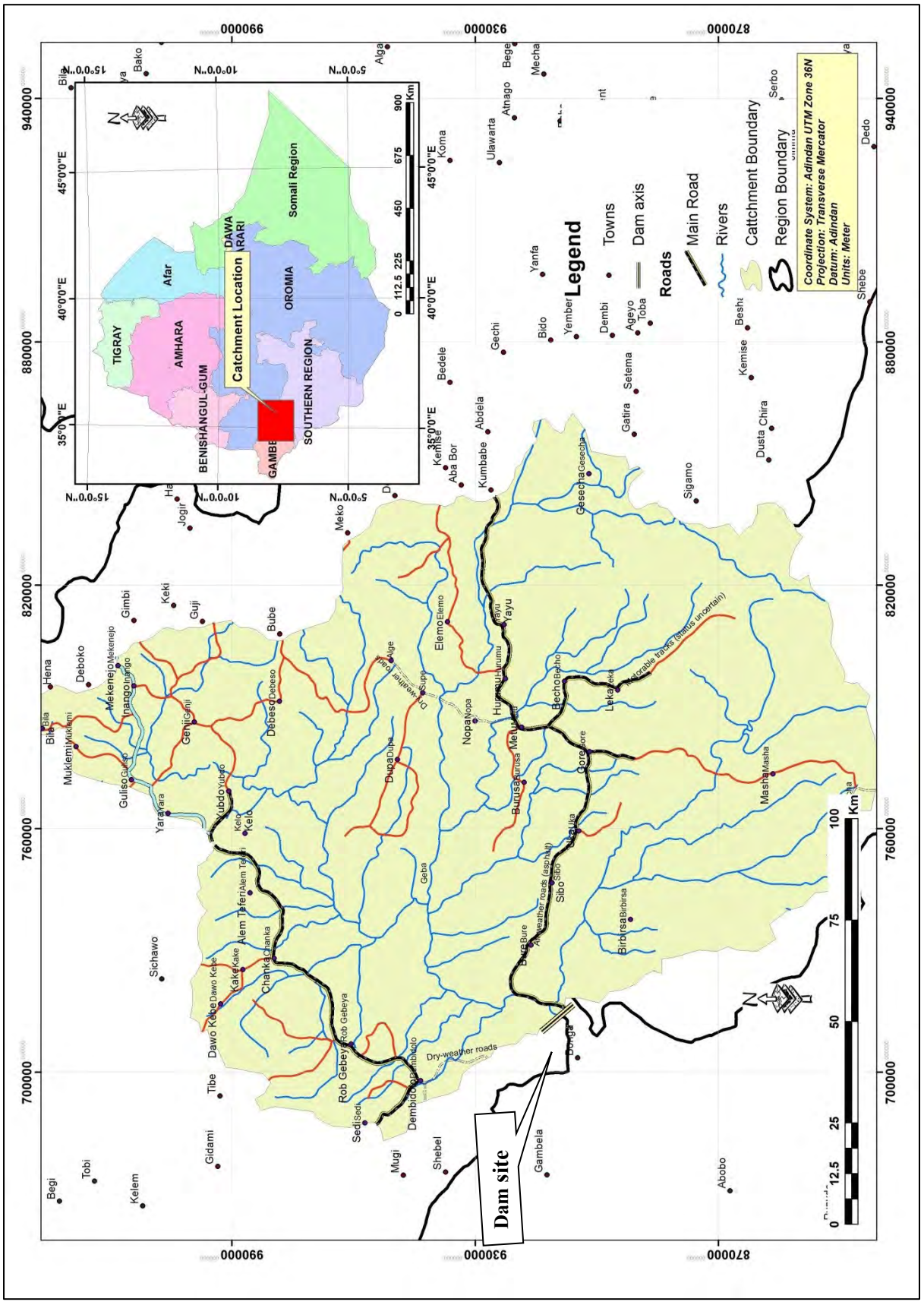

Fig. 2.8 Catchment area at dam section

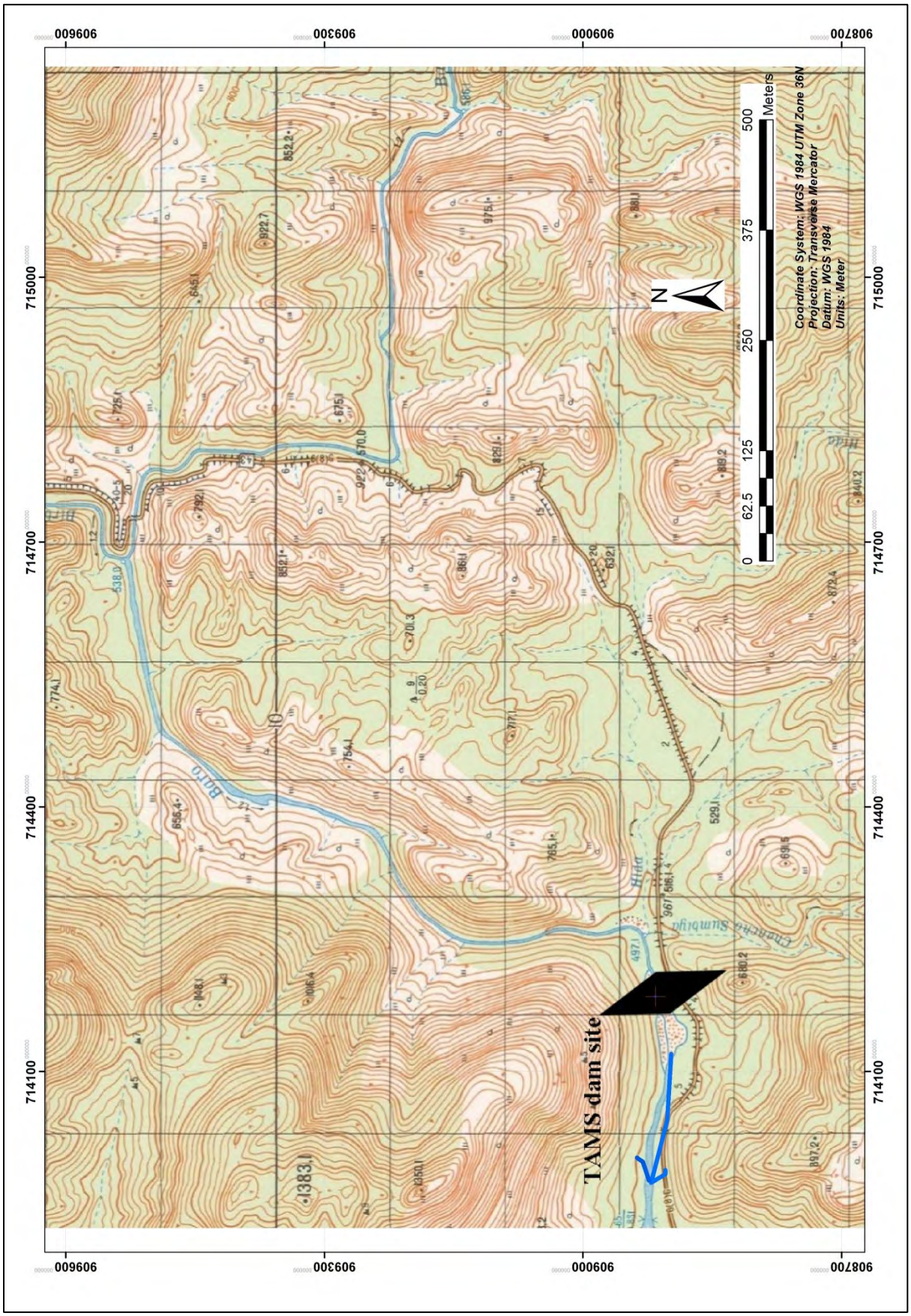

Fig. 2.9 Topographic contour map showing morphology of the project area

Intense processes of weathering could only develop in narrow zones of weak rocks which underwent a strong deformation (MoWIE, 2014). The Baro riverbed (as the upstream Birbir and Upper Baro) is mostly carved in rock as a result of a typical erosion regime in a deeply dissected landscape.

2.6 Geomorphology

The geological evolution of the interest area during the Phanerozoic (542 *Ma* to present) included first an exceedingly long-term geomorphic modeling in continental stable conditions, which in 'step 2' formed the very mature morphology (post-orogenic 'peneplain') as an inherited erosion surface. At later stages such old surface was uplifted, rifted and westward tilted to form the westward lowering an orogenic plateau, as observed in present-day geological landscape (MoWIE, 2014).

This large-scale regional morphology regards the transition belt between the lowermost and last Ethiopian relieves and the huge, flat lowlands (Sudanese plain) with intra-continental riverine wetlands including the confluence area of Akobo / Pibor and Baro (giving rise to the Sobat River)up to the junction with the White Nile (MoWIE, 2014).

Such flat area (very slowly decreasing in elevation, from the around 405 m of Baro-Pibor confluence to the around 400 m of Sobat-White Nile has to be considered the local base-level of the erosion. It is a composite mosaic showing a great micro-topographic complexity. The entire lower course of Baro from near Bonga hamlet downstream, toward the town of Gambella, belongs to this flat flood area rather than to the Ethiopian highlands. Between the mentioned local base-level and the area downstream Bonga, a typical aggradation zone is formed as indicated by the morphological change to braided river (MoWIE, 2014). (Plate 2.1)

Upstream TAMS option site, the Baro riverbed is in a prevailing erosion regime, allowing just a very limited and local deposition of alluvial sediments on the outcropping bedrock. The white arrow in the Plate2-2 points out the secondary summit (725 m a.s.l.) made of outcropping meta-granite, on the right side 1 km downstream the dam axis (MoWIE, 2014). To be noted in the above the substantial lack of any Quaternary deposit and the overall outcropping conditions of the crystalline basement rocks (non-deformed to mildly deformed meta granite). Fig 2.10 shows slope map of the dam site, it is clearly shown that most of the slope at dam site ranges 7-20, while at the most top parts it goes up to 52.

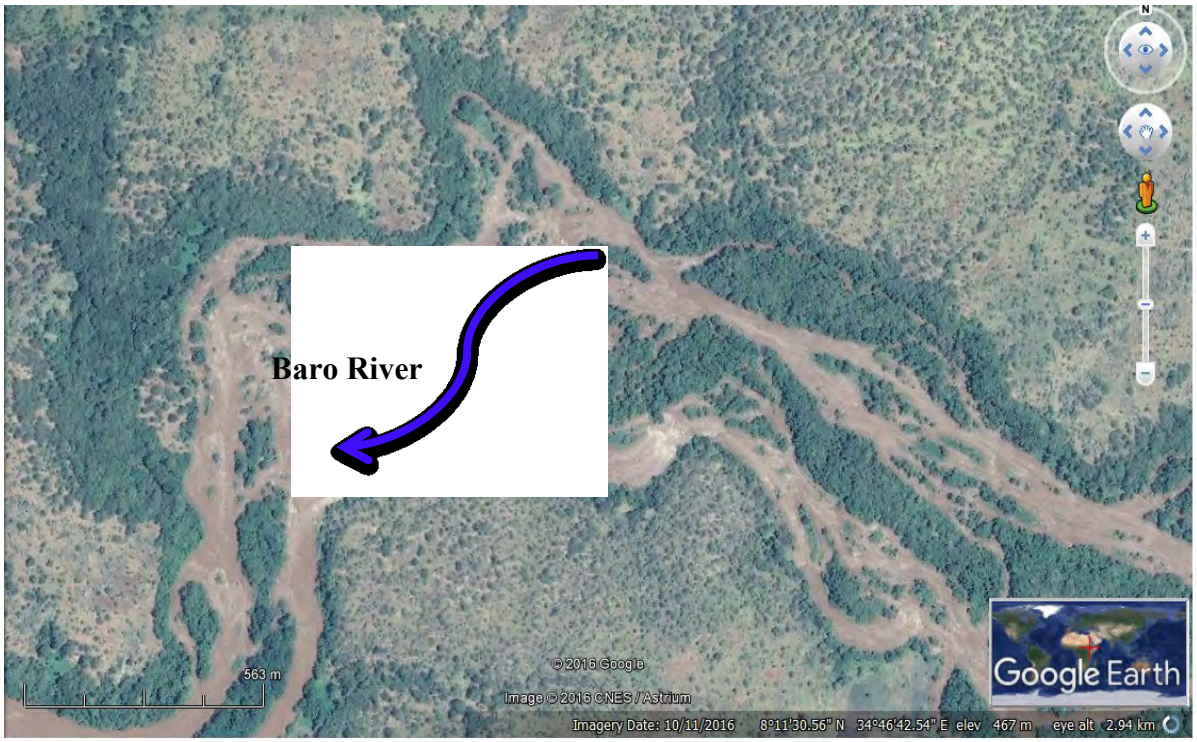

(Source: Google Earth image: Date 10.11.2016; 8°11'30.56" N; 34°46' 42.54"E)

Plate 2.1 Braided morphology of Baro River, approximately 8 km downstream Bonga hamlet

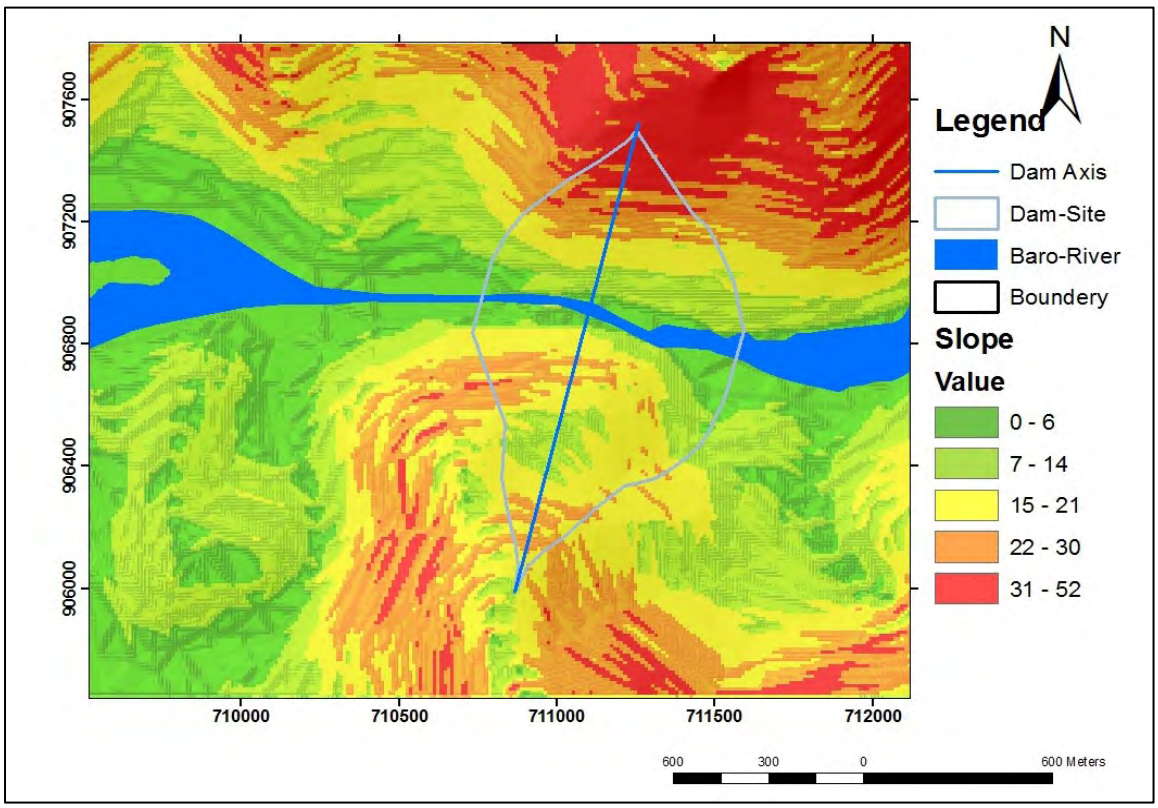

Fig. 2.10 Slope Map of the Dam site

Plate 2.2 Eccentric relieve as a rising counter slope (pointed out by the white arrow), probably cut uphill by a roughly WNW-ESE brittle lineament (MoWIE, 2014)

2.7 Land use and Land cover

The Land uses and land cover map of Ethiopian shows that, the land cover of the catchments of the study area is show in Fig. 2.11. More than 37.6% of the study area is covered by wood land, more than 37.4% is covered by Forest, 14.97 % is covered by Cultivated Land; Rain fed; Cereal Land Cover System; lightly stocked, 9% is covered by Cultivated Land; Rainfed; Cereal Land Cover System; moderately stocked; and very few percent of the study area is covered by a dense woodland (Table 2.4).

Table 2.4 Land use and land cover group of the study site

S.N	Item	Sum area km^2	Percent
1.	Cultivated Land; Rainfed; Cereal Land Cover System; lightly stocked	4584.68	14.97
2.	Cultivated Land; Rainfed; Cereal Land Cover System; moderately stocked	2784.1	9.08
3.	Woodland; Dense (>50% tree cover)	256.12	0.84
4.	Woodland; Open (20-50% tree cover)	11537.7	37.66
5.	Forest; Montane broadleaf; Open (20-50% crown cover)	11472.2	37.45

2.8 Soil and Vegetation

The project area is generally covered by dense grasslands, woodlands and bushes.The vegetation is characterized by broad leafed trees, acacia and short bushes with diverse trees including planted mangos.

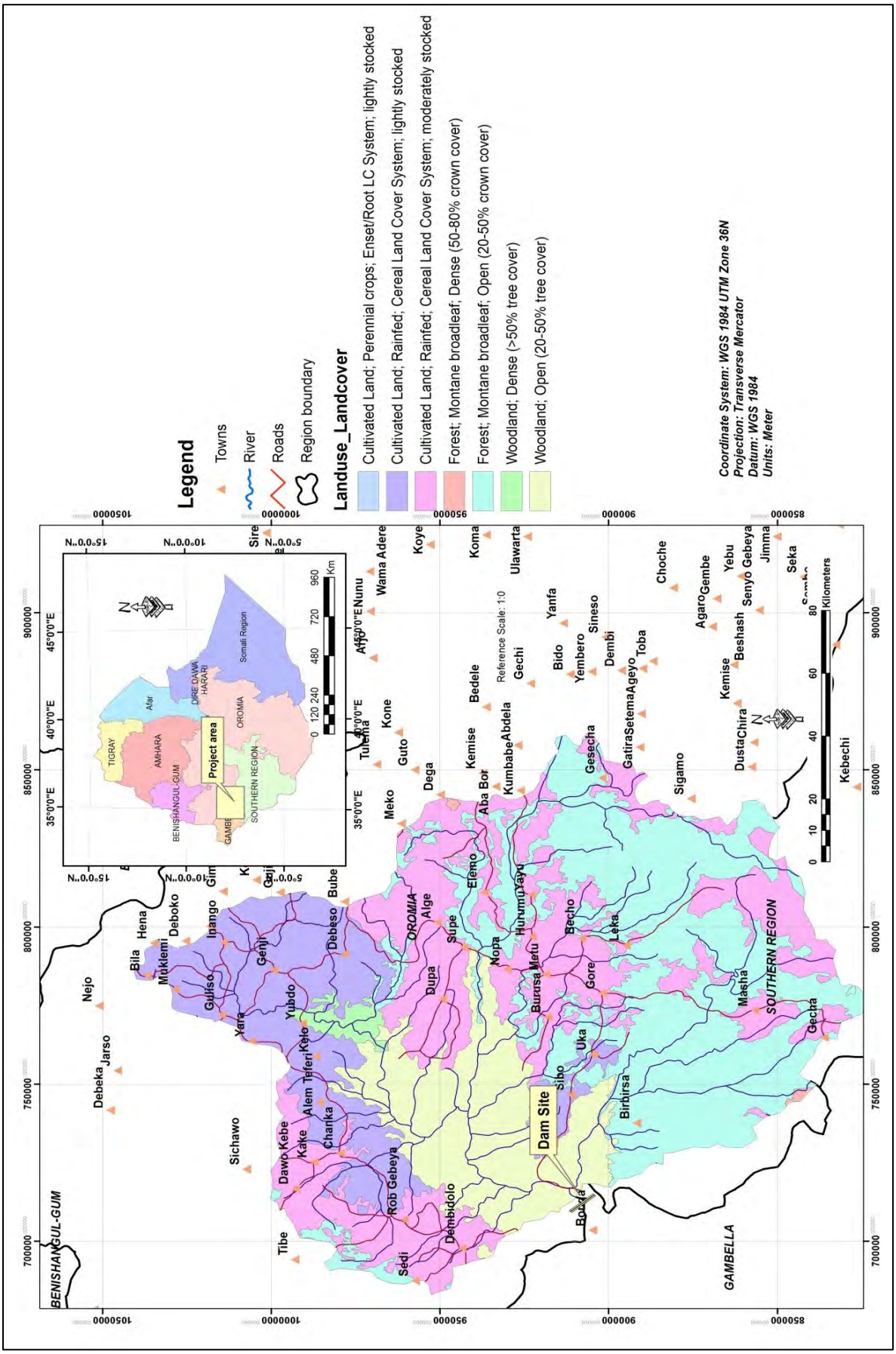

Fig. 2.11 Land use and Land cover map of the study area

Even though the region has good potential in soil fertility, agriculture is less practiced. The area as a whole could be characterized as least cultivated with traditional methods of agriculture. Though most of the area is free from population settlement, people are settled sparsely on some localities within the study area.

According to FAO (2006) soil map of Ethiopia the catchment area is mainly covered by Humic Nitosols (red, well-drained soil with a clay content of more than 30% and a blocky structure), and the rest is covered by Hypic Nitosols, Lithic Leptosol (very shallow soil over hard rock or highly calcareous material), Humic Alsols and Dystric Podzoluvoise (wetland soil hydric soil) that, unless drained, is saturated with groundwater for long enough periods to develop a characteristic gleyic color pattern), respectively. Fig. 2.12 shows the soil map of the study area and its catchment.

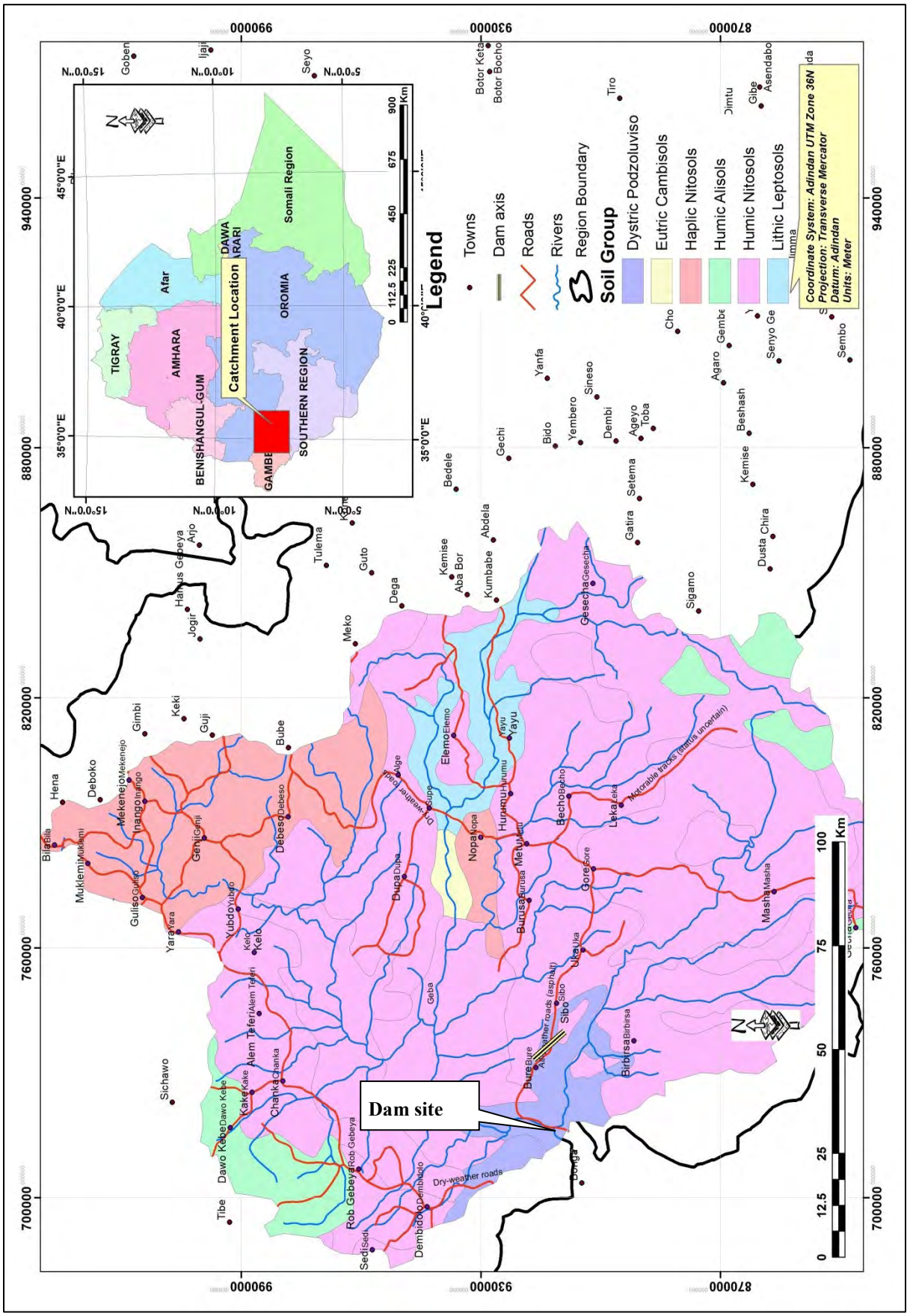

Fig. 2.12 Soil Map of the Study Area (after FAO, 2006)

*****

Chapter III LITERATURE REVEIW

3.1 Rock Mass Characterization

Rock mass characterization is the process of collecting and analyzing qualitative and quantitative data that provide indices and descriptive terms of the geometrical and mechanical properties of a rock mass. Ideally rock mass classification should provide a quick means to estimate the support requirement and to estimate the strength and deformation properties of the rock mass (Ocepec, 2006).

According to Bieniawski (1989) rock engineering classification systems play a steadily more important role in rock engineering characterization and design. The main classification systems for rock support estimates; Barton et al., (1974) Q system and Bieniawski (1989).The Rock Mass Classification system (RMR) uses the most important ground features or parameters as input. Each of these parameters is classified and each class has a given value or rating to express the quality of the ground with respect to tunnel stability.

3.1.1 Rock mass classification

A rock mass classification system is intended to classify the rock mass based on their strength, discontinuity condition , weathering, structural orientation and so on which provide a basis for estimating the deformability and strength properties, supply measureable data for support estimation, and present a platform for communication between exploration, design and construction groups (Bieniawski, 1989).

Rock mass classification schemes have been developing for over 100 years since when many scientists attempted to validate an empirical approach to tunnel design, in particular for determining support requirements in Scandinavian countries. While the classification schemes are appropriate for their original application, especially if used within the bounds of the case histories from which they were developed (Syed, 2015).

Most of the classification schemes which use multi-parameters like Wickham et.al (1972) and Barton et.al (1974) were developed from civil engineering case histories in which all of the components of the engineering geological character of the rock mass were included. Different classification systems place different emphases on the various parameters, and it is recommended that at least two methods be used at any site during the early stages of a project (Palmstrom, 2003).

It is stated that Rock mass classification schemes owe its origin in 1879 when Ritter (1879) devised an empirical approach to tunnel design for finding out support requirements (Hoek, 2007). Since then, these systems have been developing. The rock mass classification schemes that are often used in rock engineering for assisting in designing underground structures are RMR, Q and GSI systems (Palmstrom, 2003). Table 3.1 shows some well-known systems (Coscar, 2004)

Table 3.1 Major rock mass classification systems (Cosar, 2004)

Rock Mass Classification System	Originator	Country of Origin	Application Areas
Rock Load	Terzaghi, 1946	USA	Tunnels with steel Support
Stand-up time	Lauffer, 1958	Australia	Tunneling
New Austrian Tunneling Method (NATM)	Pacher et al., 1964	Austria	Tunneling
Rock Quality Designation (RQD)	Deere et al., 1967	USA	Core logging, tunneling
Rock Structure Rating (RSR)	Wickham et al., 1972	USA	Tunneling
Rock Mass Rating (RMR) Modified Rock Mass Rating (M-RMR)	Bieniawski, 1973 (last modification 1989-USA) Ünal and Özkan, 1990	South Africa Turkey	Tunnels, mines, (slopes, foundations) Mining
Rock Mass Quality (Q)	Barton et al., 1974 (last modification 2002)	Norway	Tunnels, mines, foundations
Strength-Block size	Franklin, 1975	Canada	Tunneling
Basic Geotechnical Classi-fication	ISRM, 1981	International	General
Rock Mass Strength (RMS)	Stille et al., 1982	Sweden	Metal mining
Unified Rock Mass Classification System (URCS)	Williamson, 1984	USA	General
Communication Weakening Coefficient System (WCS)	Singh, 1986	India	Coal mining
Rock Mass Index (RMi)	Palmstrom, 1996	Sweden	Tunneling
Geological Strength Index (GSI)	Hoek and Brown, 1997	Canada	All underground excavation-

3.1.1.1 Rock Quality Designation (RQD) classification method

RQD is a modified core recovery index defined as the total length of intact core greater than 100mm in length, divided by the total length of the core run. The resulting value is presented in the form of a percentage. RQD should only be calculated over individual core runs; usually 1.5 meters long (Deere, 1988).

The concept of rock quality designation, RQD, was introduced by Deere (1964). Assuming that a steady standard of drilling can be maintained, the percentage of solid core obtained depends on the strength and number of discontinuities in the rock mass concerned. RQD is

the sum of the core sticks in excess of 10cm, expressed as a percentage of the total length of core drilled.

Rock quality Designation (RQD) classification system plays an important role in characterizing a rock mass (Bieniawski, 1989). This is because the quality of the rock mass is one of the major parameters in characterizing the rock mass.

3.1.1.2 Rock Mass Rating (RMR) rock mass classification System

Bieniawski (1976) issued the details of a rock mass classification called the Geomechanics Classification or the Rock Mass Rating (RMR) system. The discussion which follows is based upon the 1989 version of the classification (Bieniawski, 1989). Both, this version and the 1976 version deal with estimating the strength of rock masses.

The following six parameters are used to classify a rock mass using the RMR system:

RMR = A1 + A2 + A3 + A4 + A5 + B…….*eq. 3.1*
Where;

A1 - Uniaxial compressive strength of rock material.
A2 - Rock Quality Designation (*RQD*).
A3 - Spacing of discontinuities.
A4 - Condition of discontinuities.
A5 - Groundwater conditions.
B - Orientation of discontinuities.

Limits

Palmstrom et al. (2006) describes that there is no input parameter for the rock stresses in the RMR system; however stresses up to 25MPa are included in the estimated RMR value. Thus, rock mass changes because of the overstressing like rock bursting and squeezing is not included in this classification system.

Whether or how faults and weakness zones are included, is unclear. No special parameter for such features is applied, however some of the parameters included in the system may represent conditions in faults, though the often complicated structure and composition in these features are generally difficult to characterize and classify. Therefore, it is probable that RMR does not work well for many faults and weakness zones. Also, swelling rock is

not included in the RMR system (Palmstrom, et al., 2006). Table 3.2 shows the rock mass classes and rock mass classes determined from the total rating after Bieniawski 1989.

Table 2.2 Meaning of rock mass classes and rock mass classes determined from the total ratings (after Bieniawski, 1989)

Parameters/Properties of rock mass	Rock Mass Rating(Rock Class)				
Rating	100 - 81	80 - 61	60 - 41	40 - 21	<20
Classification of rock mass	Very Good	Good	Fair	Poor	Very Poor
Average stand-up time	10 years for 15m span	6 months for 8m span	1 week for 5m span	10 hours for 2.5m span	30 minutes for 1 m span
Cohesion of the rock mass	>400 Kpa	300 - 400 Kpa	200 - 300 Kpa	100 - 200 Kpa	<100 k pa
Friction angle of the rock mass	$>45^0$	35^0 - 45^0	25^0 - 35^0	15^0 - 25^0	$<15^0$

3.1.1.3 The Q- rock mass classification System

The Q or NGI (Norwegian Geotechnical Institute) classification system was developed by Barton et.al (1974), primarily for tunnel design work. It expresses rock quality, Q, as a function of 6 independent parameters:

$$Q = \frac{RQD}{Jn} X \frac{Jr}{Ja} X \frac{Jw}{SRF} \ldots\ldots\ldots \textit{eq. 3.2}$$

Where,

RQD = Rock quality designation

J_n is based on the number of joint sets

J_r is based on discontinuity roughness

J_a is based on discontinuity alteration

J_w is based on the presence of water

SRF is the Stress Reduction Factor

It has been suggested that RQD/J_n reflects block size, J_r/J_a reflects friction angle and J_w/SRF reflects effective stress conditions (Barton et al., 1974).

The main advantage of the Q classification system is that it is relatively sensitive to minor variations in rock properties. Except for a modification to the Stress Reduction Factor (SRF) in 1994, the Q system has remained constant. The descriptions used to assess joint conditions are relatively rigorous and leave less room for subjectivity, compared to other classification

systems (Barton et al., 1974). Table 3.3 provides the latest version of the Q system, after Barton et al., (1974).

One disadvantage of the Q system is that it is relatively difficult for inexperienced users to apply. The J_n term, based on the number of joint sets present in a rock mass, can cause difficulty. Inexperienced users often rely on extensive line mapping to assess the number of joint sets present and can end up finding 4 or more joint sets in an area where jointing is widely spaced. This results in a low estimate of (Barton et al., 1974).

Table 3.3 Classification of rock mass based on Q- values (Barton et al., 1974)

Q	Group	Classification
10 – 40	1	Good
40 – 100		Very Good
100 – 400		Extremely Good
400 - 1000		Exceptionally Good
0.10 – 1.0	2	Very Poor
1.0 – 4.0		Poor
4.0 – 10.0		Fair
0.001 – 0.01	3	Exceptionally Poor
0.01 – 0.1		Extremely Poor

An important asset of the Q system in characterizing the rock mass is that the case studies employed for its initial development have been very well documented. The use of the Q system for the design of support has also evolved over the time. In particular Barton (1990) has introduced a design chart that accounts for the use of fiber reinforced shotcrete. This has been based on increased experience in tunneling.

Limits

As pointed out by Palmstrom and Broch (2006), the Q system has several limitations, working best between Q = 0.1 and Q = 40 for tunnels with spans between 2.5m and 30m. Though there are input parameters for overstressing, Q should be used with care in rock bursting and especially in squeezing ground. The same is the case for weakness zones; especially where swelling ground occurs.

3.1.1.4 Rock Structure Rating (RSR) classification System

Wickham et al (1972) described a quantitative method for describing the quality of a rock mass and for selecting appropriate support on the basis of their Rock Structure Rating (RSR) classification. Most of the case histories, used in the development of this system, were for relatively small tunnels supported by means of steel sets, although historically this system

was the first to make reference to shotcrete support. In spite of this limitation, it is worth examining the RSR system in some detail since it demonstrates the logic involved in developing a quasi-quantitative rock mass classification system (Wickham et al., 1972).

The significance of the RSR system, in the context of this discussion, is that it introduced the concept of rating each of the components listed below to arrive at a numerical value of

RSR = A + B + C …….*eq.3.3*

(i) Parameter A, Geology: General appraisal of geological structure on the basis of:
   a) Rock type origin (igneous, metamorphic, and sedimentary).
   b) Rock hardness (hard, medium, soft, decomposed).
   c) Geologic structure (massive, slightly faulted/folded, moderately faulted/ folded, intensely faulted/folded).

(ii) Parameter B, Geometry: Effect of discontinuity pattern with respect to the direction of the tunnel drive on the basis of:
   a) Joint spacing.
   b) Joint orientation (strike and dip).
   c) Direction of tunnel drive.

(iii) Parameter C: Effect of groundwater inflow and joint condition on the basis of:
   a) Overall rock mass quality on the basis of A and B combined.
   b) Joint condition (good, fair, poor).
   c) Amount of water inflow (in gallons per minute per 1000 feet of tunnel).

3.1.1.5 Geological Strength Index (GSI)

Hoek et.al, (1997) introduced the Geological Strength Index, as a complement to the rock failure criterion and as a way to estimate the parameters s, a and m_b in the criterion. The GSI estimates the reduction in rock mass strength for different geological conditions.

The aim of the GSI-system is to determine the properties of the undisturbed rock mass. For disturbed rock masses, compensation must be made for lowest GSI-values obtained from the same locations. Fig.3.1. shows estimation of Geological Strength Index based on field geological description used in Rock Lab. Software after Hoek and Brown, 2002.

3.1.1.6 Rock Mass index (RMi)

The Rock Mass index, RMi has been developed to characterize the strength of the rock mass for construction purpose (Palmstrom, 2006).The selected input parameters are based on earlier research and opinions in the area of rock mass classification/characterization system. The main focus of the development of RMi was on the effect of defects in rock mass that reduce the strength of the intact rock. The RMi represents only the inborn property of the rock mass. The insitu rock stresses or water pressure is not included in the Rock Mass index.

The input parameters in general strength characterization of a rock mass are selected as (Palmstrom, 1995);

- The size of blocks delineated by joints
- The strength of block material
- The shear strength of the block faces
- The size and termination of the joints

3.1.2 Rock mass failure criteria

3.1.2.1 Failure Criteria

It is more popular now to use a rock mass failure criterion and equation for deformability to estimate values for rock mass strength and deformability respectively for rock masses. A key assumption of a rock mass failure criterion is that the rock mass is isotropic. Rock mass failure criteria are often formulated in either principal stresses $\sigma_1 = f(\sigma_2, \sigma_3)$ or in normal stresses $t = f(\sigma_n)$. The parameters σ_1 and t usually denote the peak strength, but may also represent either the residual strength or yield strength (Eldbor, 2004).

3.1.2.2 Mohr-Coulomb

The peak stress of rock undergoing deviatoric loading will increase if the rock is confined. The variation of peak stress σ_1 with confining pressure σ_3 is known as criterion of failure. This consists of a linear envelope touching all Mohr's circles representing critical combinations of principal stresses (Singh et al.,2002), stated in terms of normal and shear stresses on the plain representing by the point of tangency of a Mohr circle with the envelope.

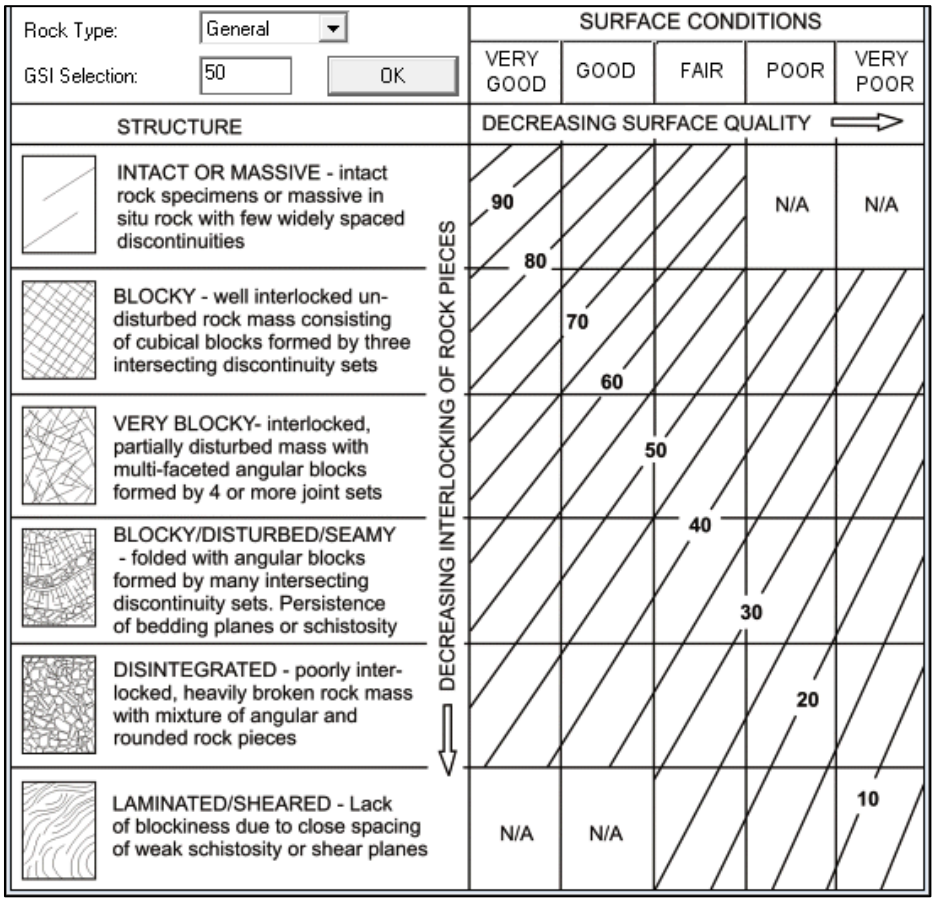

(Source: Rock Lab Guide by Hoek and Brown, 2002)

Fig. 3.1 Estimate of Geological Strength Index GSI based on geological descriptions

$\tau_p = Si + \sigma \tan Ø$……*eq. 3.4*

Where, '*Ø*' is called the angle of internal friction, it describes the rate of increase of peak strength with normal stress.τ_p is the peak shear stress or shear strength. This equation is often referred to as the Mohr-Coulomb criteria (Singh et al., 2002),

The criterion assumes that the failure occurs along a plane without any dilation. The Mohr-Coulomb criterion can also be expressed, in principal stress as;

$$\sigma 1 = \frac{2\cos Ø}{(1-\sin Ø)} + \frac{1+\sin Ø}{1-\sin Ø}\,\sigma 3$$……*eq.3.5*

The Mohr-Coulomb criterion is also used to represents the `residual' strength, i.e. the minimum strength reached by a material subjected to deformation beyond the peak. The residual shear strength may approach zero while the residual friction angle 'Ør 'will lie between zero and the peak friction angel. The equation states that `Failure' occurs when the applied shear stress less the frictional resistance associated with the normal stress on the failure plane becomes equals to a constant of the rock `Si' (Singh et al.,2002),

Some of the reason that Mohr-Coulomb criterion is often used in rock mechanics applications is that it is described by a simple mathematical equation, is easily understood and simple to use (Singh et al., 2002). To use the Mohr-Coulomb criterion one has to take the following into account.

- The failure mechanism has to be shear failure and that
- The relationship between normal and shear stress obtained by experimental tests usually show a non-linear behavior and not linear as the Mohr-Coulomb criteria predicts

3.1.2.3 Hoek and Brown Criteria

Hoek, et al. (2002) introduced their failure criterion in an attempt to provide input data for the analyses required for the design of underground excavations in hard rock. The criterion was derived from the results of research into the brittle failure of intact rock by Hoek and on model studies of jointed rock mass behavior by Brown. The criterion started from the properties of intact rock and then introduced factors to reduce these properties on the basis of the characteristics of joints in a rock mass. The authors sought to link the empirical criterion to geological observations by means of one of the available rock mass classification schemes and, for this purpose; they chose the Rock Mass Rating proposed by Bieniawski (Bieniawski, 1989). Because of the lack of suitable alternatives, the criterion was soon adopted by the rock mechanics community and its use quickly spread beyond the original limits used in deriving the strength reduction relationships. Consequently, it became necessary to re-examine these relationships and to introduce new elements from time to time to account for the wide range of practical problems to which the criterion was being applied. Typical of these enhancements were the introduction of the idea of "undisturbed" and "disturbed" rock masses Hoek and Brown, and the introduction of a modified criterion to force the rock mass tensile strength to zero for very poor quality rock masses (Hoek, et al., 2002).

One of the early difficulties arose because many geotechnical problems, particularly slope stability issues, are more conveniently dealt with in terms of shear and normal stresses rather than the principal stress relationships of the original Hoek-Brown criterion, defined by;

$$\sigma_1 = \sigma_3 + \sigma_{ci}\left(m\,\frac{\sigma 3}{\sigma ci} + S\right)^{0.5} \quad \ldots\ldots\ldots\ldots eq.\ 3.6$$

Where,

σ_1'and σ_3' are the major and minor effective principal stresses at failure

σ_{ci} the uniaxial compressive strength of the intact rock material and

m and s are material constants, where s = 1 for intact rock.

The popularity of the Hoek-Brown failure criterion was achieved through its intended applicability to a wide range of intact rock types despite only having two input parameters for intact rock, *m* and sc. The input parameters s_c and *m* are selected through linear regression of an existing set of triaxial tests on intact rock or in the case of *m* from tables relating *m* to rock type provided by Hoek and Brown (1980a).

3.1.2.4 Rock Mass Deformation

The closure of discontinuities, plastic and elastic deformation of the intact rock that comprises rock mass, under applied static or dynamic load is known as rock mass deformation (Palmstrom et al., 2001).The deformation of the rock mass can be measured using the modulus of deformation, E_d (Jonson, 1988).The modulus of deformation is defined as the sum of deformation that occurs with closure of joints in the rock mass under deformation (plastic) and the deformation that occurs with continued stress application after crack closure (elastic) (Jonson, 1988).

In the 1960's several attempts were made to use Deere's RQD for estimating in-situ deformation modulus, however, this approach is seldom used today (Deere 1988). Some theoretical expressions have been derived for simple joint geometries derived a mathematical procedure to calculate the deformation modulus of an equivalent continuum for a randomly jointed rock mass.

Empirical determination of the deformability of the rock mass is given by different scholars. Based on the case histories of mostly dam foundations, Serafim and Pereira (1983) developed an empirical relation by back analysis of Ed from the measured deformation; the relation works well for the rock mass for which RMR lies between 10 to 50 and UCS of intact rock 'qc' > 100 Mpa.

The Serafim and Pereira relation for RMR89 < 50 is expressed as eq. 3.7 (Serafim & Pereira, 1983)

$$Ed = 10^{(RMR-10)/40} \qquad .....eq.3.7$$

Where, Ed is in situ modulus of deformation in Gpa and RMR is rock mass rating.

Bieniawski (1978) proposed an empirical relation to determine Modulus of Deformation 'E_d' by using RMR. For the rock mass having RMR higher than 55 and UCS of intact rock 'qc' greater than 100 Mpa the relation is in close agreement with the tested valves. For RMR > 50 (Bieniawski, 1978),

$Ed = 2RMR - 100$ *.....eq.3.8, given in Mpa*

Agarwal, et al. (1991) also proposed an empirical relation to work out Ed from the RMR value. The values of E_d obtained by Agarwal, et al. (1991) relation are the closest to the actual observed data.

$E_d = 10^{(RMR-30)/50}$ *.....eq.3.9, given in Mpa*

Barton et al (1980), Barton et al (1992) and Grimstad and Barton (1993) proposed an empirical relation to determine Ed by using Q value;

$E_d = 25 \log_{10} Q$ *.....eq.3.10, given in Mpa*

Hoek and Brown (1997) proposed an empirical relation to work out modulus of deformation of rock mass. This relation works well for rock mass having UCS less than 100 Mpa.

Ed = (qc) 0.5 / 10 *10 (GSI-10)/40 *.....eq.3.11*

Where; 'qc' is the UCS of intact Rock at natural moisture content given in Mpa, Ed is modulus of deformation given in Mpa and GSI is the Geologic Strength Index. For RMR_{76} version > 18, GSI = RMR76 and RMR_{89} version > 23, GSI = RMR89 – 5

Deer and Miller (1996) presented an empirical classification of the Modulus of Deformation with its deformability. Rocks having a modulus of deformation < 5 have a corresponding very high deformability and on the other hand rocks having a modulus of deformation > 60 the rock exhibit very low deformability (Table 3.4).

3.1.2.5 Empirical Methods to determine shear strength of the rock mass

Hoek et.al (1992) developed an empirical approach to determine the strength of the jointed rock mass and formulated a failure criterion for jointed rock mass. Based on results of number of projects this criterion was modified by Hoek & Brown in 1988 and later by Hoek et al. (1992). For this empirical method Hoek and Brown utilized Bieniawiski's Rock Mass rating System (RMR) to work out the material constants.

Table 3.4 Classification of intact rock based on modulus of deformation (Deere and Miller, 1966)

Class	Modulus of deformation (Gpa), Hoek and Brown	Description of deformation
1	<5	Very high
2	5-15	High
3	15-30	Moderate
4	30-60	Low
5	>60	Very low

Direct determination of Shear Strength Parameters from RMR

Bieniawski (1989) proposed direct empirical relations to workout shear strength parameters i.e. Cohesion and Angle of internal friction by using Rock Mass Rating System (RMR).

Cohesion 'C' = 0.05 RMR ……*eq. 3.12*

Angle of internal friction 'Ø' = 0.5RMR + 5 ……*eq. 3.13*

3.1.3 Application of RMR in determination of Rock Slope Stability Condition

3.1.3.1 Slope Mass Rating (SMR)

For evaluating the stability of the rock slopes, Romana (1985) proposed a classification system called slope mass rating (SMR) system. Initially, Romana developed SMR to account for plane and toppling mode of failure and wedge mode was considered as a special case in which two wedge forming planes were considered individually later, this was modified by Anbalagan et.al (1992) to account for wedge mode of failure as a separate individual mode. The SMR can be expressed as an expression give in eq. 3.14.

$SMR = RMR_{basic} - (F1 * F2 * F3) + F4$……..*eq. 3.14*

Where; RMR_{basic} is evaluated according to Bieniawski (1979).

The F1, F2 and F3 are adjustment factors related to joint orientation with respect to slope orientation and F4 is the correction factor for method of excavation.

F1 – depends upon parallelism between joints and slope face strikes.
$(\alpha_j - \alpha_s)$ where, α_j is joint strike and α_s is slope strike.

F2 – refers to joint dip angle (β_j) or plunge of line of intersection of two wedge forming planes (β_i).

F3 – depends upon relationship between joint dip or plunge of line of intersection of two wedge forming planes and slope inclination. $(\beta_j - \beta_s)$ or $(\beta_i - \beta_s)$ where, α_s is the inclination of the slope.

F4 – Method of Excavation. It includes the natural slope, or the cut slope excavated by pre splitting, smooth blasting, normal blasting, poor blasting and mechanical excavation.

3.1.4 Seismic Refraction and its role in characterizing the rock mass

3.1.4.1 General about Seismic refraction

Seismic refraction survey is one of the geophysical methods most closely related to rock mass properties because the longitudinal seismic wave velocity that is sent from source varies with the main features, which characterizes the rock mass (rock properties, jointing, stresses etc.). Therefore, the results from such seismic measurements may assist Geologists/Engineers in site selections and in rock engineering. The seismic survey methods utilize the propagation of compression or primary seismic waves. The ratio of the shear (or transverse) and longitudinal sonic velocities can be used to determine the dynamic moduli of the rock (Sjögren, et al., 1979).

Seismic refraction is generally used for determining the depth to very hard layers, such as bedrock. The seismic refraction method is performed according to ASTM D 5777 procedures and involves a mapping of Vp arrivals using a linear array of geophones across the site, as illustrated in Fig.3.2, for a two-layer stratification. In fact, a single geophone system can be used by moving the geophone position and repeating the source event. In the SR method, the upper layer velocity must be less than the velocity of the lower layer. An impact on a metal plate serves as a source rich in P-wave energy. Initially, the P-waves travel solely through the soil to arrive at geophones located away from the source. At some critical distance from the source, the P-wave can actually travel through soil-underlying rock-soil to arrive at the geophone and make a mark on the oscilloscope. This critical distance (x_c) is used in the calculation of depth to rock (Sjögren, 1984).

Seismic wave velocities are calculated from the slope in a 'travel time versus distance' graph worked out from the registrations in geophones placed along the measured profile. The determination of the seismic velocities and the thickness of the various layers of is a complex process, and a great deal of practical experience is required of the operator before the results can be regarded as reliable. Fig 3.2 shows field setup and procedures for seismic refraction method.

In the ground there are several factors that, in a complex way, may influence the propagation of seismic velocities. The main contributions stem from,

- The inborn properties of the rock material; and
- The in situ rock mass conditions, i.e. distribution of rock types, jointing, rock stresses, and ground water condition.

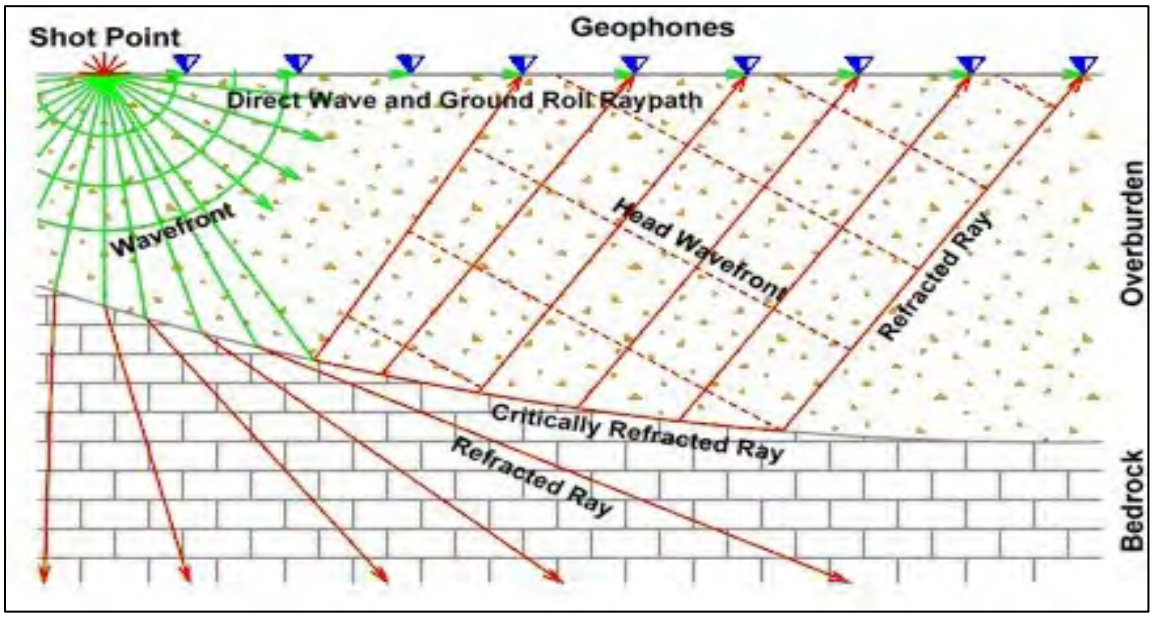

Fig. 3.2 Field Setup & Procedures for Seismic Refraction Method (ASTM D 5777)

Velocities of longitudinal waves vary considerably with the type of rock which is determined by the mineral composition, texture, density, porosity, anisotropy and degree of weathering. A representative selection of typical longitudinal (compressional) seismic velocities is given in the fig. 3.2. In addition, saturation, pressure, and temperature influence.

3.1.4.2 Characterization by Seismic refraction

Rock masses can be characterized through seismic refraction surveys; this is because different rocks have their own distinct seismic velocities. The physical properties of the rock mass such as strength and deformation parameters or permeability may differ substantially from those of the rock materials as the properties of the rock mass is strongly influenced by the type of discontinuities (joints), their orientation, spacing, persistence, aperture and filling, roughness, waviness, etc. (Palmstrom 1996). Fig 3.3 shows typical ranges of longitudinal seismic velocities for intact rock after Sjögren, 1984.

Sjögren et al. (1979) conclude from their investigations that, other than the influence from the inherent rock properties, the in situ longitudinal velocities in un-weathered (fresh) rock masses are mainly determined by:

- Stresses acting;
- Degree of jointing;
- Presence of open joints or joints with filling; and
- Ground water conditions.

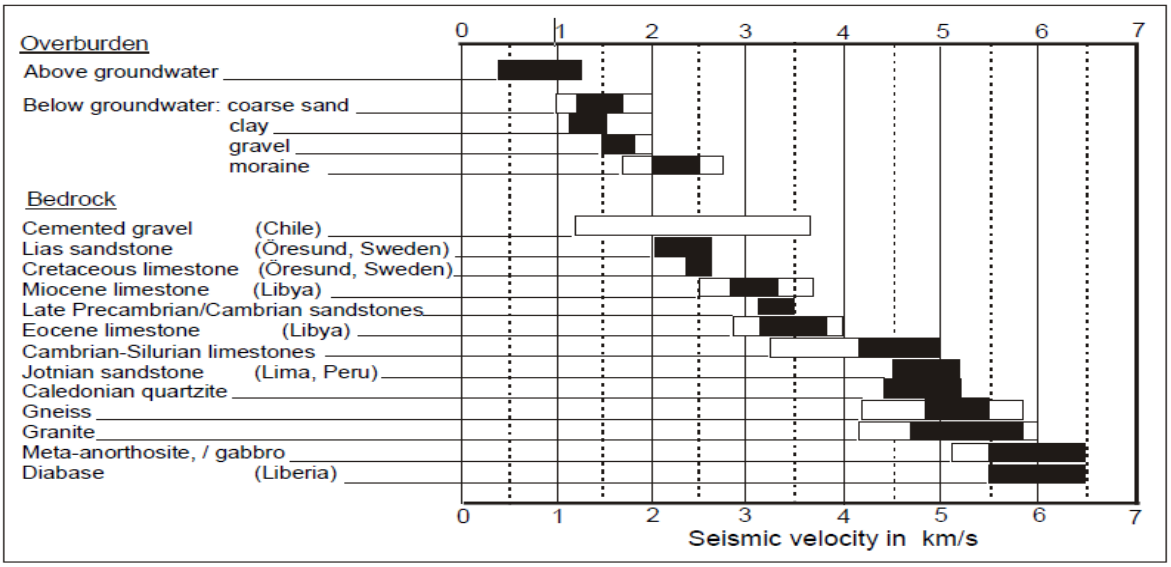

Fig. 3.3 Typical ranges of longitudinal seismic velocities for intact rocks (Sjögren, 1984)

Seismic refraction measurements cannot be used to assess the condition of the joint itself (roughness and alteration of the joint surface; hilling and size of the joint). Cecil (1971) points out that clay and other weak or low friction joint fillings, which may cause instability in a rock mass with few joints, may not influence the seismic velocity. On the other hand, one or two open joints that may not have any effect on the stability of an opening can significantly lower the seismic velocity and give the impression of low quality rock. The possibility that such conditions may exist, must be considered in the geological interpretation of the seismic refraction results.

The density of the rock is one factor, which affects the velocity of longitudinal sonic waves. In the elastic wave theory the velocity decreases with increasing density. The effect of density is, however, overruled by the dynamic stiffness of the rock, which generally varies with the density. Therefore, the sonic velocity seems incorrectly to vary with the density of the rock as shown in the figure below. Fig 3.4 shows mean longitudinal pulse velocity versus density of the rock proposed by Sjögren et al., 1979.

Although there is a clear correlation between jointing and seismic refraction velocities, the latter also includes the averaged effect of other factors such as rock properties and stress conditions as further dealt with later in this section.

There are limitations in the use of seismic refraction interpretations of jointing assessments (Palmstrom, 1982).These mainly stem from the fact that there are several properties and features influencing on the seismic velocity, and it is impossible to avoid uncertainties when

variations in the velocity is linked mainly to one or more of these. Knowledge of the geological conditions linked with comprehensive experience in refraction seismic measurements is important in reducing these limitations.

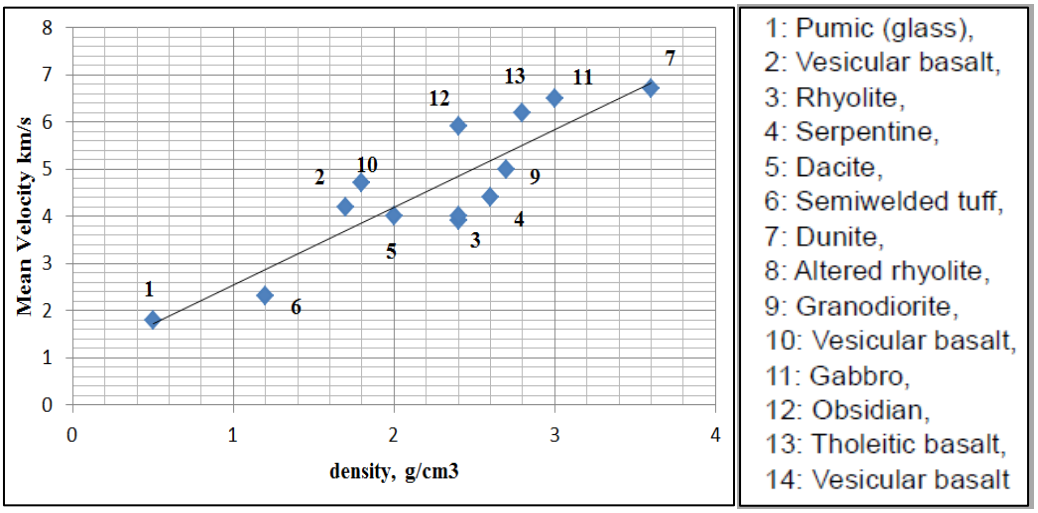

Fig. 3.4 Mean longitudinal pulse velocity versus density of the rock. (After Sjögren et al., 1979)

3.1.5 Integration of Geotechnical and Geophysical Techniques

A case study for the tropical Environment study by Andy et al. (2012), revealed that the seismic velocity has a direct relationship with the geotechnical parameters of the rock mass. They used seismic refraction survey to locate the exact value of seismic velocities which can be correlated with the SPT-N values and RQD values from borehole data set. This seismic tomography result was processed using geophysical software.

For correlation between rock quality and seismic velocity analysis, they split the methods used into two parts. The first part is velocity determination from the seismic refraction survey and the second part is laboratory analysis for rock samples to determine their P-wave velocity. From the obtained results they found correlation for seismic velocity and rock quality. Table 3.5 shows Approximate Connections between Refraction Seismic Velocities, Rock Mass Conditions and Rock Support in Scandinavian Tunnels (partly based on Sjögren et al., 1979).

From selected study sites Andy et al. (2012) also determined correlation between apparent P-wave velocities and penetration strength. Penetration strength shows a strong influence on P-wave velocity for tropical granitic rock. Fig. 3.5 shows the empirical correlation between apparent P-wave velocities with penetration strength values for the study site.

Table 3.5 Approximate Connections between Refraction Seismic Velocities, Rock Mass Conditions and Rock Support in Scandinavian Tunnels (partly based on Sjögren et al., 1979)

Insitu velocity m/s	Probable ground conditions	Possible Rock Support
<3000	Cavities in the bedrock filled with soil, or completely crushed and fragmented rock material in weakness zones	Extensive rock support
<4000	Ground related to faults, contact zones etc. with highly fractured rock	High amount of rock support
4000 - 4400	Strong- moderately jointed rock masses	Moderate to high amount of rock support
4500 - 5000	Slightly- moderately jointed rock masses	Small to moderate amount of rock support
>5000	Massive rock masses	Generally little need for rock support

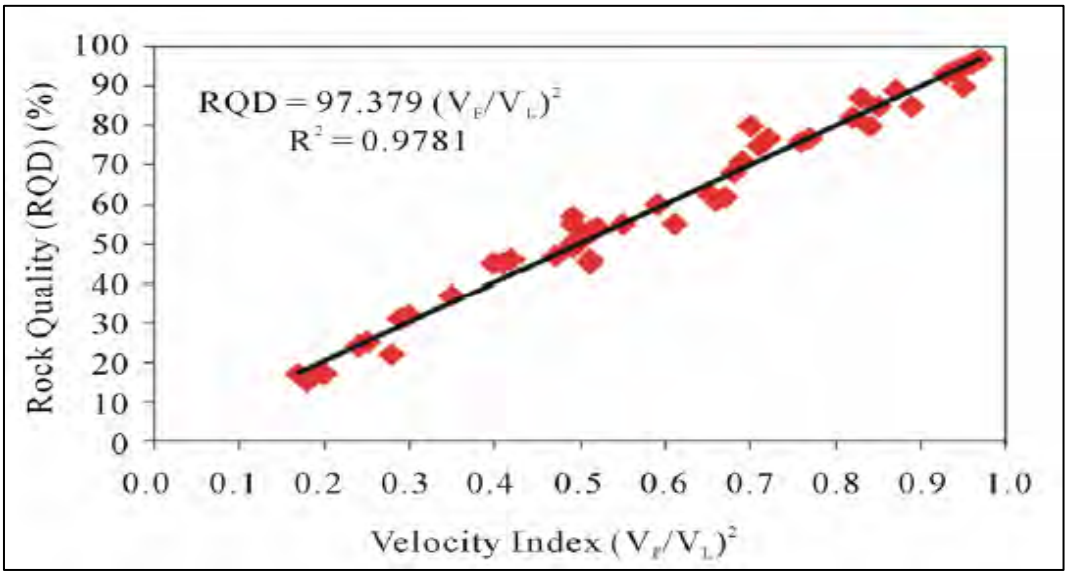

Fig. 3.5. The trend of relationship between rock quality and velocity index.

Table 3.6 Relationship between RQD, velocity index and N value (After Andy, et.al 2009)

Quality Description	RQD	Velocity(V_F/V_L)2	SPT- N Value
Very poor	Less than 25	0 – 0.25	50 – 65
Poor	25 – 50	0.25 – 0.53	65 – 70
Fair	50 – 75	0.53 – 0.75	70 – 75
Good	75 – 85	0.75 – 0.85	75 – 85
Excellent	Over 85	Over 0.85	Over 85

For their study Andy et al. (2012) concluded that, an integrated approach using P-wave seismic velocity values and geotechnical parameters are applicable for tropical environmental study. The estimation can help in predict the engineering characterizations and seismic P-wave velocity of the subsurface material (soils and rocks). In this study, the selected areas in

the tropical regions both have same type of bedrock (Tropical Granitic Bedrock). Present study however, has attempted other areas with different type of weather condition and latitude region. The different weather and latitude also influence the weathering rate of rock. Thus, the parameters obtained will considerably be influenced by the surrounding condition.

3.1.6 Genesis of Methodology for the Present Study

A thorough and extensive literature review was undertaken to gain the necessary background knowledge about the present research topic encompassing both published and unpublished reports of investigations, case studies, text books and Journals which were found related to the research topic.

From this literature review, it was clearly understood that safe design and feasibility evaluation of a large scale hydropower project, such as TAMS dam project would require complete understanding of pertinent geological features and geotechnical information of the actual surface and subsurface materials. Through an integrated approach for planning, design and implementation of engineering structures such as dams, spillways, powerhouses, tunnel alignments, etc. detailed investigation is essential.

Because of the aforementioned justifications a theoretical methodology for characterization of the rock mass was initiated. This rock mass characterization used an integrated approach mainly the rock mass classification and seismic refraction survey as a tool to characterize the rock mass.

*****

Chapter IV GEOLOGY AND STRUCTURES

4.1 Regional Geology and Structures

4.1.1 Regional Geology

TAMS Dam site is located in the western end of the lowering Ethiopian relieves, which make a gradual transition to the lowlands of Sudanese plain. The site lies within the last relieves which border the western alluvial plain of Baro-Akobo fluvial system and corresponds to the deeply dissected western margin of the Ethiopian Plateau. Due to tectono-metamorphic, volcanological and geomorphological evolution of Ethiopia, these relieves are made of ancient crystalline basement rocks, in this area lacking of the cover of Tertiary volcanic rocks. Bedrock is also lacking of any relevant coverage of Quaternary deposits, so that the outcropping conditions can be considered as very good to excellent. The inherited, N-S trended, overall structure of the bedrock, which is crossed by the almost E-W flowing Baro River (MoWIE, 2014).

4.1.2 Rocks and stratigraphy

The area lies within a wide boundary zone, about N-S trended, separating the Baro Group or Domain to the West, the 'interlayered' meta-granites (syn-tectonic granites) in the middle, and the Birbir Group or Domain to the East. The lithological units involved are (MoWIE, 2014):

- Pgn-2 (biotite gneisses and para-gneisses of Baro Domain hypothetically dated as Archean to early Proterozoic);
- Pgt-1 (syn-tectonic granites, so defined based on degree of deformation and geometry of contacts with the host metamorphic rocks, having a geo-chronological age ranging between late Proterozoic to early Paleozoic);
- Pss-1 (meta-sediments and meta-volcanic schists, psammitic and pelitic schists, marbles, chlorite schists, amphibolites, quartzites and orthogenesis of Birbir Domain, hypothetically dated upper Proterozoic).

Both the definition of the aforementioned geological units and their description are found in good quality, according to the Geological Map at a 1:250,000 scale, Gore sheet (EIGS, 1987), and the Final Report of the Gore- Gambela Geo traverse (Ayalew Tadesse & Moore, 1989), respectively.

Fig. 4.1 shows the regional geological map of the study area (after Mengesha Tefera et.al 1987, Ethiopian Institute of Geological Survey).

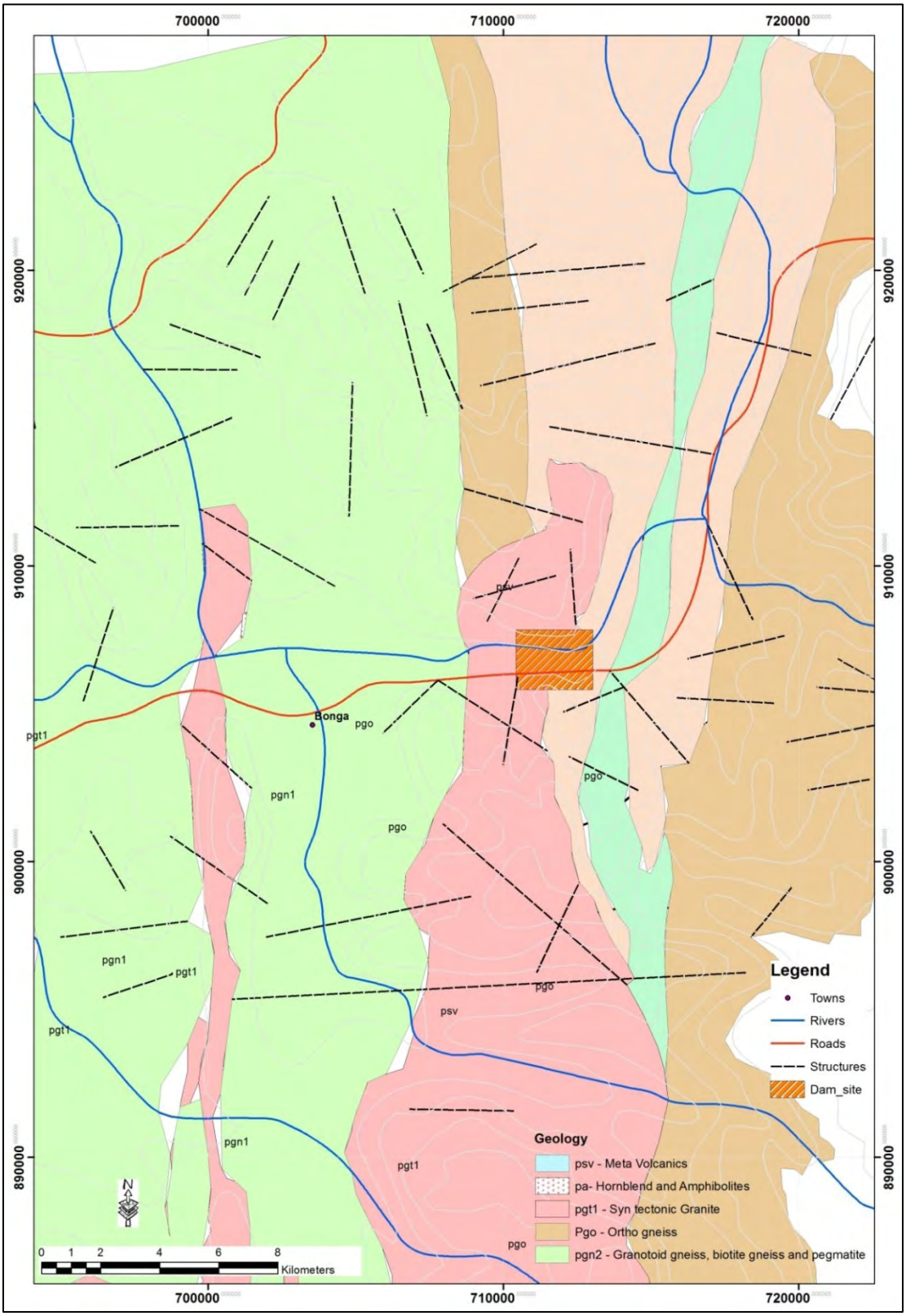

Fig. 4.1 Regional Geologic Map of the study area (after Mengesha Tefera et.al 1987, Ethiopian Institute of Geological Survey)

The uncertainty in the definition of radiometric ages of the most ancient rocks (presence or not of true Archean rocks) is due to the late Proterozoic-early Cambrian tectono-thermal event which partly reworked the oldest crystalline basement rocks. The recorded events mostly span an around 1000 to 550 Ma geological time although like, the traditionally postulated superposition by unconformity of the (supra-crustal) Precambrian low grade metamorphic rocks onto an older gneissic basement should still be confirmed. In any case, some U-Pb radiometric ages measured on zircons crossed the Paleo-Proterozoic-Archean limit at 2500 Ma, thus suggesting the presence of a very ancient, reworked continental crust (Ayalew Tadesse & Moore, 1989).

The following description synthesizes the lithological characteristics of;

(i) Baro Domain,
(ii) Birbir Domain,
(iii) Variously deformed intrusive rocks.

A. The gneiss and migmatites group belonging to **Baro Domain** includes several type of gneiss like (Mengesha Tefera et.al. 1987):

- **Biotite** and **hornblende-biotite gneisses** (layered medium-grained quartz-feldspars gneisses with abundant mafic minerals, mostly derived from tonalite to granodioriteprotoliths, subordinate garnet-bearing paragneisses, with some minor quartzite and amphibolite layers, several sub-concordant lenses and some discordant veins and ponds of granite and pegmatite);
- **Garnet-amphibole gneisses** (intercalated layers of coarse-grained, mafic gneisses);
- **Garnet-sillimanite paragneisses** (interlayered aluminous and calc-silicate gneisses with subordinate impure quartzite, as a possible meta-chert);
- **Calc-silicate gneisses** (fineto medium-grained, weakly foliated gneisses with hornblende and biotite associated with calcium-silicates like garnet, epidote, diopside);
- **Muscovite-bearing gneisses and schists** (a thin layer in the eastern boundary zone of Baro domain, probably as a retrograde metamorphic equivalent of 1b).

B. The volcano-sedimentary protolith and intrusive / extrusive rocks of **Birbir Domain** has been synthesized as metamorphosed sedimentary, volcanic and hypabyssal rocks. These group are:

- **Meta-sedimentary schists** (meta-greywacke and meta-pelite with various degree of foliation, generally very schistose, with subordinate inter-layered coarse volcano-clastic and carbonate rocks, somewhere showing some preserved primary structures like sedimentary bedding and lamination);
- **Hornblende and biotite schists** (mafic schists probably deriving from hypabyssal and volcanic protoliths);
- **Muscovite-quartz schists** and **conglomerates** (fine- to medium-grained biotite-muscovite quartz schists, somewhere with garnet and staurolite, somewhere with chlorite; subordinate layers of quartzite; rare lenses of quartz pebbles conglomerate);

- **Marbles** (small lenses of calcite-bearing, pure marbles, and impure marbles with calcium-silicates). As previously mentioned, these rocks are found in some parts of the Baro catchment area far from the dam, but not in the dam site nor in the reservoir area.

C. The Precambrian metamorphic rocks are intruded by a set of **younger magmatic rocks**, widely ranging in both ages (pre- syn- and late- to post-kinematic as previously mentioned, referred to tectono-metamorphic and tectono-thermal episodes) and chemical and mineralogical composition (with progressively increasing SiO2: gabbro, diorite, tonalite, granite, leucogranite). As for the geological age and petrology, local-scale information is provided by Ayalew Tadesse and Moore (1989), regarding the area where the TAMS project is located in.

The magmatic rock type which crops out in the TAMS option dam site, close to a major fluvial bend of Baro, some 5 km downstream the Upper Baro-Birbir confluence, belongs to a group of discordant granite stocks emplaced along the tectonic boundary between Baro and Birbir Domains. This granite body is mapped in Geological Map, Gore sheet, as N-S elongated mass, crossing the Baro River and well exposed on both sides of the valley. The granite is mildly deformed, showing a metamorphic foliation which is generally easy to identify in the field, however results somewhere less evident. It is massive, medium-grained, containing elongated minerals like hornblende amphibole. Its western boundary with the gneisses of Baro Domain is discordant and shows a complex magmatic contact zone with xenolites, whereas the eastern boundary is a much more deformed zone with evidence of shear and mylonitic bands, both in the intrusive and in the host rocks. The collected samples (with record of the original orientation) are intended to be analyzed by means of thin sections

microscope study too, in order to better define the deformation style and thus the expected mechanical characteristics (MoWIE, 2014).

As a final remark about the bedrock, it is worth to observe that, due to its location, the TAMS Dam site lies west, and downstream, of the other hydropower projects along Upper Baro River. This means the lack of Tertiary to Quaternary volcanic rocks (lava flows, mostly basalts, and subordinate pyroclastic deposits) covering the crystalline rocks of the West Ethiopian Shield. These metamorphic and intrusive rocks, having better mechanical characteristics than the volcanic multilayer as a whole crop out in both the dam site and in the reservoir area and subsequently offer more favorable geological conditions for designing and building a dam and its appurtenant structures, compared with the upstream projects (MoWIE, 2014).

As for the Quaternary deposits, it has to be noted the minimal amount of loose materials covering either the slopes or the riverbed. The latter is prevailingly cut in the bedrock, with a very scarce and discontinuous presence of thin alluvial deposits, without a good grain-size selection and mostly made of coarse sand. The only deposit with a significant component of fine-grained material (clay-bearing loam), is found east of TAMS option dam site some 5.4 km along the paved road. The slopes underwent a long-term, high energy geomorphic process of denudation and residual soils are substantially lacking. At few places, where the topographic surface offers relatively adequate depressions, show thin layers of colluvial deposits. Slope deposits (gravitative) are found at the base of right side or just below the steepest cliffs (again, in the right side) and consist of block deposits due to toppling.

4.1.3 Regional Structures

Western Ethiopia including TAMS Project location belongs to a special area of African continent whose complex geological history is directly or indirectly due to a concatenation of several interacting tectonic episodes, which can be schematically grouped in the following 'steps':(EIGS, 1987).

(i) The mountain-building processes and continental accretion (due to the mostly late Proterozoic East African Orogeny or EAO, formerly called 'Pan-African') giving rise to the roughly N-S trended thrust-and-fold belt;

(ii) The post-tectonic long-term erosion in a relatively stable continental environment (giving rise to a typical peneplain at the beginning of Phanerozoic);

(iii) The first (late Paleozoic to Cretaceous) rejuvenation of inherited structures during the multi-stage break-up of the Gondwana continental mass formed after 'step' 1, and the related tectonics, mostly extensional and subordinately dominated by horizontal shear. Intra-continental rift basins (like the Melut basin) formed as the result of extensional to trans-tensional stresses: the latest phases produced the first important changes in the preexistent physiography, both continental and oceanic;

(iv) The Cenozoic beginning of vertical deformations, due to asthenospheric upwelling (modeled in 'Mantle Plumes' theory), and the subsequent continental-scale rifting. The combination of the two produced both the Main Ethiopian Rift (MER) and the Ethiopian Plateau, as well as the related volcanism and seismicity;

(v) The Quaternary to present-date active tectonics as a prosecution of main former processes but with a counter-clockwise rotation of the regional stress-field and related deformations. Approximately E-W lineament formed as a surficial result of deep structures and allowed the westward presence of both seismicity and volcanism far from its 'natural' source, which is the MER.

These 'steps' are more or less important for the geological setting and actual conditions of TAMS Project area. 'Steps' 1 and 2 controlled the formation of rock types as the Project site bedrock and determined its outcrop conditions and overall structural geometry. 'Step' 3 gave rise to some regional NW-SE trended structures which may indirectly influence the local tectonics and geomorphology. 'Step' 4 is very important regarding the geo-morphological evolution of the natural drainage network. 'Step' 5 and related E-W tensile to trans-tensional faulting is able to form important brittle lineaments, like the Ambo / Yerer-TulluWellelVolcano-Tectonic Lineament (whose possibly related deformation seems to interest the roughly E-W trended part of upper Birbir course). Anyway, 'steps' 3 to 5 mostly regard the highest elevations of Ethiopian Plateau, east of the TAMS Project area (which in turn is indirectly affected as a distal effect (MoWIE, 2014).

4.2 Local Geology and Structures

4.2.1 Local Geology

The main rock types which form the local geology of the project area are: Mildly deformed to non-deformed granite, Foliated granitoids (mostly tonalite); Gneisses (both ortho- and para-

gneisses); Schists (various kinds of meta-sedimentary and meta-volcanic schists); Amphibolites, and Quaternary Deposits (MoWIE, 2014).

4.2.1.1 Mildly deformed to non-deformed granite

This rock type belongs to the group of younger magmatic rocks intruded in Precambrian metamorphic rocks (MoWIE, 2014). In the area, this discordant granite stock is emplaced along the tectonic boundary between Baro and Birbir Domains. It is mapped in Geological Map (Fig.4.1), Gore sheet, as N-S elongated mass, crossing the Baro River and well exposed on both sides of the valley. The granite is mildly deformed, showing a metamorphic foliation which is generally easy to identify in the field, however results somewhere less evident. It is massive, medium-grained, containing elongated minerals like hornblende amphibole. Its western boundary with the gneisses of Baro Domain is discordant and shows a complex magmatic contact zone with xenolites, whereas the eastern boundary is a much more deformed zone with evidence of shear and mylonitic bands, both in the intrusive and in the host rocks (MoWIE, 2014).

The intrusive rocks is found exposed at the right side of Baro valley in the TAMS dam site, forming a very massive relieve, culminating in the 1383.1 m summit of Agag Mountain. It is generally fresh (non-weathered sound rock), hard, massive, fine- to medium-grained, rarely coarse-grained, holo-crystalline, with great compactness, almost homogeneous in fabric, and hence practically isotropic. Its mineralogical composition usually groups feldspars (both potassic and plagioclases) and quartz, accompanied with a minor amount of mafics (biotite mica and amphiboles), which have a different resistance to chemical weathering in tropical climate, ranging from very high (chemically stable quartz) to average (feldspars, prone to be transformed in clay minerals) to low (mafics, that is iron-rich minerals, easily oxidized). Jointing in depth is not very intense (MoWIE, 2014), since the observed fractures are dueto tectonics and generally persistent in the surficial layers only.

4.2.1.2 Foliated granitoids

This kind of syn-tectonic magmatic rock is intruded in the Precambrian rocks. It is strongly to average foliated intrusive rock type cropping out in the left side of Baro valley, at the dam site. It locally underwent strong deformation, which can produce narrow weak zones. In its fresh and undeformed states its mechanical characteristics is very similar to the ones of the non-deformed granites. At places, it is cut by a network of discordant quartz veins and pegmatites (MoWIE, 2014).

4.2.1.3 Gneisses (both ortho- and para-gneisses)

Many rocks which belong to both previously described Baro and Birbir Domains are characterized by a medium degree of deformation, giving rise to the typical gneissic texture (a coarsely foliated texture with a rough separation of differently shaped metamorphic minerals in alternate layers around 0.5 to 2 mm thick, due to a penetrative but not too dense schistosity, which produces slightly irregular, undulated surfaces as cleavage plains) can be grouped here, because of their rather similar mechanical characteristics. These rocks may include intercalated (generally concordant) layers of quartzite, whose characteristics can be compared to the ones of host rock, due to their minor thickness.

4.2.1.4 Schists (various kinds of meta-sedimentary and meta-volcanic schists)

This group is characterized by a very dense set of platy, parallel, regular planes of schistosity as a result of a very strong, pervasive deformation, as well as an important amount of less hard phyllo-silicates as a mineral component of the rock. In the dam site, these rocks are found to the east of meta-tonalite band and, in a minor 'inclusion' set due to folding, within the meta-tonalite body some 500 m downstream the dam site (MoWIE, 2014). These rocks belong to Birbir Domain.

The strong deformation produced a very close set of discontinuities and fractures which, where steeply dipping to sub-vertical and relatively opened in the surficial layer of the bedrock, allow a strong chemical weathering (mainly evident as oxidization). This weathering can involve a thickness up to 4-5 m from the topographical surface toward the depth, as easy to observe in several outcroppings.

4.2.1.5 Amphibolites

As minor rock bodies, strongly deformed, elongated and somewhere boudinated, some amphibolites are observed in association with the previously described 'schists'. Where the thickness exceeds some few meters, this kind of rock is very hard, massive (MoWIE 2014), however these good conditions seldom occur because of the complex interlayering of relatively thin, different metamorphic rock types giving rise to a bulk mass which has to be considered weak as a whole.

True amphibolites are mafic metavolcanic rocks which underwent medium-grade metamorphism up to the amphibolite facies (temperatures higher than 500 °C and pressures less than 1.2 Gpa.

4.2.1.6 Quaternary deposits

No place covered with a relevant layer of quaternary deposits, exceeding some 4-7 m as in BH-07 and BH-04 was observed at the dam site. The steepest parts of the right side (where the bedrock is in overall outcropping conditions) show some Talus and colluvial deposits made of toppled blocks, under the rocky cliffs. In any case, these thin deposits are laterally discontinuous.

4.2.2 Local Structures

According to MoWIE (2014), the westernmost part of the Ethiopian Plateau is carved by both Birbir and Upper Baro rivers, and in particular in the Birbir catchment area just below an approximate elevation of 1500 m, a dense set of roughly E-W lineament, very 'fresh' from a morphological point of view, is clearly identified in the satellite imageries.

Satellite images of the study area shows the local structures E-W trended physiographic / tectonic lineaments of the westernmost part of the Ethiopian Plateau. More detailed visualization of the area, allowing identifying the evident morphological lineament along the E-W trended segment of Birbir River, east of Dembidolo, and other minor, similarly trended lineaments.

4.3 Geology of the Dam site and Structures

4.3.1 Geology of the Dam site

Rock exposures in the study area are generally around the Bonga village, belonging to the Baro domain; representing pre/syn tectonic granite and granitic gneiss. The Baro domain comprises pre/syn-tectonic granites, grano-diorites, diorite and monzodiorite (Ayalew Tadesse and Moore, 1989).

4.3.1.1 Granite

Nearly circular granites are found on the left and right parts of the study area, which represents the earliest /syn-tectonic granite plutonism. This unit makes a circular chain of granite hills rising over 790 m a.s.l. and makes Baro River course a clockwise turn. The granite is characterized by creamy, coarse grained, strong and dense.

Plate 4.1 shows an exposure of granite on the left side of the study area. The granite is found in boulder size.

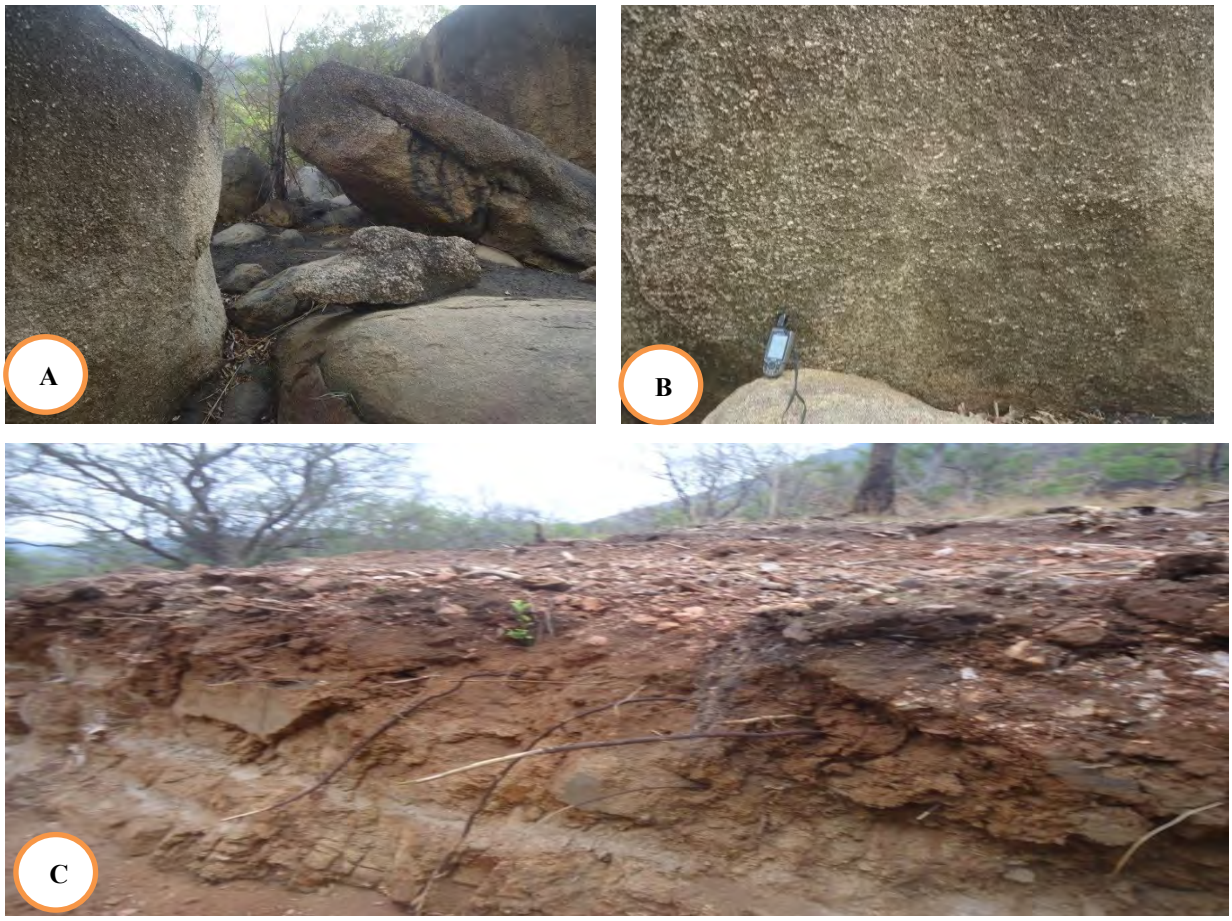

Plate 4.1 Photo showing Granite exposure on the left side of the study area (A&B), Residual soil found at the right bank (C)

4.3.1.2 Pegmatite Intrusion

A pocket of pegmatite intrusion is found on the left side of the study area up stream of the dam axis. The deposit found to be highly weathered, weak and jointed state.

4.3.1.3 Residual/ Colluvial Deposit

Residual soils and Colluvial soil units are found near the Baro River. All of them are located on top of decomposed bedrocks and/or reworked materials one on top of the other with variable thicknesses. Top soils are found at the top associated with different sizes of grass and bush roots. Its thickness varies from 20cm to 60cm. The grain sizes of the soil are ranging from clay size to sandy silt sizes with different plasticity characteristics and appearance colors.

4.3.2 Structure of the Dam site

The dam site area of Baro River is in a prevailing erosion regime; hence its riverbed is mostly cut in the bedrock with a minor degree of alluvial deposits coverage. The bedrock is deeply

carved and polished by a high-energy water flow, which washed away the weakest rocks (formed after both chemical alteration and tectonic processes). In this area, the RMR data as well as the discontinuity data point were located. In these stations, meta-granites predominate as the outcropping rock type.

Plate 4.2 shows a rather solid and compact rock, whose mechanical discontinuities are arranged in three families, forming cubic blocks. The rock-mass conditions in this place are hence considered as good.

Plate 4.2 Structural discontinuity at the Baro River, downstream of the dam axis

In Station , the family of joints 090°-110° / 80 is prevalent, the background of discontinuities is dominated by the lineament 02°/70° crossing at low-angle the previous system; another family of joints has planes oriented at 320°-330°/25°. Fig 4.4 shows the statistical analysis of the recorded discontinuities.

Compared with the natural outcrops along the Baro's riverbed, those on the Gore-Gambela road show a very fractured rock. Such a difference can be partly due to the nature of the outcrop, since the road cut displays disturbed conditions due to both weathering and blasting.

The Station RMR 8 is about 350 m upstream of the dam axis. The exposed outcrop length is 30 m. As shown in Plate 6.2., the rock underwent intense tectonic processes which produced faulting, folding, and gave rise to narrow belt with mylonitic textures.

The statistical analysis allows identifying several sets of diaclases, in addition to the wavy schistosity planes. By summarizing, the rock-mass is typical of a strongly deformed zone.

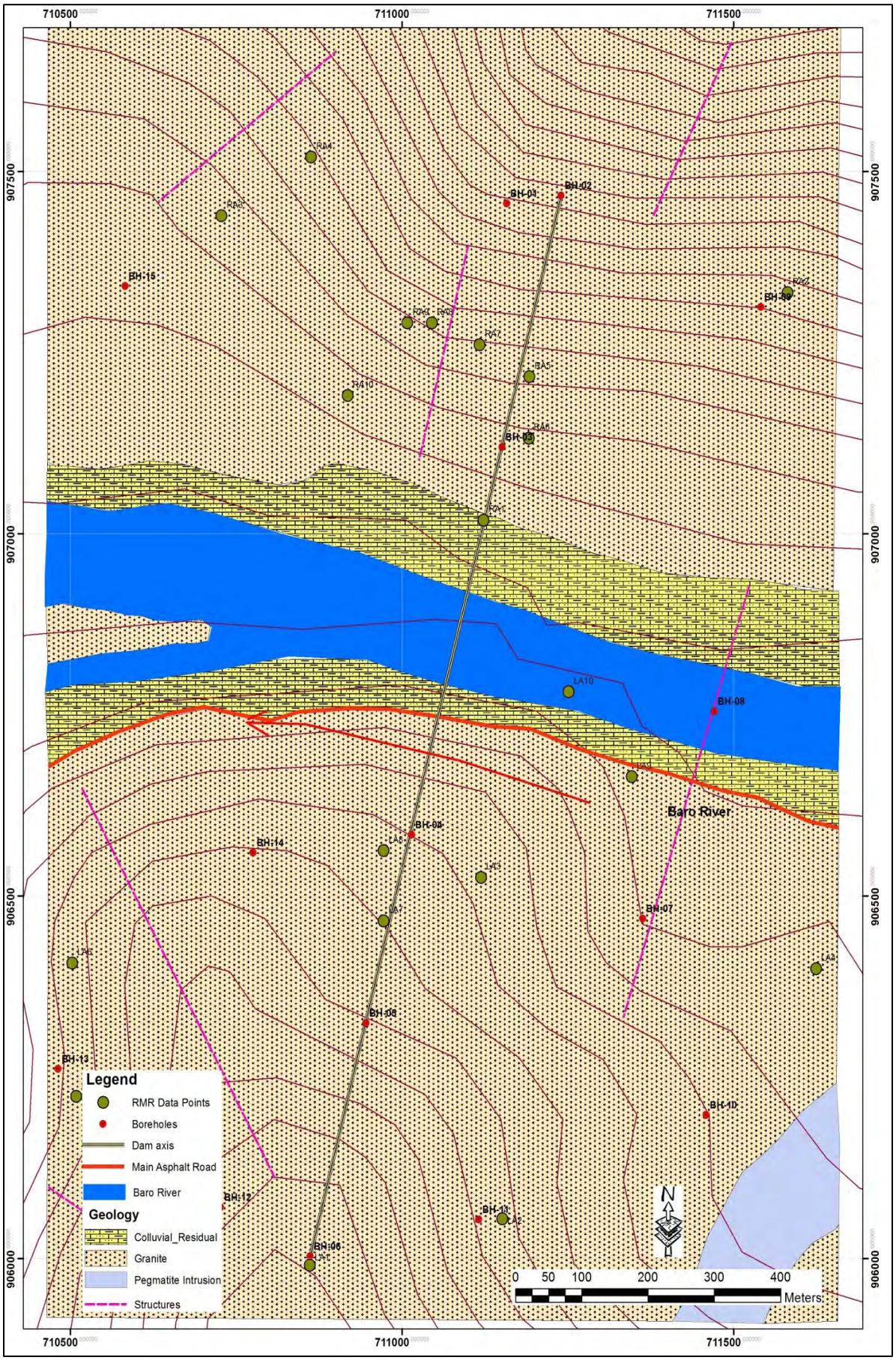

Fig. 4.2 Geological Map of the Study area (produced by the author)

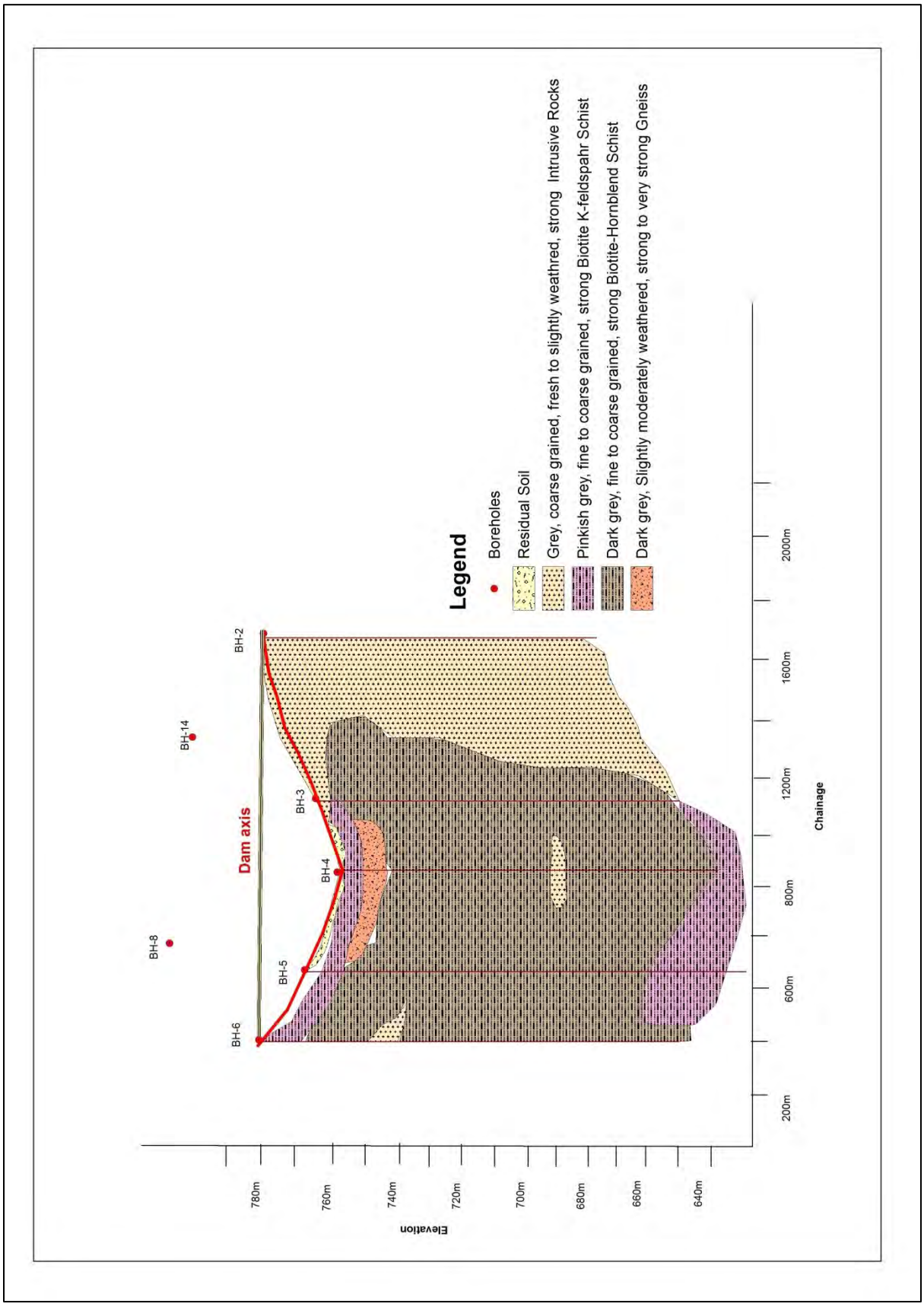

Fig. 4.3 Geological cross section at the Dam axis

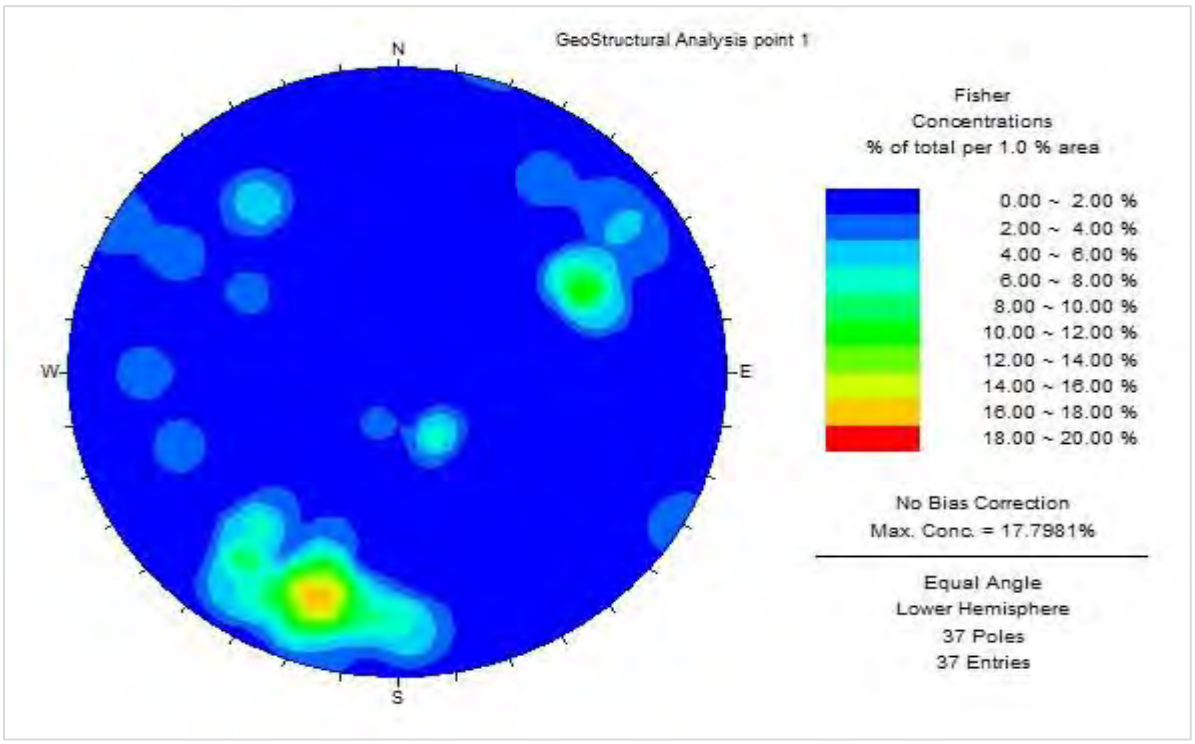

Fig. 4.4 Stereo plot for the structural discontinuity data near the dam site

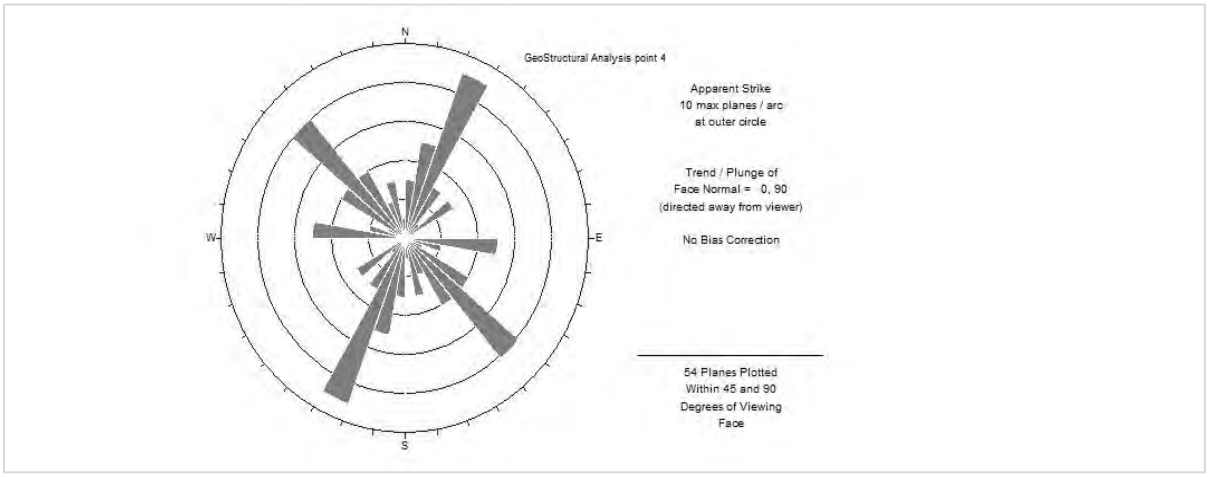

Fig. 4.5 Rose diagram showing the structural discontinuity along Gambella main road

4.4 Seismicity

Recent and active deformations (Pliocene to Quaternary) with the counter-clockwise rotation of the regional stress field, caused the change in opening of the MER from orthogonal (roughly NWSE trended tensile stress) to oblique (almost E-W trended stress). Such a rotation is an efficient geodynamic 'engine' for triggering tensile and trans-tensional deformations, which can be expected to mostly follow the roughly E-W structural trend (Gouin, 1979).

The NW-SE and NNW-SSE extensional structures (grabens, semi-grabens, rifts, often with a horizontal shear component generating trans-tensive faulting) overprinted the formerly described, inherited N - S to NNE - SSW tectono-metamorphic regional structures and lithological anisotropies. Such structures are due to 'step' 3 but may locally interfere with the youngest almost E-W structures. In particular, TAMS site is located close to the eastern border fault zone of Melut Rift. The deformation referred to this 'step' is the source of the seismicity affecting Ethiopia and the surrounding regions. Due to the importance of this topic, some more detailed information with regard is provided in the following pages (Gouin, 1979).

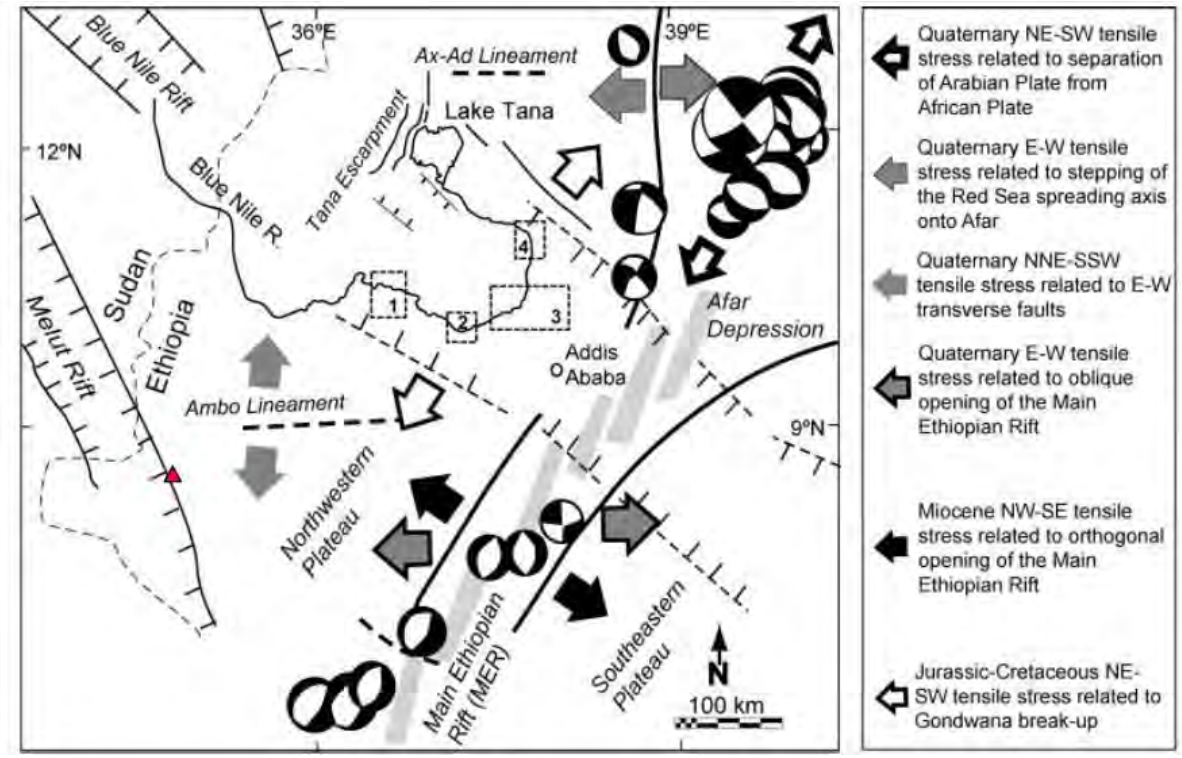

Fig.4.6 Sketch-map showing the relationships between the main tectonic structures, the stress regime and the seismicity, in the Ethiopian and eastern Sudan region (Gouin, 1979)

The Organization of African Geological Surveys - OAGS is carrying out since January 2011 the"*Seism tectonic Map of Africa*" (SeTMA) International Project, which should provide a reference map at a 1:10,000,000 scale. Figure 4.5 shows the 2013 update of seismicity: as a general remark, seismicity of the androgenic East Africa produced earthquakes up to >7 magnitude south of Turkana Depression; the northernmost high-energy epicenter corresponds to Juba (Sudan) earthquake of May 20th, 1990 (M = 7.1 - 7.4: ALHASSAN *et al*., 2007), which is roughly located at the northern end of EARS western ('Albertine') branch (Midzi, et al, 1999).

The westernmost zone of Ethiopia, including TAMS site, and the easternmost N-S stripe of South Sudan and Sudan territory , in the right side of Nile valley, lie within an oval-shaped, N-S elongated zone of relative low-seismicity. This zone is bordered by: (1) an eastern alignment which follows the Main Ethiopian Rift - MER; (2) the area of Juba and an approximately E-W to WNW-ESE elongated cluster; (3) an uneven and low-density, irregular, almost N-S, western alignment running parallel to, and not far from the White Nile riverbed up to Khartoum. Unlike the typical inter-plate seismicity along divergent margins, which certainly corresponds to the rift region in Ethiopia highlands (including Gibe III), the low seismicity within the mentioned crustal block along the Sudan-Ethiopia border seems to be intra-plate type (Gouin, 1979). Fig 4.7 shows seismic hazard map of Ethiopia, accordingly the project site fall on the seismic zone 0, where there is no damage.

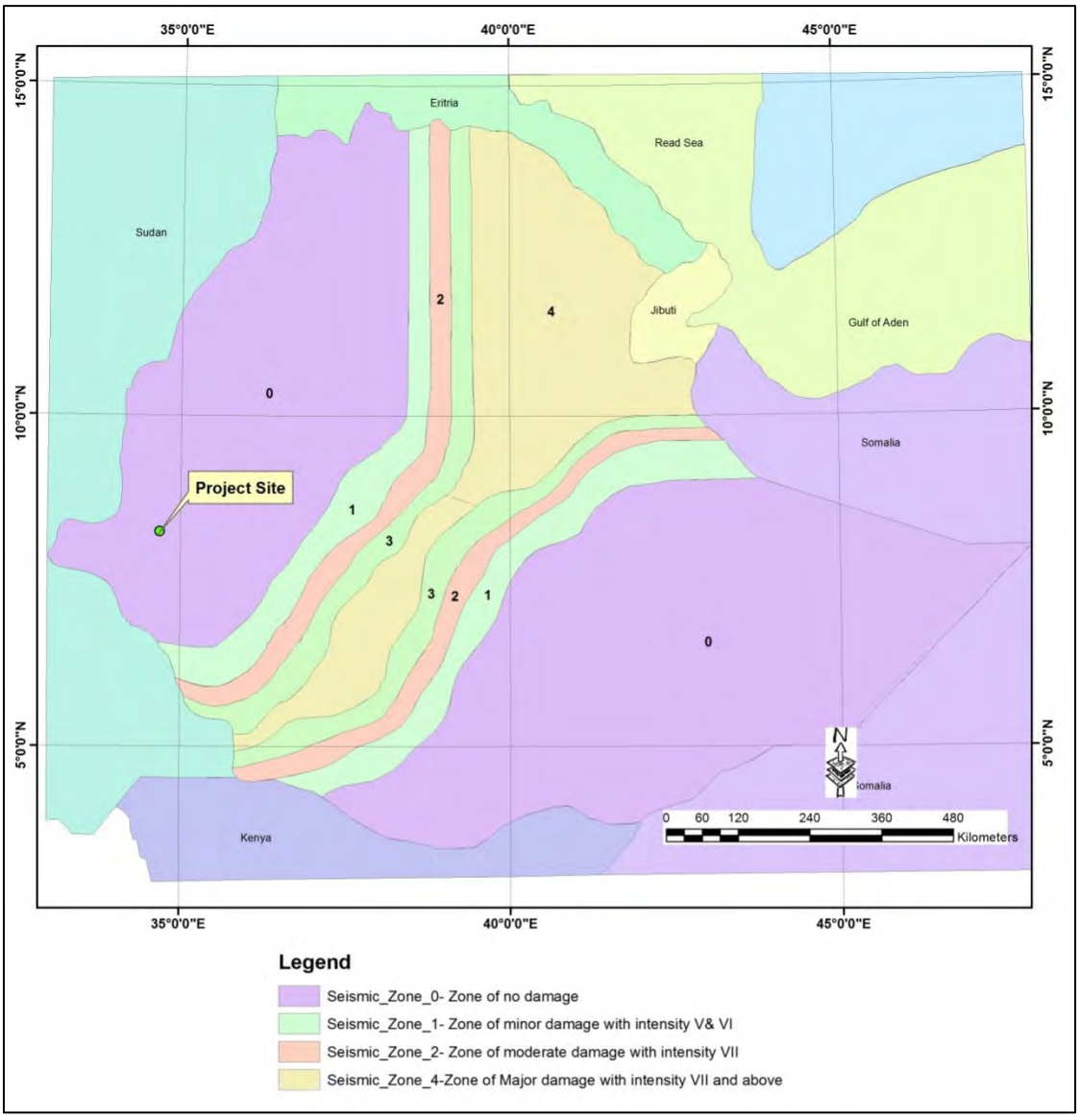

Fig.4.7 Seismic Map of the Project Site. (after L.Asfaw, 1986)

Fig.4.8 shows Seismic hazard map, showing PGA values, expected at 10% probability of exceedance in 50 years. PGA is by classes of values, indicated by colors from green to red, the dam site is pointed as red.

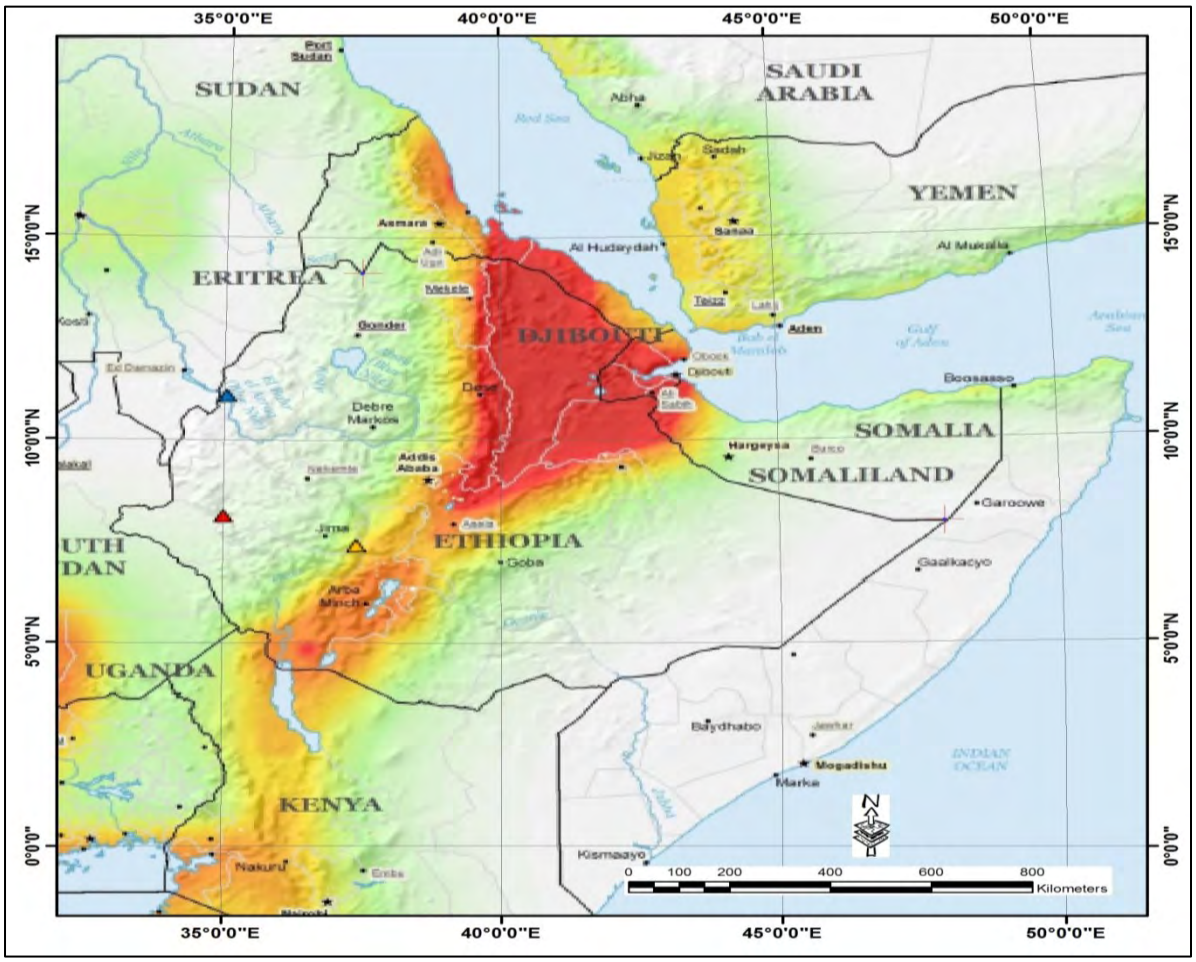

(Source: http://www.seimo.ethz.ch/static/GSHAP/)

Fig.4.8 Seismic hazard map, showing PGA values, expected at 10% probability of exceedance in 50 years. PGA is by classes of values, indicated by colors from green to red.

4.5 Hydrogeology

The geology in both the dam site and the reservoir area shows a regional- to local-scale fabric made of N-S trended litho-tectonic units, with prevailing N-S trended metamorphic foliation, as an inherited overall structure. This structure is transversally cut by the westward-flowing Baro River, whose riverbed is often modeled along EW and WNW-ESE brittle lineaments and true faults. The silicate-bearing metamorphic rocks which crop out in the interest area have a very low primary permeability. This permeability is due to different kinds of porosity. As a general remark, mildly deformed, fine-grained and homogeneous meta-intrusive rocks (i.e. syn-tectonic meta-granite) have a very low primary permeability, whereas their inclusions (especially the discordant ones) like quartz veins, pegmatite veins and ponds have

a higher hydraulic conductivity. A feature which obviously lowers the impervious behavior of meta-granitoids and ortho-gneisses is the occurrence of post-metamorphic tensile and shear stresses driven micro-fracturing along axial planes cleavages, especially in syn-form structures, and dense foliation along shear zones and litho-tectonic boundaries (MoWIE, 2014).

The primary porosity (ratio: void-space volume / bulk volume of the rock material, generally expressed in per cent values) of crystalline rocks like intrusives and silicate-bearing metamorphic typically ranges between 1% and 1.17% (MoWIE, 2014).

The determining of in-situ porosity within crystalline rocks, in order to assess its retention properties, can be estimated by subtracting the porosity due to micro-cracks from the total porosity determined in laboratory. Hydrostatic compression tests on granite specimens are usually performed with loading up to 50MPa and 100MPa. For comparison, similar tests performed in the Precambrian crystalline basement granites of Baltic Shield (Fennoscandia, Northern Europe), indicated that major closure of micro-cracks generally occur at 50MPa and that the in-situ porosity is approximately 10–15% less than the total porosity, as measured in the laboratory (MoWIE, 2014).

In any case, the rock types which crop out in the interest area should be considered substantially impervious as a whole, due to a very low primary porosity. A very important feature is the lack of carbonate rocks (like marble and calc-silicate rocks within the Birbir Domain meta-sedimentary assemblage) in masses of any significant volume.

The permeability of these normally impervious crystalline rocks depends on the combination of primary porosity and secondary permeability (fracturing), which can be found in presence of dense fracture sets, or fault zones. In this geological context, permeability is a typically anisotropic property, since lower if measured normal to the metamorphic foliation (MoWIE, 2014). The overall NS trend is a favorable geological feature for the hydrogeological characteristics, since it should minimize the possible seepage toward downstream in the dam footprint.

The fracture porosity (secondary permeability) due to brittle deformation affecting the rock mass in the project site will be carefully assessed by means of remote sensing techniques in the further steps of TAMS project development (MoWIE, 2014).

*****

Chapter V METHODOLOGY AND DATA COLLECTION

5.1 Permeable

For the present study, systematic data was collected from the field as well as laboratory testing on representative samples was carried out. In general, data used in the present study can be categorized as primary and secondary. Primary data included data obtained from core logging, field mapping, rock mass rating (RMR) data as well as laboratory studies. These data sources were used for the characterization of the rock mass. The synthesis of this data finally, resulted into rock mass characterization for the study areas. Fig.5.1 show a general methodology followed in the present study.

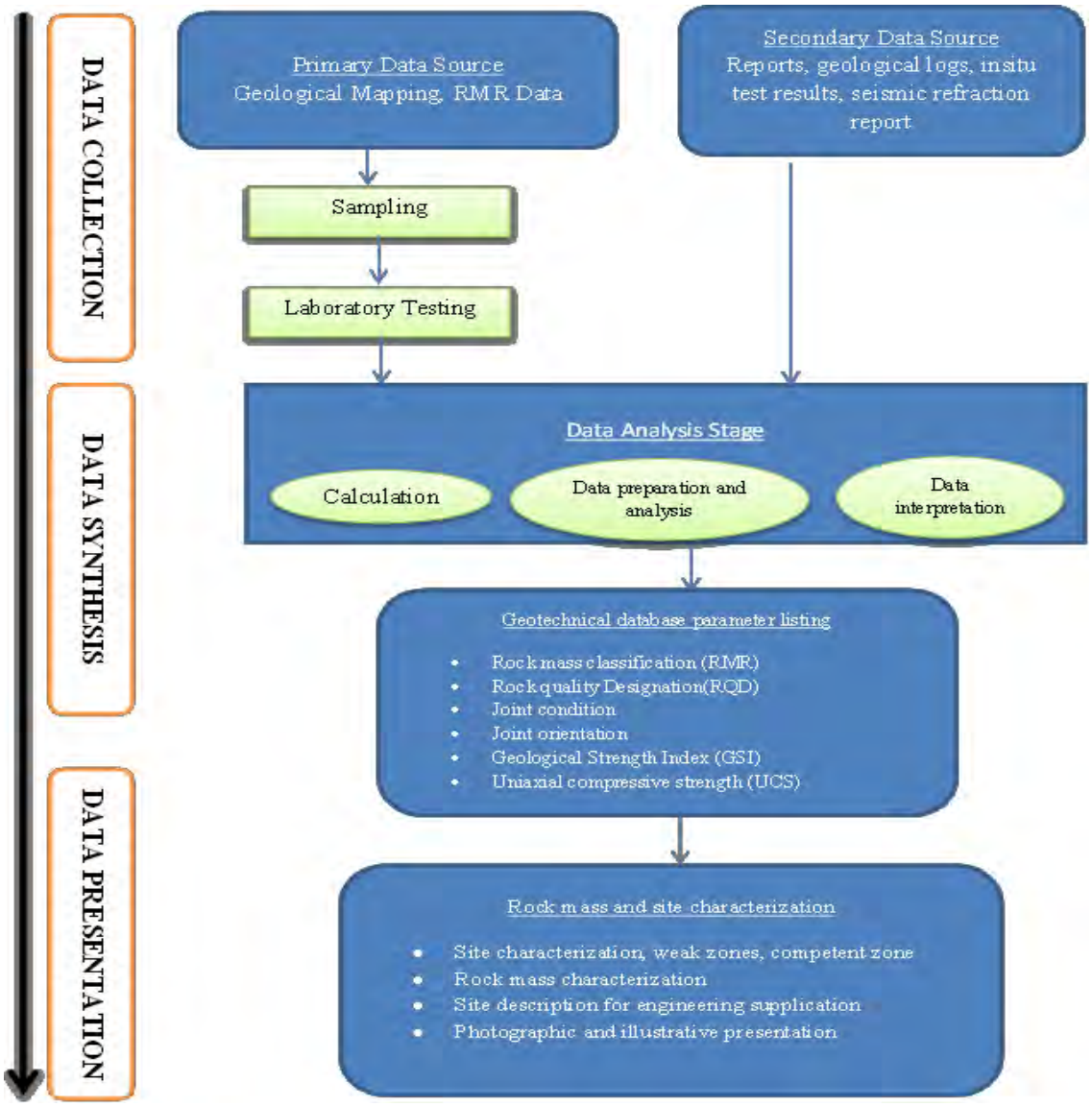

Fig. 5.1 Flow chart for methodology and data collection.

5.2 Primary Data Collection

5.2.1 Geological and Structural Data collection at the Dam Site

The Geological and Engineering geological mapping of the dam site is designed to acquire detailed and wide ranging geo-information at a scale of 1:10,000, which includes comprehensive overview of the geomorphologic, lithological, degree of weathering and structural setting of the study area.

In order to achieve the objectives of this study the methods followed include:

- Review of existing data and compilation of base geological map based on acquired previous maps and digital images in the office. These data were used as a working base map together with the topographic maps.
- Field investigation and data collection. The field investigation and data collection included detailed section logging, description of lithological units, sketching or photographing of important geological, structural and geomorphological features. These features are included as illustration where found necessary.
- Analysis and integration of all acquired data (geomorphology, lithology and structure) in terms of engineering geological aspects.
- Preparation of component maps at the scales required for this specific research.

5.2.2 RMR Data collection at surface outcrops

To have the rock mass property at the dam site: field data collection was carried out at surface exposures. Twenty representative sites were selected based on systematic judgmental description and accessibility to the characteristics of the rock mass visual description. The location of the points is shown in Table 5.1 and Fig. 5.2. To determine the rock mass rating (RMR) the previously mentioned six parameters were used. The discontinuity data like dip, dip direction, strike and slope direction was measured in the field at selected outcrops. Rock quality is determined by using Palmstorm (1982) relation (eq.5.1).

$$RQD = 115 - 3.3 J_v \quad \text{....eq.5.1,}$$

Where J_v is the discontinuities count, more than 10cm long, in 1mx1m exposed rock surface.

Spacing is determined by simple measurement through measuring tape. Visualization, condition of discontinuities, ground water condition and orientation of discontinuities were determined by characteristics of the geological condition (Plate 5.1).

Plate 5.1 Field Insitu Strength testing and data collection

Table 5.1 Field RMR Data collection Points

RMR ID	Easting	Northing	Elevation	Lithology	Remark
RA1	711123.00	907019.00	504.00	Granite	Right Abutment
RA2	711581.00	907333.00	645.00	"	
RA3	710728.00	907439.00	586.00	"	
RA4	710863.00	907520.00	619.00	"	
RA5	711192.00	907217.00	586.00	"	
RA6	711191.00	907132.00	529.00	"	
RA7	711117.00	907261.00	602.00	"	
RA8	711045.00	907291.00	625.00	"	
RA9	711008.00	907291.00	604.00	"	
RA10	710918.00	907191.00	530.00	"	
LA1	710861.00	905991.00	761.00	Granite	Left Abutment
LA2	711151.00	906055.00	642.00	"	
LA3	711119.00	906526.00	596.00	"	
LA4	711624.00	906400.00	532.00	"	
LA5	710509.00	906224.00	547.00	"	
LA6	710503.00	906408.00	616.00	"	
LA7	710972.00	906466.00	661.00	"	
LA8	710972.00	906563.00	619.00	"	
LA9	711346.00	906665.00	508.00	"	
LA10	711251.00	906782.00	509.00	"	

The uniaxial compressive strength (UCS) has been determined by Schmidt Hammer and the Barton and Choubey, 1977, relation has been used to work out UCS from the Schmidt rebound number by using eq. 5.2

$$Log_{10}(\sigma_c) = 0.00088\gamma R + 1.01 \quad ...eq.5.2$$

Where; 'σc', uniaxial compressive strength in MPa, 'γ' is the Dry rock density in KN/m^{3}and'R' is the Schmidt rebound number.

5.2.3 RMR data collection from drilled boreholes

5.2.3.1 Descriptive rock Core Logging

The geological description on logging addressed the rock type identification, color and textural description, the degree of weathering, rock strength class, intensity of rock fracturing, and the type and extent of secondary infilling minerals. The weathering grade classification was made in accordance to ISRM (1981) strength classification. The RQD data were collected following the standard practice as proposed by Deer (1964) and expressed as,

$$RQD\ (\%) = \frac{\sum Full\ diameter\ drill\ Core\ samples\ with\ length \geq 10cm}{core\ run\ length} \ldots\ldots eq.\ 5.3$$

In all the drilling operation of current investigation, the core samples were obtained with double tube core barrel and proper precautions in place to avoid or minimize core sample disturbance. To measure the length of the core, piece of core were measured along the centerline from tip to tip, or along the fully circular barrel section. Core breaks caused by the drilling process were evidenced by rough fresh surfaces thus fitted together and considered as one piece for RQD data collection.

5.2.3.2 Discontinuity Description

5.2.3.2.1 Joint separation

Joint separation is related to the aperture that is measured across the joint. Separation has an effect on the stiffness of the joint (ISRM, 1981). This is more so if the joint has soft infill such as clayey material which may have a lubrication effect when shear forces are experienced in the joint (ISRM, 1981). Joint separations were measured for each observation points. Average values were considered for the RMR determination.

5.2.3.2.2 Joint roughness

Joint roughness can be classified as primary (first order) or secondary (second order) ISRM, 1981), and describe the large and small scale roughness respectively. During the preset study joint roughness was determined by touch and feel and accordingly observations were made for RMR.

5.2.3.2.3 Joint weathering

When joint walls are highly weathered, the strength that this joint can achieve is limited to the bearing capacities of the asperities during shearing (ISRM, 1981). During the present

study the joint weathering was determined by observing the joint walls upon touching them and also by looking out for any color changes due to oxidation or chemical reactions with fluids that may have passed through the discontinuity.

5.2.3.2.4 Joint sets

The joint set number is a description and differentiation of joint groupings with variable causes. They are differentiated and determined on account of dip, and dip direction and other characteristics such as roughness, spacing, etc. Joints belonging to the same group exhibit similar characteristics including closely related values for dip and dip direction (ISRM, 1981).

On un-oriented core, it can be difficult to differentiate one joint set from the other. Careful observation of the rock core, especially in a core run in which two joints belonging to different sets are found to be close to each other, can help to differentiate between the joint sets. The same observations were made for joint sets in the present study.

5.3 Secondary Data Collection

5.3.1 Boreholes Data

Boreholes drilled at the dam site were used as a secondary data source for the characterization of the rock mass. A total of eight boreholes were used to characterize the rock in the dam Foundation area. These boreholes are designated as BH-2, BH-3, BH-04, BH-05, BH-14, and BH-06 and are located along the proposed dam axis. A total of 1001.27 m of borehole depth was used to have relevant information on rock mass. Table 5.2 shows the detail summary of the drilling data, used in this research.

Table 5.2 Summary table showing the borehole drilling location and total depth

BH-ID	Location	Total Depth (m)	UTM Coordinates (Zone 36)		Elevation (m)
			Easting	Northing	
BH-02	AXIS CREST-RS	80	710840.73	907476.03	589.34
BH-03	AXIS-RA	125.5	711173.38	907198.52	565.56
BH-04	AXIS-RIVERBED	140	711087.16	906849.62	487.28
BH-05	AXIS-LA	132.55	710974.00	906427.16	615.66
BH-06	AXIS CREST-LS	145	710865.03	905989.99	776.19
BH-07	PLINTH-LS RIVERBED	102.72	711525.87	906603.03	492.57
BH-08	PLINTH-RS RIVERBED	135.5	711578.00	906873.99	494.22
BH-14	DOWNSTREAM DAM TOE	140	710722.18	906833.85	495.03
TOTAL		**1001.27 m**			

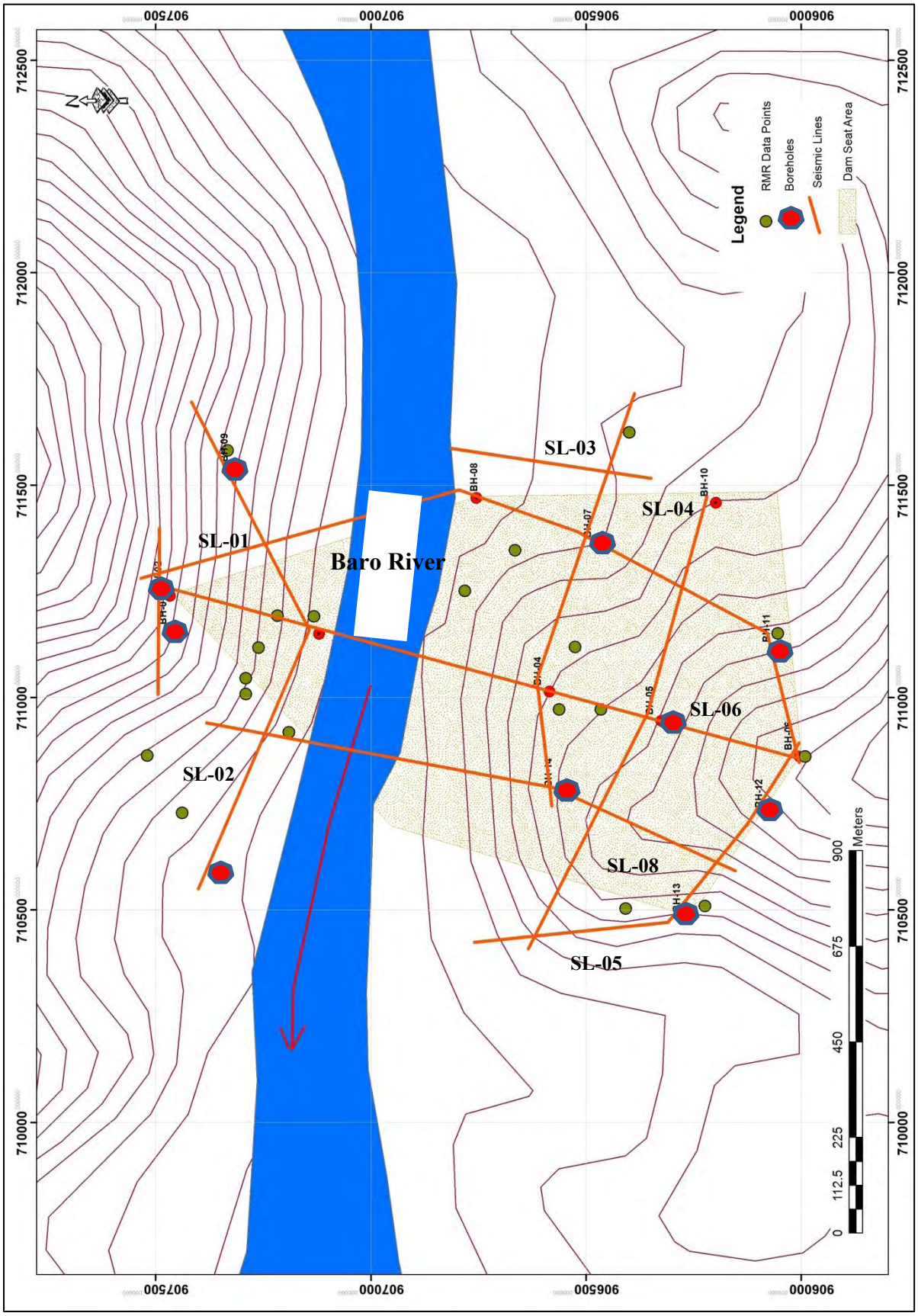

Fig 5.2 Figure Showing Primary and secondary data collection Points

5.3.2 Insitu Permeability Test Data Collection

Water pressure test data were used to characterize the permeability condition of the foundation rock. The permeability tests were conducted in each borehole in every five meters interval, where the rock is capable to inflate the gland. The method consisted of five consecutive tests or runs, each of ten or five minute duration, and with a particular corresponding pressure magnitude. The five testing pressures were applied in the order of A-B-C-B-A with increasing and decreasing sequences where, C = stands for the peak applied testing gauge pressure, B = moderate applied testing pressure and equals two-third of the peak applied pressure, and A= low applied testing pressure magnitudes and equals one-third of the testing peak gauge pressure. For this particular study from six boreholes a total of 124 permeability test data were used.

5.3.3 Seismic Refraction Data Collection

Seismic refraction data were used for the present study. The geophysical observations were made along the survey lines, which had been laid out at pre-selected sites as shown in Fig 5.2. The surveying work was mainly intended to determine: (i) the direction and layout of seismic lines and (ii) the marking and leveling of seismic shot points and geophone locations.

Accordingly, the geophysical profiles were pegged and labeled every 10 m interval all over the area. In addition, the shot points were marked at every 50 m of spacing, along the lines. A total of 16 lines were surveyed in the area which has a total length of 17,650 m. These include 11 nearly south-north extending denoted as ST-01, ST-02, ST-03, ST-04, ST-05, ST-06, ST-07, ST-08, ST-09, ST-10 & ST-11 and nearly east west spreading lines.

The refraction seismic study was carried out by Geomatrix P.L.C using Smart-Seis unit of Geometrics of U.S.A, which is 24-channel seismograph, microprocessor based with the latest hardware and software and interfaced with plotter. For the wave signals reception geophones type PE-3 (10Hz) and for energy source explosives were used. The field data were all processed in the conventional manner, by manual work in which the p-wave velocities determined from the first arrivals was used for the interpretations. The frequency filtering options of the instrument were utilized to eliminate unwanted signals or noise. The Seismograms were produced using the internal computer of Smart-Seis exploration seismograph with the following standard processing parameters:

5.4 Sampling and Laboratory analysis

A total of 14 index and engineering properties of intact rock samples were studied and tests were performed to determine: bulk unit weight and strength (Uniaxial Compression and Point load) of rock specimen. The tests were conducted at the central laboratory of Ethiopian Construction Design and Supervision Works Corporation.

Table 5.3 shows the borehole ID, location of the samples, field lithological descriptions, sampling depth and the type of parameter test conducted on the rock samples.

Table 5.3 Summary table showing sample location and tested parameters

S.N	BH ID	Location	Field Lithological Description	Sampling Depth (m)	Tested Parameters	
					UCS (Point Load)	Unit weight
1.	BH-04RS-2	Center of Dam Axis	Meta Granodiorite	10.77-11.00	✓	
2.	BH-04RS-5		Meta Granite	25.75-26.05		✓
3.	BH-04RS-6			32.40-32.60	✓	
4.	BH-04RS-9			91.68-92.10	✓	✓
5.	BH-04RS-10		Meta Volcanic	62.75-63	✓	
6.	BH-14RS-3	Downstream of Dam Axis	Meta Volcanic	34.95-35.30	✓	✓
7.	BH-14RS-4		Meta Granodiorite	39.30-39.45	✓	✓
8.	BH-14RS-7		Meta Granite	75.08-75.35	✓	✓
9.	BH-05RS-3	Center of Dam Axis	Meta Volcanic	61.15-61.75	✓	✓
10.	BH-05RS-5			99.00-99.76		✓
11.	BH-05RS-7		Meta Tonalite	130.00-130.60	✓	✓
12.	BH-06RS-3	Spillway and Dam Axis	Meta Diorite	29.40-30.00	✓	✓
13.	BH-06RS-5		Granite Pegmatite	82.85-83.40		✓
14.	BH-06RS-6		Ortho Gneiss	85.85-86.45	✓	

5.5 Rock mass characterization Methodology

5.5.1 Permeable

A complete engineering geological rock mass description contains details of the rock material and the natural discontinuities (Hoek et al, 1995). Adequate descriptors, a uniform format and standard terminology are used to properly describe rock foundation condition. In this work the descriptive scheme is adopted to systematically characterize the rock material and rock mass properties. (IAEG, 1981).

The description of the rock involves:

- Determination of the fundamental rock name (lithological rock name).
- Description of the properties of the rock material (color, texture, state of weathering and strength).
- Description of additional properties necessary to describe the features of the rock mass (discontinuities and weathering profile).

5.5.2 Foundation Characterization

5.5.2.1 Rock Mass Classification

Geomechanics Classification (Rock Mass Rating System) developed by Bieniawski (1989) was used for the classification and interpretation of the quality of the foundation rocks at the proposed dam site. The six parameters as proposed by Bieniawski (1989) were used to classify the rock mass using RMR system. Data on these parameters was collected from the field and from the laboratory test results.

The rock mass was first divided in: homogenous "geotechnical units", based on geophysical profiles, fracture density and evenness as displayed by weighted RQD. These regions are assumed to be more or less uniform in certain geotechnical features. Because the seismic values can be affected by the rock type and rock mineralogy, other than rock mass properties, calibration was made to the geotechnical parameters of the drilled cores.

5.5.2.2 Rock mass Strength and Failure Criteria Approach

Laboratory results on core samples are not representative of a rock mass of significant volume. On the other hand, in-situ strength tests of the rock mass are seldom practical or economically feasible (Hoek et al, 1995). There is major deficiency of laboratory testing of rock specimens, as the specimens are limited in size and therefore represent a very small and highly selective sample of the rock mass from which they were removed. In a typical engineering project, the samples tested in the laboratory represent only a very small fraction of one percent of the volume of the rock mass. In addition, since only those specimens which survive the collection and preparation process are tested, the results of these tests represent a highly biased sample.

For this specific research the most commonly and accepted method is used.i.e Hoek-Brown failure criterion and estimation on the required parameters was made with the help of rock mass classification. The shear strength parameters (cohesion and angle of internal friction) were determined based on the result of the rock mass rating, as proposed by Bieniawski et al. (1989). Further, Hoek Brown failure criteria (Hoek et al, 1995) were also utilized to estimate the shear strength parameters.

5.5.2.3 Deformability Assessment

According to Argawa, et.al 1991 deformation of a rock mass is the change in volume or shape of the rock mass;

- Shear displacements along discontinuities, or opening, and/or
- Closure of discontinuities.

The rock mass modulus is related to the rock substance strength, but in particular to the nature of the discontinuities, including spacing, opening, degree of infilling and orientation relative to the load direction.

A number of empirical methods were used to characterize the foundation deformability of the rock mass. A more recent correlation between in-situ modulus of deformation and the RMR Classification system was developed by Serafim and Pereira (1983) that included an earlier correlation by Bieniawski (1978), Agarwal et al (1991), Barton et al Relation (1980), Hoek and Brown (1997) and Hoek et al.(2002) relations were used for the present research study.

5.5.2.4 Foundation Permeability

Permeability is a measure of the ease in which water can flow through a soil or rock volume. It is one of the most important geotechnical parameters (Houlsby, 1976). However, it is probably the most difficult parameter to determine. It directly affects the (i) quantity of water that will flow toward an excavation and (ii) design of cutoffs beneath dams in permeable foundations

For the present study the foundation permeability data were interpreted and hydraulic domain classifications are suggested to be made based on the permeability classification of rocks given by Lashkaripour and Ghafoori (2002):i.e.

- Impervious, if Lugeon Value is 0-3,
- Low permeability, if Lugeon Value is 3-10,
- Medium permeability, if Lugeon Value is 10-30,
- High permeability, if Lugeon Value is 30-60,
- Very high permeability, if Lugeon Value is >60,

Fig 5.3 shows the interpretation of different Lugeon patterns with its description and interpretation chart proposed by Houlsby (1976).

5.5.2.5 Bearing capacity estimation

The safe load bearing capacity of the foundation rock were calculated empirically based on UCS and RQD values proposed by Bowles (1996), and using a factor of safety of 3 as:

$$Safe\ Load\ Bearing\ Capacity = \frac{UCS*(RQD)2}{Factor\ of\ Saftey} \ldots\ldots\ldots eq.\ 5.4$$

On the other hand Hoek-Brown Criteria (2002) and Roc-Lab software developed by Rock-science were used to evaluate the safe load bearing capacity of the foundation rock mass for this particular study.

BEHAVIOR	PRESSURE STAGES	LUGEON PATTERN	DESCRIPTION	REPRESENTATIVE LUGEON VALUE
LAMINAR	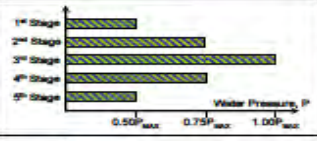	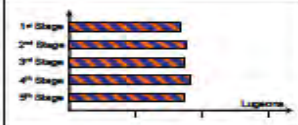	All Lugeon values about equal regardless of the water pressure	Average of Lugeon values for all stages
TURBULENT	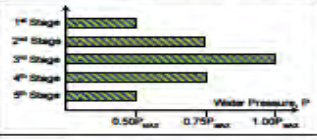		Lugeon values decrease as the water pressures increase. The minimum Lugeon value is observed at the stage with the maximum water pressure	Lugeon value corresponding to the highest water pressure (3rd stage)
DILATION	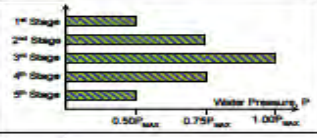	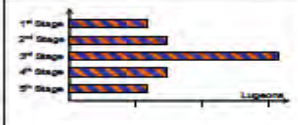	Lugeon values vary proportionally to the water pressures. The maximum Lugeon value is observed at the stage with the maximum water pressure	Lowest Lugeon value recorded, corresponding either to low or medium water pressures (1st, 2nd, 4th, 5th stage)
WASH-OUT	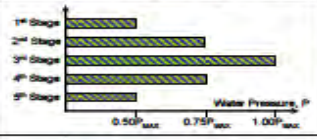		Lugeon values increase as the test proceeds. Discontinuities' infillings are progressively washed-out by the water	Highest Lugeon value recorded (5th stage)
VOID FILLING	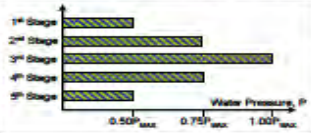	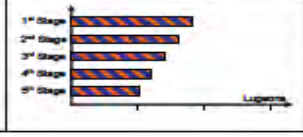	Lugeon values decrease as the test proceeds. Either non-persistent discontinuities are progressively being filled or swelling is taking place	Final Lugeon value (5th stage)

Fig 5.3 Lugeon Pattern Interpretation Chart (Houlsby, 1976)

5.5.2.6 Seismic Refraction in characterizing the rock mass

For the present study the seismic refraction data were used in characterizing the rock mass, specifically its seismic velocity is used to characterize the rock mass in terms of its quality, strength, degree of weathering and other related parameters. Besides, the seismic data were used in conjunction with the borehole data to characterize the rock mass of the given foundation.

*****

Chapter VI RESULTS, INTERPRETATIONS AND DISCUSSION

6.1 Preamble

The rock mass characterization carried out in the present research work is specific for the evaluation of the foundation condition in terms of its Rock quality, bearing capacity, deformability and permeability using an integrated geotechnical and geophysical approach.

The study is based on the primary and secondary data analysis. The required data was obtained from the field investigation, borehole data, insitu tests and seismic refraction results at the dam site in conjunction with cross-validation of actual conditions. This chapter forwards results and interpretations as well as discussions based on the research findings.

6.2 Rock mass classification

6.2.1 Rock mass classification from exposed rock

For the present study the data pertaining to RMR has been collected from both abutments along the excavated road cut slopes and naturally exposed sites at several locations. Based on the observed conditions, the ratings for each of the parameters were assigned from the standard RMR table. Later, sum total of all the ratings for each of the parameters provided RMR value. The uniaxial compressive strength (UCS) has been determined through insitu measurements by Schmidt Hammer. The Schmidt Hammer rebound values were used to determine UCS by using the empirical formula proposed by Barton and Choubey (1977).

6.2.1.1 Intact Rock Strength

For the present study UCS for surface rock exposure has been determined by Schmidt rebound number by using eq. 6.1 (Barton and Choubey, 1977);

From the results of UCS it was found that the rock strength value at the dam site ranges from 22 – 100 Mpa. The variation in the strength of the intact rock at the dam site is because of variability in the rock composition, degree of weathering and discontinuity characteristics.

6.2.1.2 Rock Quality Designation (RQD)

The Rock Quality Designation (RQD) has been determined by using Palmstorm's Volumetric Count method (Palmstrom, 1982), using the previously mentioned relationship.

Accordingly from this relationship the RQD of the rocks found in the dam site ranges from 52 – 96 %. Based on the classification given by Deer (1964) the rock mass in general fall in Fair to Excellent class.

6.2.1.3 Condition and Spacing of Discontinuity

For the present study the condition and spacing of the discontinuity was assessed based on guidelines as proposed by ISRM (1981). The area is characterized by massive intrusive rocks therefore, the spacing of discontinuity ranges from 50 – 200 cm. Further, the condition of the discontinuity at the dam foundation is in general having separation less than10 mm and the surfaces of discontinuities are generally rough and at places it's smooth.

6.2.1.4 Ground Water Condition

Ground water condition is the important parameters used in the classification of the rock mass. For the present study an attempt was made to know the ground water condition in the rock mass at the dam foundation. Based on the site investigations and data from the boreholes no ground water was detected on surface exposures and at shallow depths through boreholes. Thus the rock mass condition at surface and shallow depth is characterized as completely dry.

6.2.1.5 Orientation of discontinuity

The orientation of the discontinuities was measured at and near the dam foundation. In general, the orientations of the discontinuities are favorable as per the Beniawsk's RMR classification system (Bieniawski, 1989).

Table 6.1shows the RMR location points, the parameters used, the ratings assigned and the total RMR values for the corresponding rock mass class.

Table 6.1 RMR data for various locations at the dam Abutments

RMR Data Points	*Parameter Ratings*										*RMR_{89}*	*Rock Mass Class*
	UCS(Mpa)			*RQD*			*Spa.*	*Con.*	*GWC*	*Ori*		
	SHV	*UCS*	*Ra*	*JV*	*RQD*	*Ra*						
Left Abutment												
LA1	42	66.881	7	18	55	13	8	20	15	-2	61	Good
LA2	30	47.772	7	19	52	13	8	20	15	-2	61	Good
LA3	14	22.294	7	15	65	13	10	20	15	-2	63	Good
LA4	26	41.402	7	19	57	17	10	20	15	-2	67	Good
LA5	38	60.511	7	9	86	17	10	20	15	-2	67	Good
LA6	33	52.549	7	12	75	17	10	20	15	-2	67	Good
LA7	38	60.511	7	6	95	20	15	20	15	-2	75	Good
LA8	38	60.511	7	21	46	13	10	19	15	-2	62	Good
LA9	59	93.952	7	16	62	13	8	17	15	-2	58	Fair
LA10	58	92.359	7	17	59	13	8	17	15	-2	58	Fair
Right Abutment												
RA1	54	85.99	7	10	82	17	10	22	15	-2	69	Good
RA2	62	98.729	7	11	82	17	10	20	15	-2	67	Good
RA3	63	100.32	7	9	82	17	10	20	15	-2	67	Good
RA4	59	93.952	7	8	89	20	15	22	15	-2	77	Good
RA5	39	62.104	7	14	82	13	10	20	15	-2	63	Good
RA6	42	66.881	7	12	75	17	10	20	15	-2	67	Good
RA7	51	81.212	7	14	69	13	10	20	15	-2	63	Good
RA8	51	81.212	7	15	66	13	10	19	15	-2	62	Good
RA9	54	85.99	7	6	96	20	10	19	15	-2	69	Good
RA10	46	73.25	7	11	79	17	10	20	15	-2	67	Good

UCS *– Uniaxial compressive strength,* ***SHV*** *– Schmidt hammer Value,* ***Ra*** *– Rating,* ***Jv****- Volumetric count,* ***RQD*** *– Rock quality designation,* ***Sp.*** *– Spacing of discontinuity,* ***Con.*** *– Condition of discontinuity,* ***GWC*** *– ground water condition,* ***Ori*** *– Orientation of discontinuity,* ***RMR*** *– Rock mass rating*

Based on the RMR data (Table 6.1) an attempt was made to zone the rock mass at the dam foundation by using Arc GIS. Accordingly, 50% of the foundation rock mass falls in RMR class 66 – 70, 40% falls in 61 – 65 and the rest 10% falls in class 70 – 80. Fig 5.1 shows these RMR zones at the dam site, with location of boreholes, dam axis and anticipated structures.

6.2.2 Rock mass classification from boreholes

6.2.2.1 Preamble

Geomechanics classification (RMR) was used for classifying and interpreting the quality of the foundation rocks at the proposed Dam site through bore holes data. For the purpose of classification the rock mass at dam foundation was first divided in to structural regions, based on fracture density and evenness as displayed by weighted RQD. These regions are assumed to be more or less uniform in certain geotechnical features.

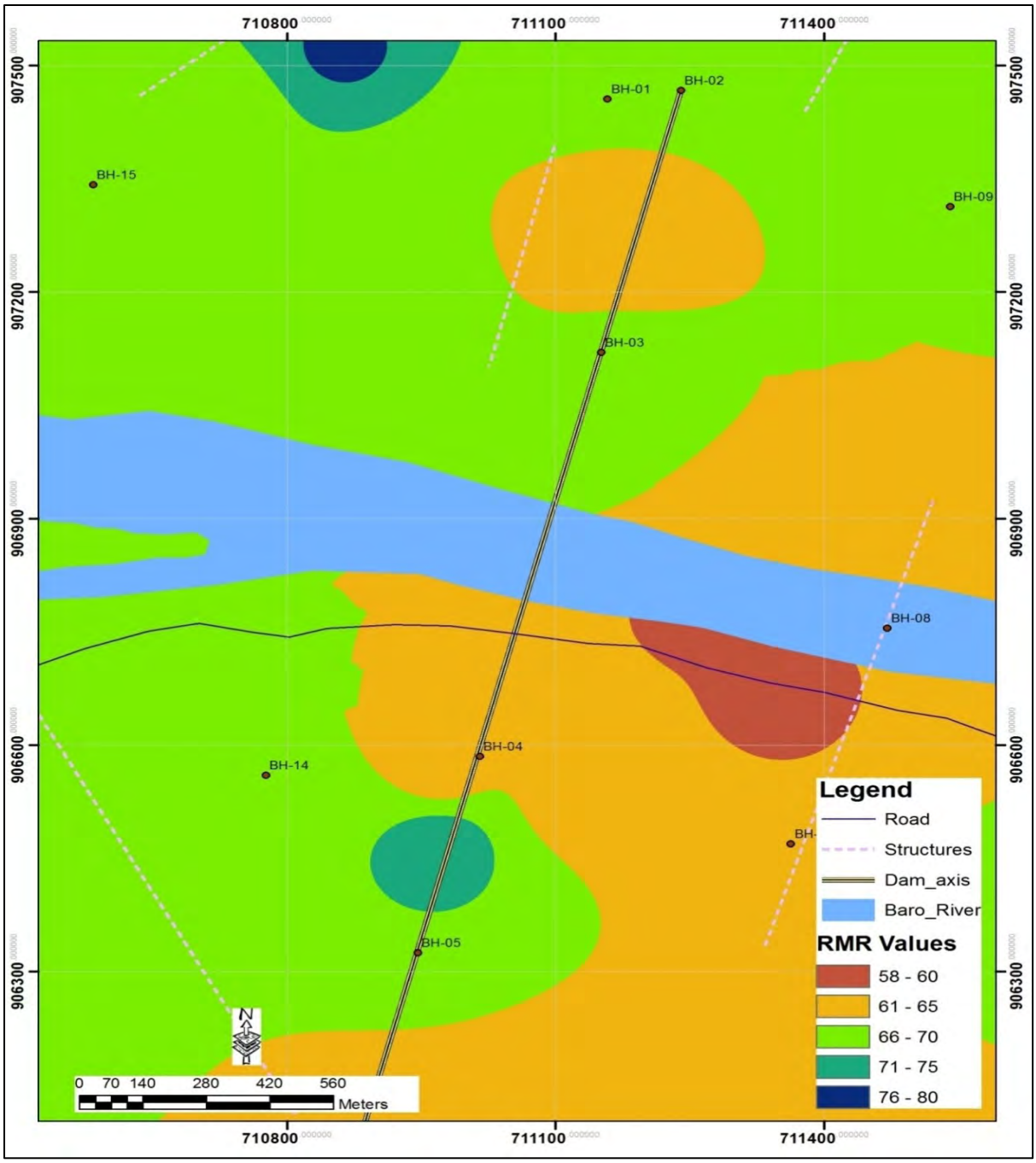

Fig 6.1 RMR zone map at the Dam Site

6.2.2.2 Intact Rock Strength

Intact rock strength for various rock types present at the dam foundation was determined through Uniaxial Compression Strength (UCS) tests conducted on representative core samples at the laboratory. These strength values were used in rock mass classification system using Beniawsk's (1989) RMR system. Almost all the rock samples tested showed relatively high values for UCS. Table 6.2 shows summary of laboratory test results on rock core samples, taken from different locations and depths at the dam foundation.

Table 6.2 Laboratory Test Result for different rock core samples from the Dam foundation

S.N	BH ID	Location	Lithological Field Description	Sampling Depth(m)	Unit Weight	Point Load (Mpa)	UCS (Mpa)
1.	BH-04RS-2	Center of Dam Axis	Meta Granodiorite	10.77-11.00	2.95	-	-
2.	BH-04RS-5		Meta Granite	25.75-26.05		9.98	-
3.	BH-04RS-6			32.40-32.60	2.64	-	-
4.	BH-04RS-9			91.68-92.10	-	-	403.59
5.	BH-04RS-10		Meta Volcanic	62.75-63	-	8.12	178.72
6.	BH-14RS-3	Downstream of Dam Axis	Meta Volcanic	34.95-35.30	2.89	6.26	360.02
7.	BH-14RS-4		Meta Granodiorite	39.30-39.45	-	-	374.77
8.	BH-14RS-7		Meta Granite	75.08-75.35	2.68	9.94	-
9.	BH-05RS-3	Center of Dam Axis	Meta Volcanic	61.15-61.75	2.91	-	363.00
10.	BH-05RS-5			99.00-99.76	-	5.33	-
11.	BH-05RS-7		Meta Tonalite	130.00-130.60	2.69	3.57	198.09
12.	BH-06RS-3	Spillway and Dam Axis	Meta Diorite	29.40-30.00	2.79	4.69	-
13.	BH-06RS-5		Granite Pegmatite	82.85-83.40	-	13.49	-
14.	BH-06RS-6		Ortho Gneiss	85.85-86.45	-	-	324.55
15	BH-06RS-7		Ortho Gneiss	132.35-132.7	2.59	-	276.51

6.2.2.3 Rock Quality Designation (RQD)

Rock mass quality is an important geological parameter for the design and construction of a dam project. The rock mass quality is highly influenced by the presence of geological structures; such as joints, faults and shear zone in addition to the grade of weathering. For the present study, the RQD data was collected by following standard practice as proposed by Deer (1964). The rock quality at the proposed dam foundation ranges from very good to excellent, and in general the RQD values increases with depth. Fig 6.2 shows the RQD value of selected boreholes at different depth. Perusal of graph (Fig. 6.2) clearly shown that the RQD value for rock mass in BH-7at certain depths is almost 100 %.

6.2.3 Estimation of Rock Mass Quality

6.2.3.1 Rock Formations Intercepted

Generally, the area is characterized by rock formations starting from the top soil materials. The lithological units encountered during field survey are mainly syn tectonic granites and Meta volcanic rocks at places. The granite material is characterized by light gray in color, with a coarse matrix composed of feldspathic materials. There are also pegmatites in various places along the formations. Amphibolite interceptions are few in the dam site area at the depth of the drill holes.

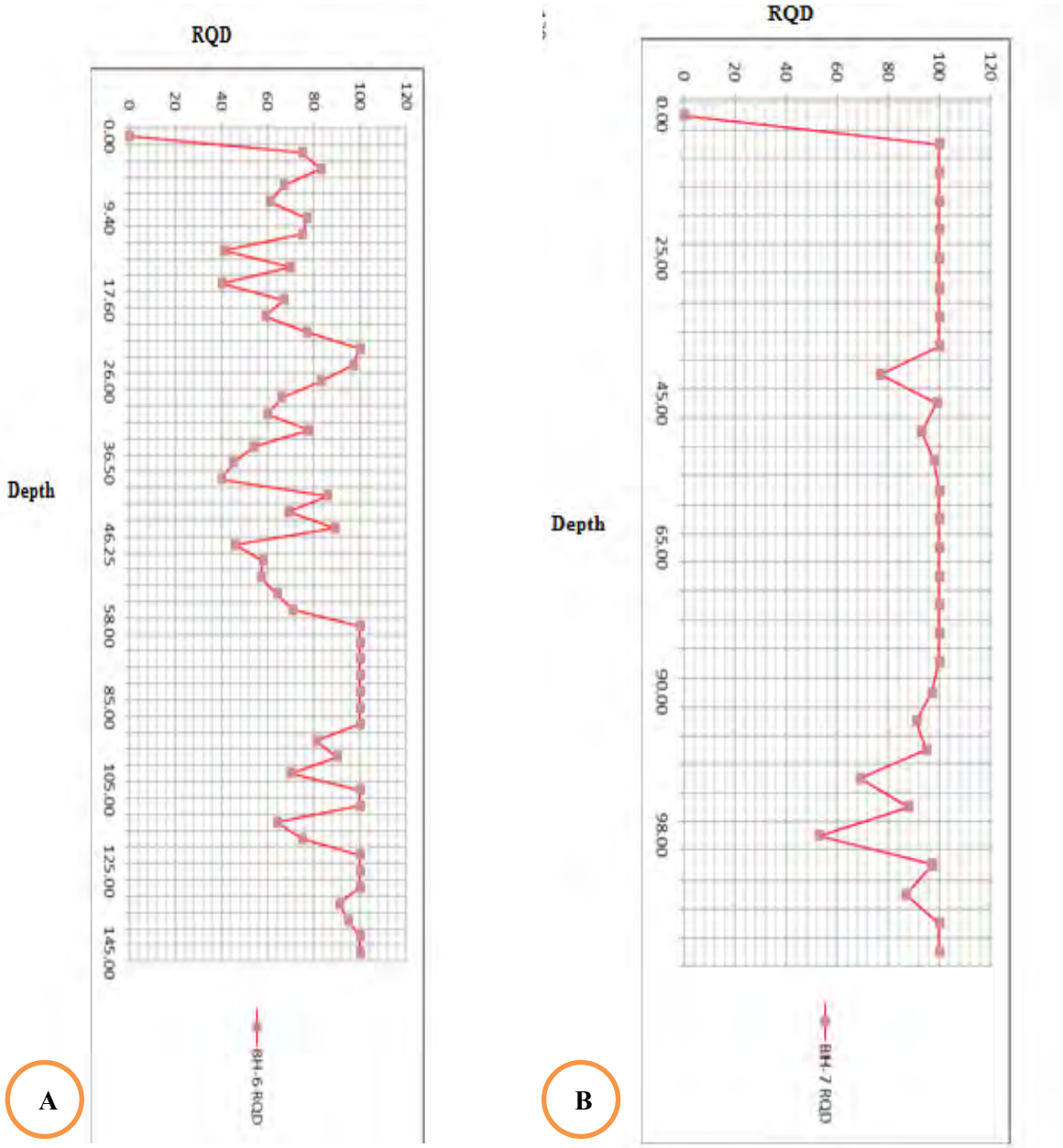

Fig 6.2 RQD value at selected boreholes A) BH-6 & B) BH-7

6.2.3.2 Rock mass quality Estimation using Geological Strength Index

According to the GSI classification, Most of the surface RMR points correspond to the structural category 2 and 3, that is blocky (well interlocked undisturbed rock-mass consisting in cubical blocks formed by three intersecting discontinuity sets) and very blocky (interlocked partially disturbed mass with multifaceted angular blocks formed by 4 or more joints sets), respectively (Hoek et al., 2002).

Table 6.3 RMR classification from Drilled boreholes at the Dam site

BH-ID	Zoning Depth	Location	Rock Description	UCS (Mpa)	Average RQD (%)	Spacing of Discontinuities (mm)	Condition of Discontinuities	Ground Water	Total RMR Rating	Rock mass Class Number	Description
BH-4	18.0 – 41.40m	Dam axis	Meta-Granite	249	58	60mm	<10mm separation, rough surfaces	Damp	69	II	Good
			Rating	15	13	8	23	10			
	41.50 – 62.50m		Meta-Volcanics	178.72	86	300mm	<1mm separation, Slightly rough surfaces	Damp	72	II	Good
			Rating	12	17	10	23	10			
	90 – 109.10m		Meta-Granite	403	97	>700mm	<1mm separation, rough surfaces	Damp	84	I	Very Good
			Rating	15	20	15	24	10			
BH-5	59.0 – 63.10m	Dam axis	Biotite Schist	366	100	>600mm	<1mm separation, Slightly rough surfaces	Damp	83	I	Very Good
			Rating	15	20	15	23	10			
	64.30 – 94.15m		Meta-Diorite	128	100	450mm	<1mm separation, Slightly rough surfaces	Damp	71	II	Good
			Rating	12	20	10	19	10			
	125.0 – 132.5m		Meta - Tonalite	198	100	300mm	<1mm separation, Slightly rough surfaces	Damp	75	II	Good
			Rating	12	20	10	23	10			
BH-6	27.20 – 47.50m	Dam axis and Spillway	Meta-Diorite	56	66	120mm	<1mm separation, Slightly rough surfaces	Damp	59	III	Fair
			Rating	7	13	8	21	10			
	84.0 – 129.8m		Ortho-Gneiss	324	91	>600mm	<1mm separation, Slightly rough surfaces	Damp	84	I	Very Good
			Rating	15	20	15	24	10			
	130 – 145m		Gneiss intercalated with metavolcanic	276	97	>600mm	<1mm separation, Slightly rough surfaces	Damp	84	I	Very Good
			Rating	15	20	15	24	10			

Table 6.3 Cont'd…..

BH-ID	Zoning Depth	Location	Rock Description	UCS (Mpa)	Average RQD (%)	Spacing of Discontinuities (mm)	Condition of Discontinuities	Ground Water	Total RMR Rating	Rock mass Class Number	Description
BH-7	10.20 – 62.0m	Upstream of Dam axis	Meta Granodiorite	369	98	>600mm	<1mm separation, rough surfaces	Damp	81	I	Very Good
			Rating	15	20	15	21	10			
	87.20 – 102.8m		Meta-Syenite	122	89	300mm	<1mm separation, Slightly rough surfaces	Damp	72	II	Good
			Rating	12	17	10	23	10			
BH-14	8.30 – 36.0m	Downstream of Dam axis	Metagranite intercalated with metavolcanic	360	87	120mm	<1mm separation, Slightly rough surfaces	Damp	83	I	Very Good
			Rating	15	17	8	21	10			
	39.0 – 54.40m		Meta-Granodiorite	374	62	100mm	<10mm separation, Slightly rough surfaces	Damp	62	II	Good
			Rating	15	13	8	16	10			
	60.25 – 108.4m		Meta-Granite	248	69	150mm	<1mm separation, Slightly rough surfaces	Damp	64	II	Good
			Rating	12	13	8	21	10			

As a general remark about the quality of the joints which cut the bedrock, they are very closed without presence of water. Only some surfaces show the local presence of iron oxides. Due to these characteristics, the surface quality of such joints has been referred to the category 2 (good, rough slightly weathered and altered surfaces) (Hoek et al., 2002).As an input for the GSI chart, the choosed value zone is between 60 and 70, which corresponds to a good quality of rock mass. Fig 6.3 shows Geological Strength Index chart for the rock mass found in the present dam foundation.

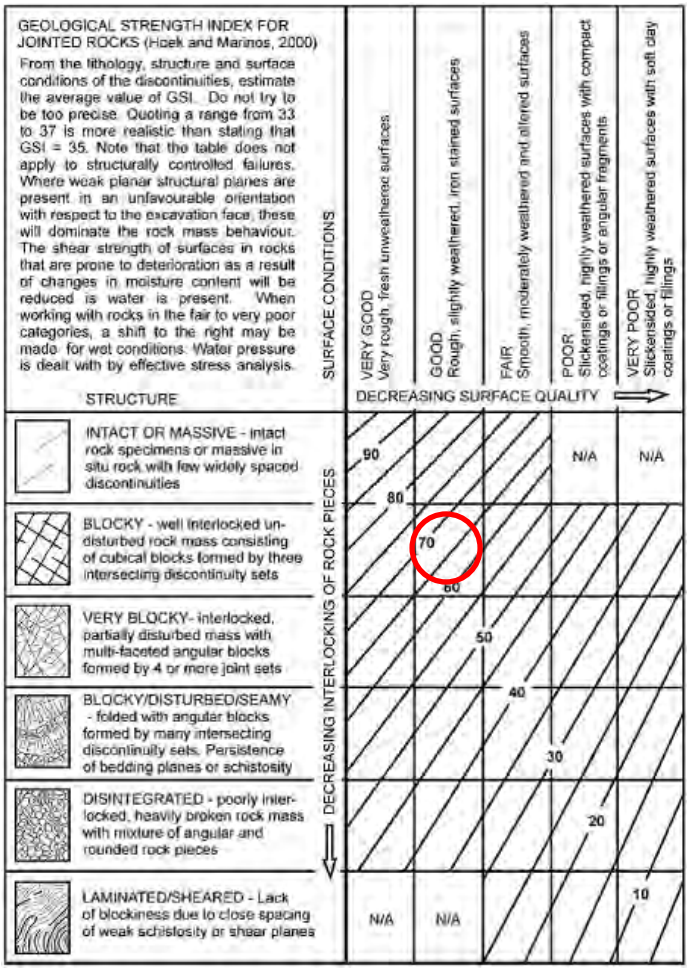

Fig 6.3 GSI chart showing rock mass quality at the dam foundation

6.2.3.3 Weak Zones

Some of the weak zones in the study area have been found at the contacts of lithological rock formation. Other weak zones as observed were due to low strength weathered zones, decomposed rock mass and rock mass affected by leaching. In this regard, the most notable weakness zones within the rock mass were demonstrated by highly decomposed and broken

or leached segments of the rock mass as shown in Plate 6.1on the right bank of the study area, especially on the Biotite-hornblende schist.

Plate 6.1 shows the weak formations on biotite-hornblende schist formation on the right bank of the dam site. These weak zones are associated with high foundation permeability as observed during insitu packer permeability test results.

Plate 6.1 Rock core showing zone of weakness, decomposition at the contact zone (Borehole 3)

6.2.3.4 Overall quality of the Rock mass

Surface mapping and boreholes drilled at the dam site and other appurtenant structures greatly enhanced better understanding of surface and subsurface configuration of geotechnical layers. General observations of the site; visual observations of the drill core recovered from boreholes and in situ, test pits and trench excavated on the dam site and laboratory tests conducted on representative samples enabled the determination of the geotechnical layers at the dam site.

With the exception of some very soft rocks and heavily jointed media, the majority of the rock masscan be classified as an excellent foundation material.However, there is a need to accurately estimate the ultimate bearing capacity of the foundation rock mass and to evaluate possible foundation treatment for the incompetent geological formations and structures. When the rock mass is considered, it is inferior to that of the intact rock material due to the presence of jointing and weathering (Fig. 6.4).

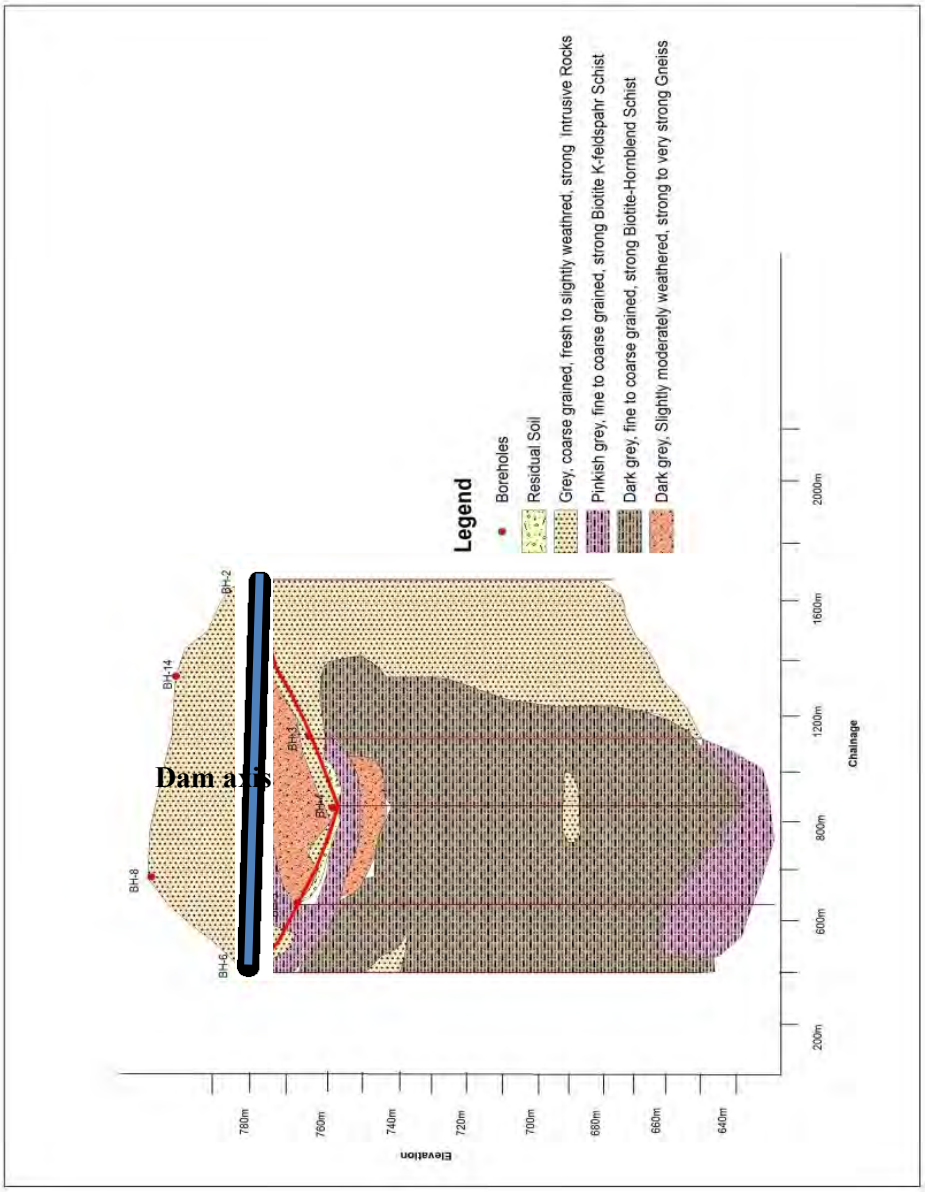

Fig. 6.4 Fence diagram showing the Engineering Geological condition of the Dam site

6.3 Engineering Geological Mapping

An engineering geological map is a type of geological map, which provides a generalized representation of all those components of geological environment, which are significant in land use planning, design, construction, and maintenance, as applied to civil engineering applications. These maps may play an important role in planning and decision making in the early stages of development of a project. Another use of the map is to identify potential problems or favorable conditions existing at the proposed project site (Hack et al., 2002).The engineering geological mapping of the TAMS Dam site has been carried out on the basis of engineering characterization of the rock mass and the soils. For mapping purpose the rocks

have been characterized based on the strength, weathering grade and the jointing intensity (RQD). Whereas the soils of the dam site area has been classified based on the unified soil classification system. Fig.6.5 presents the engineering geological map of the study area.

6.4 Estimation of Deformability

The assessment of rock mass deformation properties is essential for the foundation of the dam and appurtenance structures. The stability and deformability of the rock foundation is dependent on the strength and deformability of the rock mass. The index properties of the intact rock samples are not the only criteria on which a design is based as the rock mass is typically heterogeneous and anisotropic than intact rock due to the presence of discontinuities, apart from the chemical weathering of the rock mass (Agarwell et al., 1991).

The deformation modulus of the rock mass may often be the critical parameter in the design of an engineering structure on rock. Similarly, to the problem of predicting the rock mass strength, it is also very difficult and expensive to determine in the field. The rock mass deformability is complicated by the lack of a suitable method to determine the effect of the discontinuity network upon the deformability of the rock mass. Similar to the strength of jointed rock, the modulus of jointed rock varies significantly depending on the proportion of the intact rock in a rock mass (Agarwell et al., 1991).

In the present study Modulus of deformation ‘Ed’ of the rock Mass has been determined empirically by using relations proposed Agarwal et al. (1991) and Hoek and Brown (1997).

6.5 Estimation of Shear Strength

6.5.1 Hoek and Brown failure criteria

Hoek and Brown (2002) developed an empirical approach to determine the strength of the jointed rock mass and formulated a failure criterion for jointed rock mass. For the present study Rock mass strengths were calculated using the principles outlined in the generalized Hoek-Brown failure criterion with the parameter results from mapping, core logging and laboratory testing.

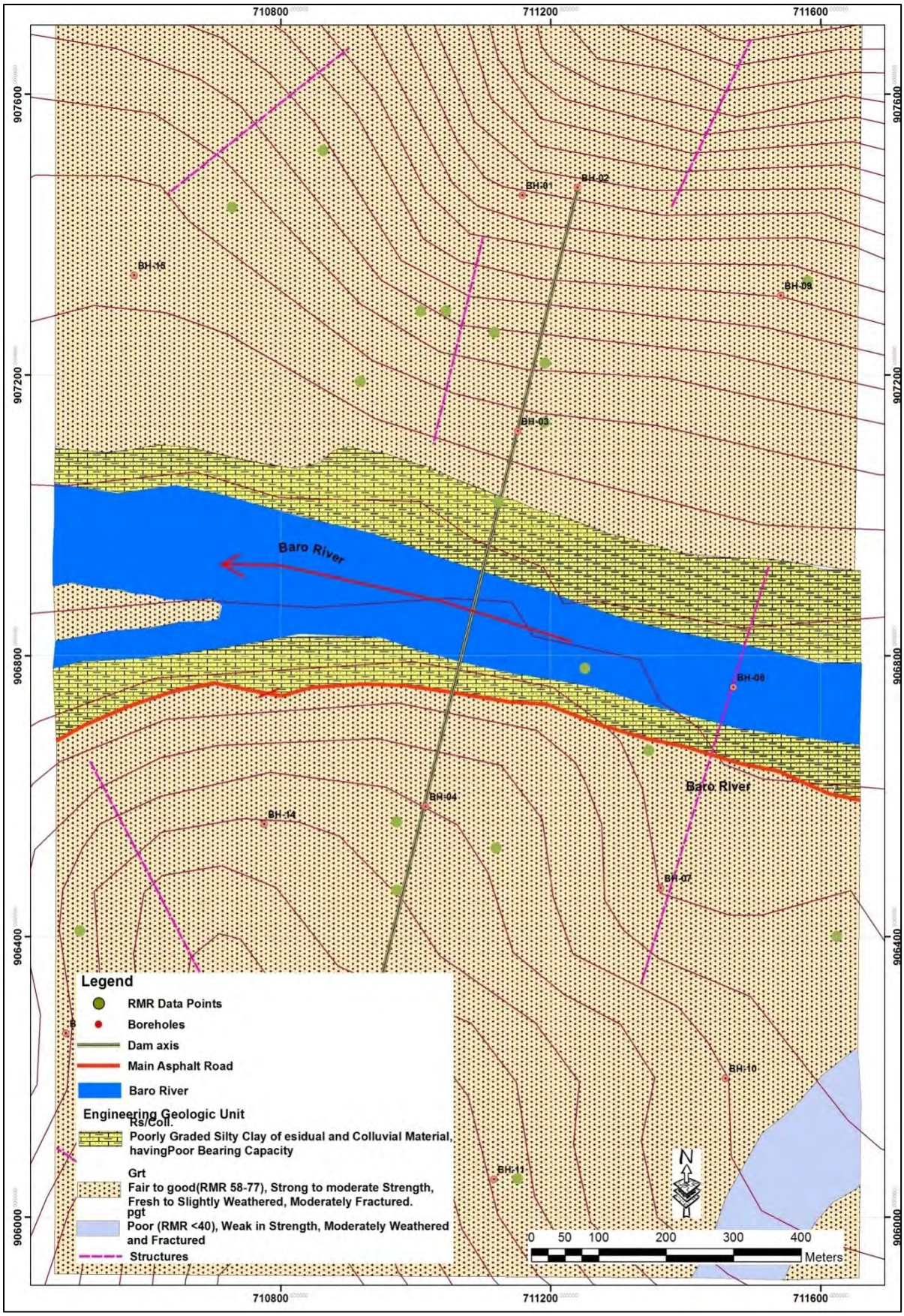

Fig 6.5 Engineering Geological Map of the Dam Site with Borehole Locations and RMR data points (produced by the author)

Table 6.4 Shear strength Parameters and Modulus of Deformation 'Ed' as determined from RMR

RMR Data Points	*RMR_{89}*	*Elevation*	*Modulus of Deformation 'Ed' in (kg/cm2)*	*Shear Strength Parameters*	
			Argawal (1991).	*C*	*Ø*
LA1	61	761	4.17	3.05	35.5
LA2	61	642	4.17	3.05	35.5
LA3	63	596	4.57	3.15	36.5
LA4	67	532	5.5	3.35	38.5
LA5	67	547	5.5	3.35	38.5
LA6	67	616	5.5	3.35	38.5
LA7	75	661	7.94	3.75	42.5
LA8	62	619	4.37	3.1	36
LA9	58	508	3.63	2.9	34
LA10	58	509	3.63	2.9	34
RA1	69	504	6.03	3.45	39.5
RA2	67	645	5.5	3.35	38.5
RA3	67	586	5.5	3.35	38.5
RA4	77	619	8.71	3.85	43.5
RA5	63	586	4.57	3.15	36.5
RA6	67	529	5.5	3.35	38.5
RA7	63	602	4.57	3.15	36.5
RA8	62	625	4.37	3.1	36
RA9	69	604	6.03	3.45	39.5
RA10	67	530	5.5	3.35	38.5

Table 6.5 shows the *mi* values, Rock mass constants, GSI for the rock and Disturbance factor D, for estimating various rock parameters in the Generalized Hoek-Brown failure criterion. In Table 6.5 the average intact rock strength is calculated along the borehole from similar rock formations. The parameters are calculated and simulated from the generalized Hoek-Brown failure criterion (Hoek et al 2002) with the excel sheet version for academic purpose developed by Raghuvanshi, (2017).

It is expressed as:

$$\sigma_1' = \sigma_3' + \sigma_c \left(mb \frac{\sigma_3}{\sigma_c} + S \right)^a \qquad \text{……..eq.6.1}$$

Where, `$m_b$' is the value of the constant 'm' for the rock mass, `s' and `a' are constant which depend upon the characteristic of the rock mass, σc is the uniaxial compressive strength of the intact rock pieces and σ_1' & σ_3' are the axial and confining effective principal stresses, respectively.

Table 6.5 Rock mass strength of the TAMS dam area, based on estimated mi values from Raghuvanshi, 2017 and UCS test values from selected boreholes at Dam seat area

Borehole ID	UCS (Mpa)	RMR_{89}	D	Average GSI	*mi*	Rock mass constants			Rock mass compressive Strength(Mpa)	Mohr Columb fit	
						s	*a*	*mb*	*σcm*	C	ϕ
Dam axis											
BH-4	403	84	0	79	37	0.097	0.501	15.588	230.2	42.75	49.25
BH-5	128	71	0	50.04	27	0.0229	0.502	8.017	50.04	10.6	43.88
BH-7	122	72	0	67	35	0.0256	0.502	10.77	54.97	11	46.88
BH-14	374	62	0	57	35	0.0084	0.504	7.536	137.86	29.6	43.46

Fig 6.6 shows the relationship between major principal stress and minor principal stress incorporating both the Hoek-Brown criteria and Mohr-Column criteria based on the calculated parameters shown in Table 6.5.

Similarly for surface RMR data collected from various locations on the abutments has been used as an input parameter for strength estimation. The uniaxial compressive strength has been determined by Schmidt hammer at all representative sites from where RMR data has been collected. The value of material constant 'mi' has been directly adopted from the standard table (Hoek and Brown, 2002). The other material constant m_b and S were determined by using GSI.

Table 6.6 shows the results of the average intact rock strength calculated from RMR at both abutments of the dam site. The parameters are calculated and simulated form the generalized Hoek-Brown failure criterion (Hoek et al., 2002) with the unpublished modified version developed by Raghuvanshi (2017).

Fig 6.7 shows the relationship between major principal stress and minor principal stress incorporating both the Hoek-Brown criteria and Mohr-Column criteria based on the calculated parameters shown in Table 6.6 for selected RMR points on both abutments at the dam site.

6.6 Abutment Slope Stability

6.6.1 Preamble

Slope stability of the abutments is very important for the safe functioning of any dam project. The instability of abutment slopes may pose serious problems during the construction stage. Identification of instability of the slopes in the initial stages may help in evolving proper

remedial measures. Therefore, it is essential to carry out the stability analysis of the abutment slopes in the initial stages of investigation and planning (Hoek and Bray, 1977).

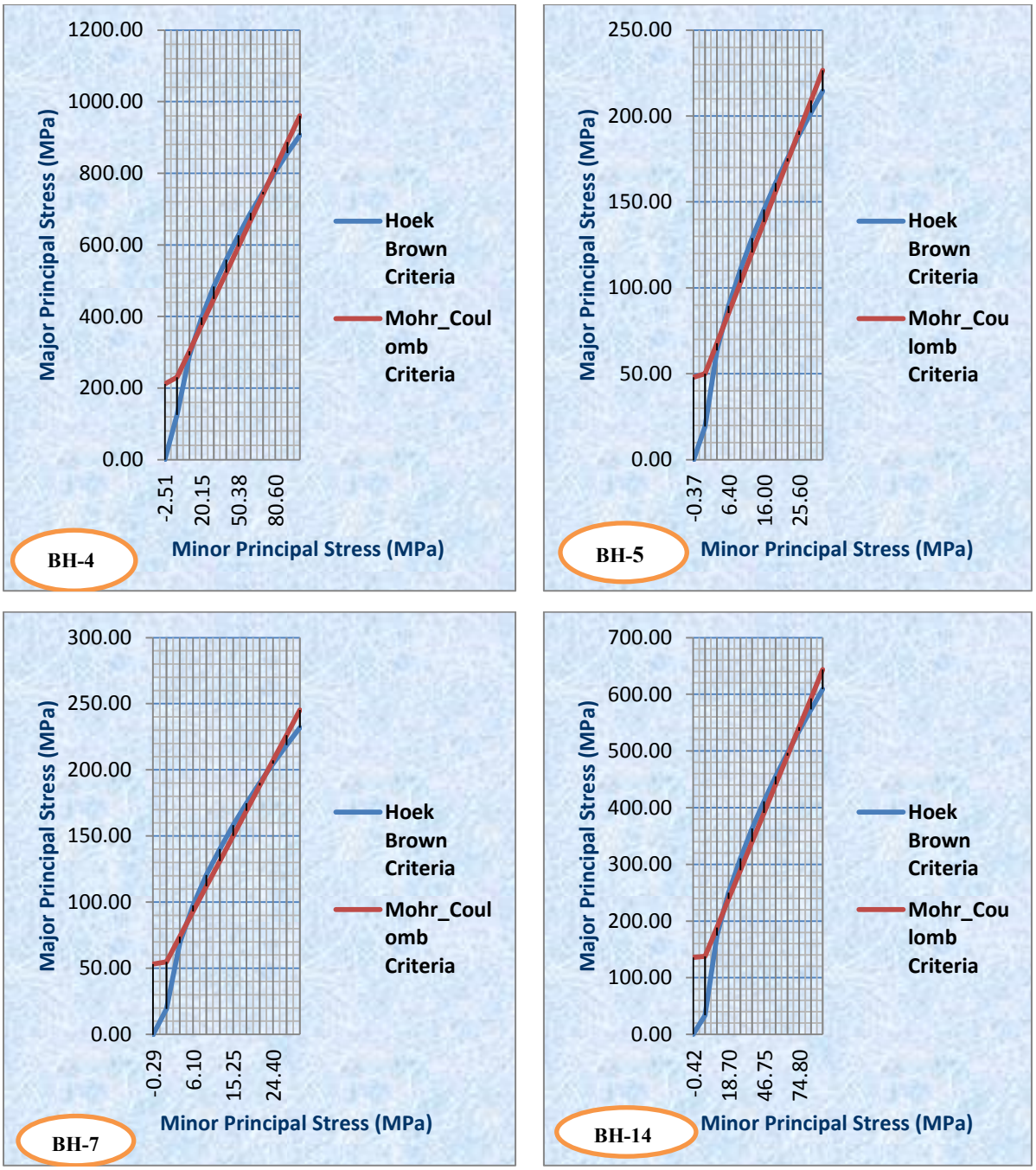

Fig.6.6 Rock mass strength, based on estimated mi values from Hoek and Brown, 2002 and UCS test values from selected boreholes at Dam site.

For the present study, the kinematic analysis was performed using the stereographic projection method which is a strong tool to use for systematic data collection and presentation. Data required to perform the stereographic projection are dip and dip direction of each discontinuity plane, slope inclination and the shear strength of the discontinuity

planes. Because of the limited outcrop on the right abutment, the kinematic check was done only for the left abutment of the dam site.

Table 6.6 Rock mass strength of the TAMS dam area, based on estimated mi values from Hoek and Brown, 2002 and RMR data results from abutments

RMR point	UCS (Mpa)	RMR_{89}	D	Average GSI	*mi*	Rock mass constants			Rock mass compressive Strength (Mpa)	Mohr Columb fit	
						s	*a*	*mb*	*σcm*	C	ϕ
Left Abutment											
LA1	66.88	61	0	56	33	0.075	0.504	6.856	23.53	5.15	42.66
LA3	22.29	63	0	58	32	0.094	0.503	7.14	7.92	1.72	42.98
LA6	52.55	67	0	62	34	0.014	0.502	8.751	20.88	4.358	44.69
LA7	60.51	75	0	70	34	0.0357	0.501	11.646	28.39	5.59	46.99
LA8	60.51	62	0	57	32	0.0084	0.504	6.89	21.17	4.63	42.69
LA9	93.95	58	0	53	32	0.0054	0.505	5.972	30.31	6.82	41.5
Right Abutment											
RA1	85.99	69	0	64	33	0.0183	0.502	9.123	35.03	7.25	45.01
RA3	100.32	67	0	62	35	0.0174	0.502	9.009	40.71	8.44	44.93
RA4	93.95	77	0	72	33	0.0446	0.501	12.14	45.32	8.85	47.31
RA6	66.88	67	0	62	33	0.0147	0.502	8.49	26.12	5.4	44.43
RA7	81.21	63	0	58	33	0.0094	0.503	7.39	29.6	6.39	43.25
RA8	81.21	62	0	57	32	0.0084	0.504	6.89	28.58	6.26	42.69

6.6.2 Discontinuity Analysis

Discontinuities are structural weakness planes upon which movement can take place. The presence or absence of discontinuities has a very important influence upon the stability of the rock slopes and the detection of these geological features is most critical for the stability investigation (Hoek and Bray, 1977).

The most readily apparent influence of the orientation of discontinuities on rock mass strength is evident in the failure of rock slopes along one or more discontinuities; consequently in the present study the influence of joint orientation on the stability of the rock masses prevailing on the left abutments has been evaluated.

The first step of evaluation was to analyze the structural fabric of the slope to determine if the orientation of the discontinuities could result in instability of the slope under consideration. This was done by means of stereographic analysis of the structural discontinuities (bedding planes and joints) commonly referred to as kinematic analysis.

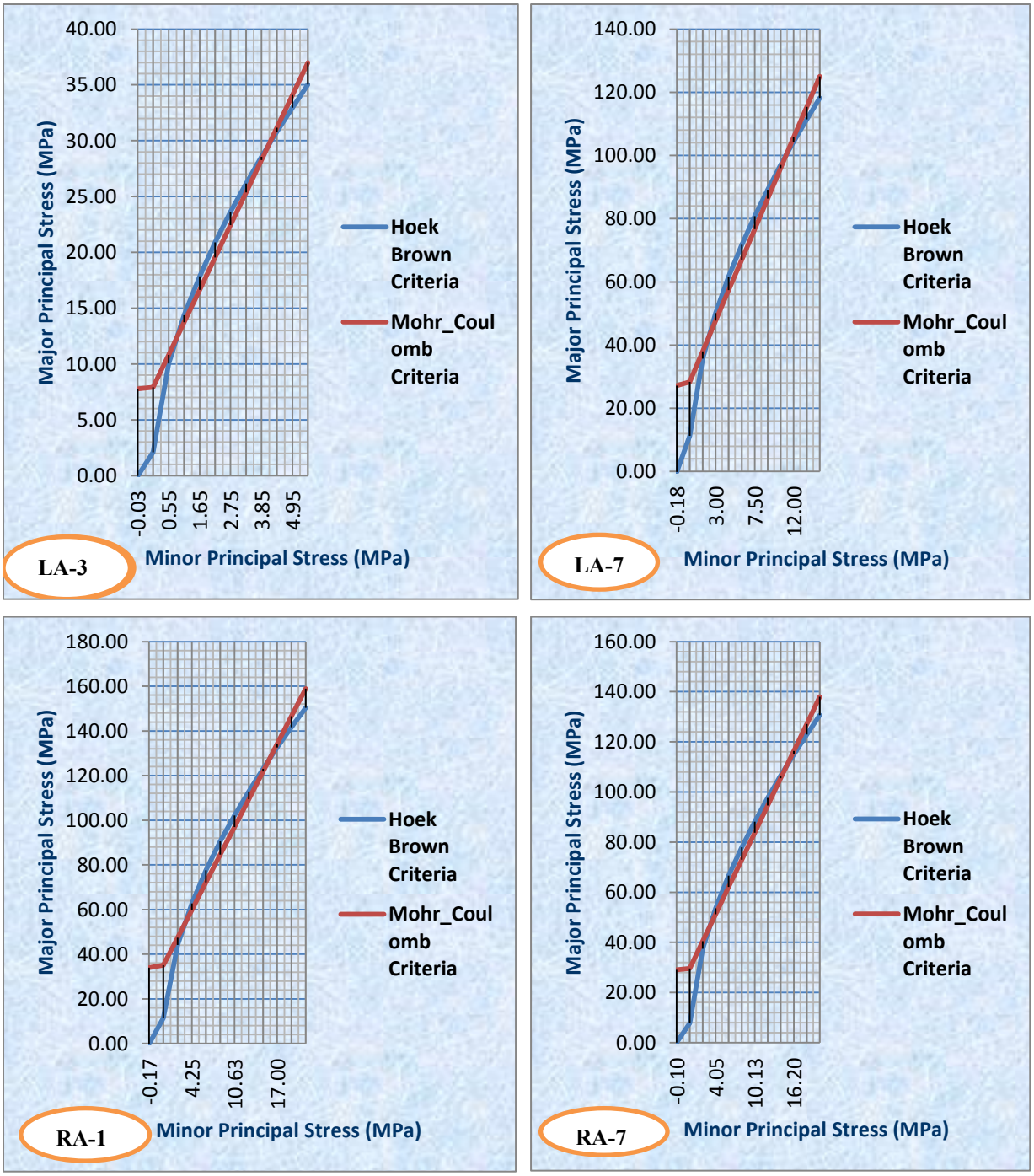

Fig.6.7 Rock mass strength of the TAMS dam area, based on estimated mi values from Hoek and Brown, 2002 and UCS test values from selected RMR points on both abutments.

The factors of primary importance to the influence of joint orientation are whether joint intersections cut or daylight the slope at less than the natural or manmade slope angle and if so whether the dip angle of joints or the plunge angle of the joint intersections exceed the angle of friction along the joint surfaces (Hoek and Bray, 1977).

The rock mass exposed on the abutment slopes are traversed by discontinuity planes mainly, joints and faults. In order to work out the preferred orientations of these discontinuity planes,

structural data, mainly, joints has been collected from both the abutment slopes in which the exposure is preferable.

At RMR point LA 8, about 350 m upstream of the dam axis the exposed outcrop length is about30 m. As shown in Plate 6.2, the rock underwent intense tectonic processes which produced faulting, folding, and gave rise to narrow belt with mylonitic textures.

Plate 6.2. RMR point 8, left side of the outcrop left abutment

The statistical analysis allows identifying several sets of dia clases, in addition to the wavy schistosity planes. By summarizing, the rock-mass is typical of a strongly deformed zone.

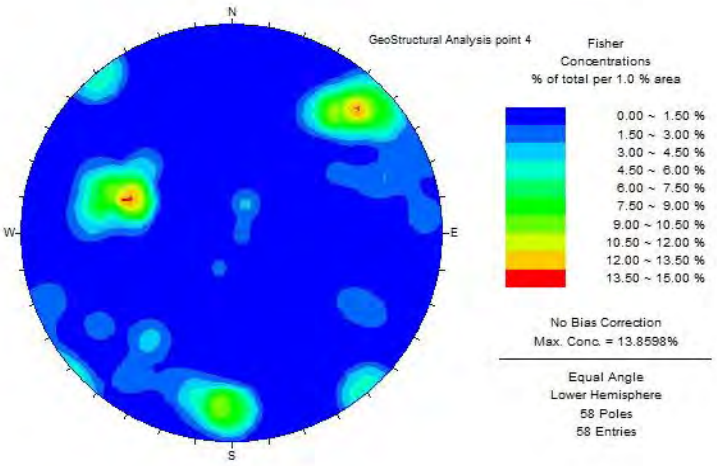

Fig.6.8 Stereo plot for RMR point 8 near the dam axis

The main schistosity ranges around 100° / 60° whereas the joint families are at least 5. There are three main families at 240° / 60°, 0° / 80°, and 030° / 60°.

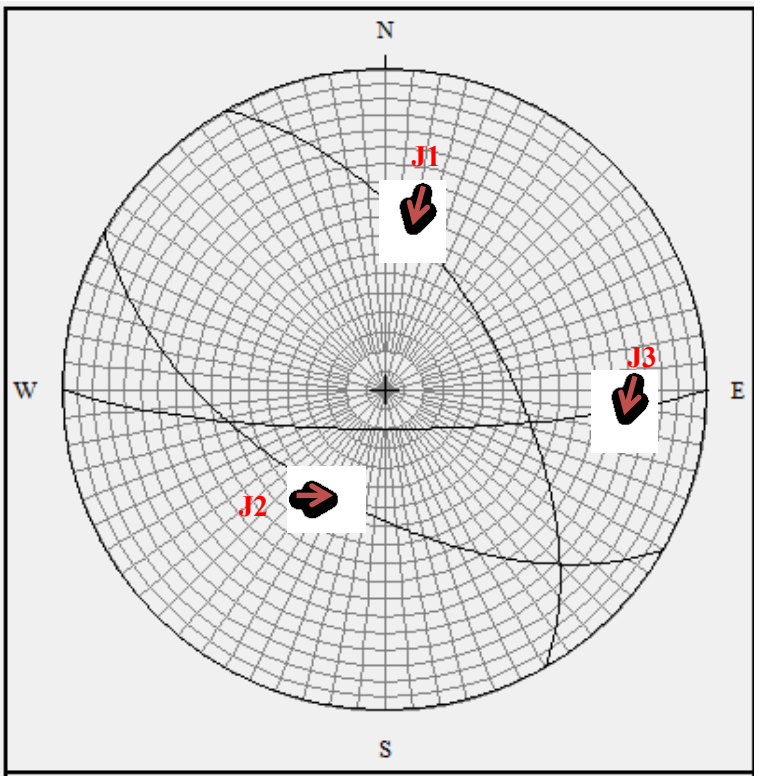

Fig. 6.9 Preferred orientations of discontinuity planes as observed on the left abutment

6.6.3 Kinematic Check

An attempt was made to check the slope stability of the abutments, due to scarcity of data and lack of exposure the kinematic check is applied only at left abutment road cut slope sections. Structural data, along with slope inclination and a 'phi circle' corresponding to angle of friction of the rock mass has been plotted on equal area projection 'Schmidt Net'. The angle of friction has been estimated from the RMR data. Fig. 6.8 presents the stereo plots to demonstrate Markland test for abutment slope sections.

Thus, in a rock slope the failure will only occur if the following conditions are satisfied;

Plane failure $\alpha_f > \alpha_p > \varphi$ *…Eq 6.2* Wedge failure $\alpha_f > \alpha_i > \varphi$ *…Eq 6.3*

Where; α_f is the slope angle, α_p is the dip of the potential failure plane, α_i is plunge of the line of intersection and φ is the angle of internal friction of the two wedges forming plane.

It has been found that the road slope cut at the left side slope sections satisfy the kinematics condition for wedge mode of failure defined by joints J2 and J3.

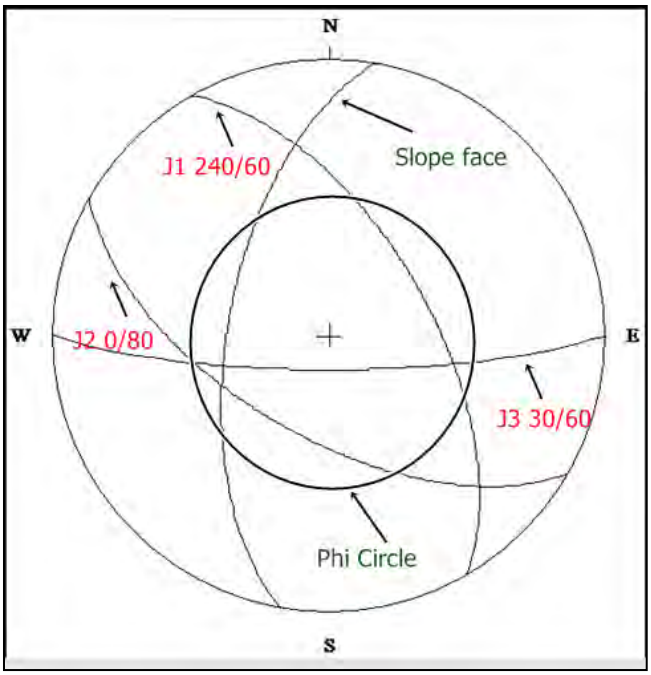

Fig 6.10 Kinematics check for potential mode of failure in left abutment slopes

However, no joint satisfies the kinematic condition for plane mode of failure. Thus, there is a possibility of wedge mode of failure in the left abutment slopes. This analysis is made with a limited point structural data, therefore it is recommended to make a detailed slope stability analysis during excavation and construction period, where there will be rock exposure and detail structural data on both of the abutments.

6.6.4 Slope Stability Analysis using Slope Mass Rating (SMR)

For evaluating the stability of the rock slopes, Romana (1985) proposed a classification system called slope mass rating (SMR) system. For slope mass rating Romana utilized Bieniawiski's Rock Mass System (RMR). Initially Romana developed SMR to account for only plane and toppling mode of failure, later this was modified by Anbalagan et al. (1992) to account for wedge mode of failure also.

$$SMR = RMR_{basic} - (F_1 * F_2 * F_3) + F_4 \quad \ldots\ldots eq.\ 6.4$$

Where; RMR_{basic} is evaluated according to Bieniawski (1976). The F1, F2 and F3 are adjustment factors related to joint orientation with respect to slope orientation and F4 is the correction factor for method of excavation.

F1 – depends upon parallelism between joints and slope face strikes.

(α_j - α_s) where, α_j is joint strike and α_s is slope strike.

F2 – refers to joint dip angle (β_j) or plunge of line of intersection of two wedge forming planes (β_i).

F3 – depends upon relationship between joint dip or plunge of line of intersection of two wedge forming planes and slope inclination.
($\beta_j - \beta_s$) or ($\beta_i - \beta_s$) where, α_s is the inclination of the slope.

F4 – Method of Excavation. It includes the natural slope, or the cut slope excavated by pre splitting, smooth blasting, normal blasting, poor blasting and mechanical excavation.

Table 6.7 Values of adjustment factors for different joint orientations (after Anbalagan et al., 1992)

Case of slope Failure		Very Favorable	Favorable	Fair	Unfavorable	Very Unfavorable
P T W	($\alpha_j - \alpha_s$) ($\alpha_j - \alpha_s$-180°) ($\alpha_i - \alpha_s$)	>30°	30 - 20°	20 - 10°	10 - 5°	<5°
P/W/T	F_1	0.15	0.40	0.70	0.85	1.00
P W P/W	(β_j) (β_i) F_2	<20° 0.15	20 - 30° 0.40	30 - 35° 0.70	35 - 45° 0.85	>45° 1.00
T	F_2	1.0	1.0	1.0	1.0	1.0
P W T	($\beta_j - \beta_s$) ($\beta_i - \beta_s$) ($\beta_j + \beta_s$)	>10° <110°	10 - 0° 10 - 120°	0° >120°	0–(-10°) >120°	<-10° -
P/W/T	F_3	0	- 6	- 25	- 25	- 60

As per slope mass rating (SMR) Romana (1985) defined five stability classes based on the above mentioned parameters. Accordingly for each parameter rating is given and the total Slope Mass Rating (SMR) is calculated. According to the Romana (1985) classification in the present case the road cut slope at the left abutment falls into Class II, the rock mass description is good; the stability condition is stable with some failure blocks. Table 6.8 shows the parameters ratings and the calculate SMR for the left abutment slope.

6.7 Assessment of Permeability

6.7.1 Foundation Permeability

Engineering geological investigations in connection with the construction of dams on fractured rocks have indicated a relationship between the stress distribution in rocks and their water transmissibility. This relationship has greater significance in the dam foundation,

Table 6.8 Values and ratings given for the parameters for the left abutment slope

Cause of slope failure	Rating
P (αj - αs)	18
T (αj - αs- 180)	
W (αi - αs)	
P/T/W	
F1 Rating	**0.7**
P(βj)	32
W (βi)	
P/W	
F2 Rating	**1**
P (βj -βs)	-10
W (βi -βs)	
T (βj +βs)	
P/W/T	
F3 Rating	**-25**
F4 Rating	**0**
RMR_{basic}	**62**
Total SMR	**79.5**

because the underlying rocks are subjected to the weight of the dam and the impounded water. Therefore, the hydrodynamics of the water flowing through the fractures have been investigated using water pressure tests in the holes drilled within the foundation. The permeability tests are based on measuring the amount of water accepted by the ground under pressure during a given time (Anbalagan, et.al, 1995).

An examination of the test results shows that the permeability in general is low in most of the bore holes drilled and the Lugeon values decreases with depth. The Lugeon values reach up to 65 in BH-3, between 15 to 60 m (Fig.6.11). Further down, the Lugeon values are less than 10. The 'Sealing of Joints' which is predominant in the stages from 32 m downwards, clearly brings out the need for washing the holes by using proper deflocculating agents before grouting. The water intake seems to be uniform irrespective of lithological variations and excellent RQD (> 90%).

During the present study, the initial interpretation was based on different flow patterns within the rock mass at dam foundation such as; laminar, turbulent and hydro fracturing blocking and unblocking in the rock mass (Louis, 1980). This can be inferred by a graphical analysis of the flow rate (Q) and pressure (P) curves during testing. These curves are plotted in the field itself, in order to control the applied pressure so that it does not exceed the critical pressure (Pc). The second phase of interpretation involves analyses to select representative permeability values based on dominant flow conditions. This is done by plotting the

histograms of permeability in terms of Lugeons against pressure steps (Houlsby, 1976). Further, due care has been taken in the interpretation of mixed flow conditions.

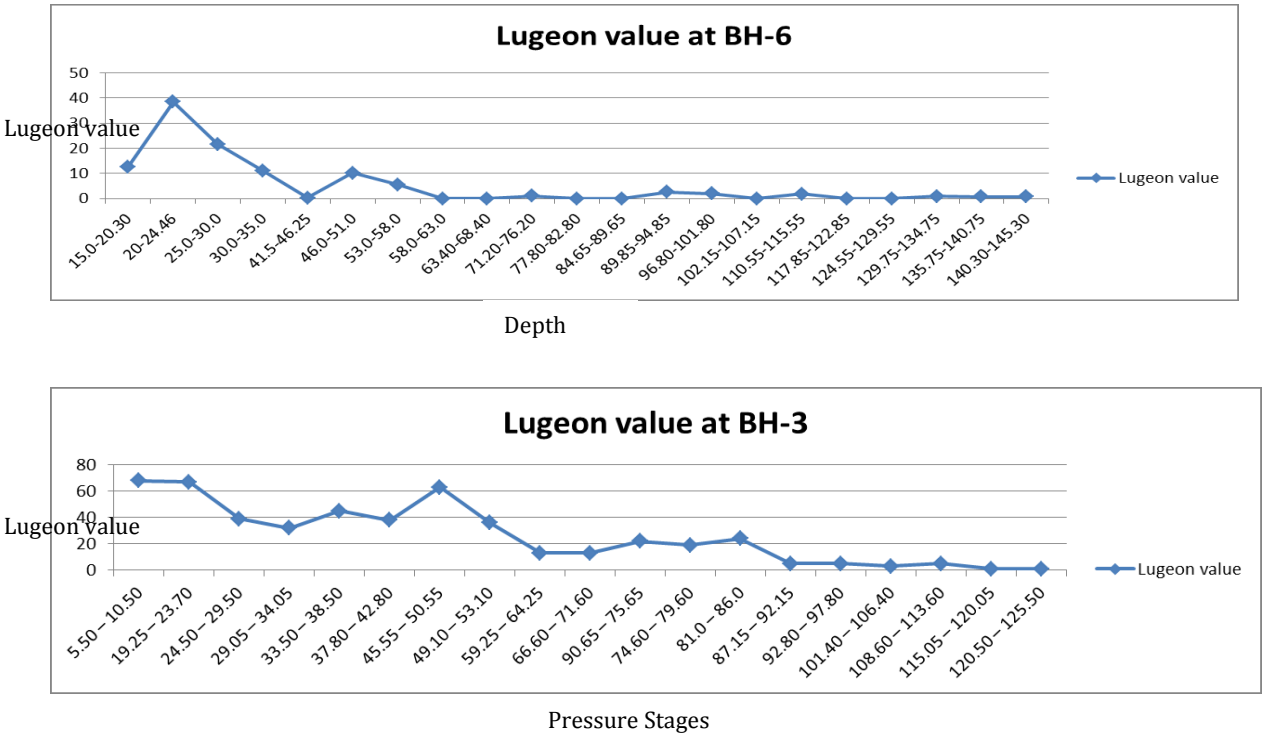

Fig 6.11. Lugeon values at selected boreholes at the dam site

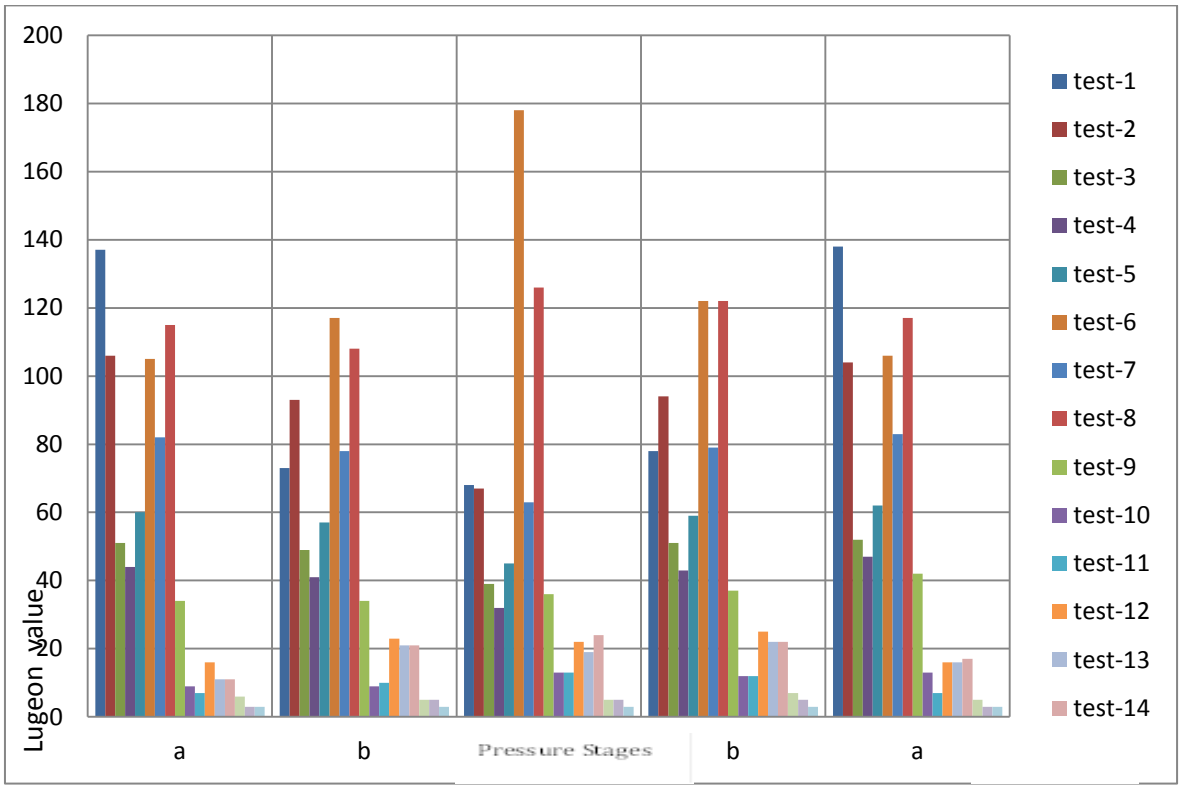

Fig. 6.12 Inferred Lugeon pattern for the test sections of the water pressure test done in drill hole BH-3

During the feasibility stage of the Project various water pressure permeability tests were conducted at the dam foundation and other appurtenant structures. Summary of Permeability test results is given in Table 6.10.Interpretations and hydraulic domain classifications were made based on the permeability classification of rocks given by Lashkaripour and Ghafoori (2002) (Table 6.9).

Table 6.9 Condition of rock mass discontinuities associated with different Lugeon values (Lashkaripour and Ghafoori, 2002)

Lugeon Range	Classification	Hydraulic Conductivity Range (cm/sec)	Condition of Rock Mass Discontinuities	Reporting Precision (Lugeons)
<1	Very Low	$< 1 \times 10^{-5}$	Very tight	<1
1-5	Low	1×10^{-5} - 6×10^{-5}	Tight	± 0
5-15	Moderate	6×10^{-5} - 2 x 10-4	Few partly open	± 1
15-50	Medium	2×10^{-4} - 6×10^{-4}	Some open	± 5
50-100	High	6×10^{-4} - 1×10^{-3}	Many open	± 10
>100	Very High	$> 1 \times 10^{-3}$	Open closely spaced or voids	>100

Fig 6.13 shows the Lugeon value of three boreholes at different test sections depth. It can be clearly seen that the permeability condition of the foundation rocks is relatively low to very low.

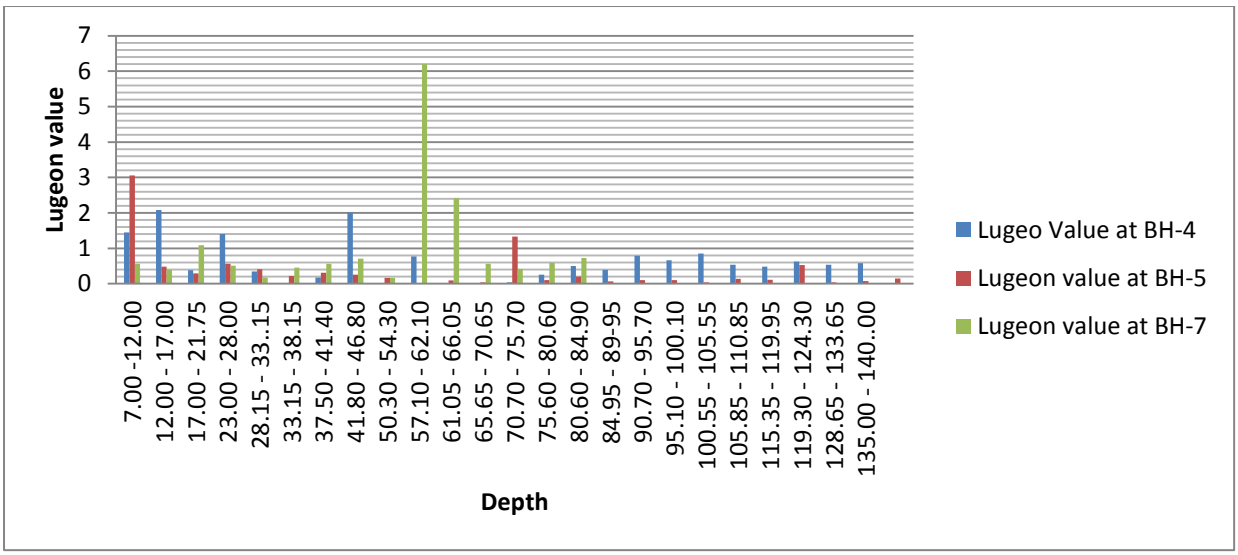

Fig. 6.13 Inferred Lugeon value for the test sections of the water pressure test done in three boreholes

For the present study six selected borehole insitu test data were used to characterize the permeability of the foundation rocks. The summary of permeability results is presented in Table 6.10 (a) and (b).

Table 6.10 (a) Summary of Permeability Results

S.N	Borehole ID	Test section length	Lugeon Value	Flow type (ugeon Pattern interpretation	Permeability Class (Lashkaripour and Ghafoori, 2002)
1	BH04	7.00 -12.00	1.45	Turbulent flow	Impervious
2		12.00 - 17.00	2.08	Voidfilling flow	Impervious
3		17.00 - 21.75	0.38	Voidfilling flow	Impervious
4		23.00 - 28.00	1.4	Voidfilling flow	Impervious
5		28.15 - 33..15	0.35	Dilation flow	Impervious
6		33.15 - 38.15	0	Dilation flow	Impervious
7		37.50 - 41.40	0.18	Dilation flow	Impervious
8		41.80 - 46.80	2.01	Turbulent flow	Impervious
9		50.30 - 54.30	0	Dilation flow	Impervious
10		57.10 - 62.10	0.77	Turbulent flow	Impervious
11		61.05 - 66.05	0,70	Turbulent flow	Impervious
12		65.65 - 70.65	0.01	Dilation flow	Impervious
13		70.70 - 75.70	0.04	Dilation flow	Impervious
14		75.60 - 80.60	0.26	Laminar flow	Impervious
15		80.60 - 84.90	0.5	Wash-out flow	Impervious
16		84.95 - 89-95	0.39	Turbulent flow	Impervious
17		90.70 - 95.70	0.79	Wash-out flow	Impervious
18		95.10 - 100.10	0.66	Wash-out flow	Impervious
1	BH-05	8.25 - 12.85	3.06	Turbulent flow	Low permeability
2		13.85 - 17.85	0.48	Turbulent flow	Impervious
3		18.45 - 22.85	0.29	Turbulent flow	Impervious
4		22.35 - 27.10	0.56	Turbulent flow	Impervious
5		27.10-32.30	0.41	Turbulent flow	Impervious
6		32.30-37.14	0.22	Turbulent flow	Impervious
7		37.30 - 42.30	0.31	Void filling flow	Impervious
8		42.52-47.52	0.26	Void filling flow	Impervious
9		47.50-52.60	0.17	Turbulent flow	Impervious
10		52.60-57.60	0.02	Void filling flow	Impervious
11		57.60-62.30	0.09	Dilation flow	Impervious
12		62.30-67.30	0.04	Turbulent flow	Impervious
13		67.30-72.30	1.33	Wash-out flow	Impervious
14		72.80-77.80	0.1	Dilation flow	Impervious
15		77.45-82.45	0.2	Void filling	Impervious
16		82.40-87.40	0.07	Dilation flow	Impervious
17		87.60-92.60	0.1	Turbulent flow	Impervious
1	BH-06	15.0-20.30	12.7	Turbulent flow	Medium permeability
2		20-24.46	38.47	Turbulent flow	High permeability
3		25.0-30.0	21.67	Turbulent flow	Medium permeability
4		30.0-35.0	11.14	Turbulent flow	Medium permeability
5		41.5-46.25	0.19	Dilation flow	Impervious
6		46.0-51.0	10.16	Turbulent flow	Medium permeability
7		53.0-58.0	5.5	Dilation flow	Low permeability
8		58.0-63.0	0.01	Dilation flow	Impervious
9		63.40-68.40	0	Dilation flow	Impervious
10		71.20-76.20	1	Dilation flow	Impervious
11		77.80-82.80	0.01	Laminar flow	Impervious
12		84.65-89.65	0.02	Laminar flow	Impervious
13		89.85-94.85	2.63	Turbulent flow	Impervious
14		96.80-101.80	2.04	Turbulent flow	Impervious

Table 6.10 (b) Summary of Permeability Results

S.N	Borehole ID	Test section length	Lugeon Value	Flow type (ugeon Pattern interpretation	Permeability Class (Lashkaripour and Ghafoori, 2002)
1	BH-07	13-16	0.56	Void filling flow	Impervious
2		19-22	0.39	Turbulent flow	Impervious
3		25-28	1.09	Turbulent flow	Impervious
4		31-34	0.51	Turbulent flow	Impervious
5		33.85-36.85	0.18	Void filling flow	Impervious
6		36.85-41.85	0.46	Turbulent flow	Impervious
7		41.85-46.85	0.56	Washout- flow	Impervious
8		46.55-50.0	0.71	Washout- flow	Impervious
9		51.05-56.05	0.17	Turbulent flow	Impervious
10		56.35-61.35	6.2	Laminar flow	Low permeability
11		63.10-66.60	2.42	Turbulent flow	Impervious
12		66.60-71.60	0.56	Void filling flow	Impervious
13		71.60-76.60	0.42	Turbulent flow	Impervious
14		76.60-81.0	0.59	Dilation flow	Impervious
15		82.15-87.15	0.73	Washout- flow	Impervious
16		89.05-94.05	26.23	Void filling flow	Medium permeability
17		94.20-99.20	0.7	Turbulent flow	Impervious
1	BH-08	15.25 – 21.25	3	Dilation flow	Low permeability
2		24.8 – 29.0	3	Dilation flow	Low permeability
3		30.7 – 35.7	37	Turbulent flow	Mediumpermeability
4		35.4 – 40.4	28	Turbulent flow	Mediumpermeability
5		47.8 – 52.8	66	Turbulent flow	Highpermeability
6		52.7 – 57.7	40	Turbulent flow	Mediumpermeability
7		58.05 – 63.05	18	Laminar flow	Mediumpermeability
8		62.5 – 67.5	13	Washout flow	Moderatepermeability
9		66.0 – 71.0	11	Turbulent flow	Moderatepermeability
10		71.35 – 76.35	5	Washout flow	Moderatepermeability
11		77.9 – 82.9	8	Dilation flow	Moderate permeability
12		83.0 – 88.0	5	Void filling flow	Moderate permeability
13		90.55 – 95.55	10	Turbulent flow	Moderate permeability
14		97.1 – 102.1	35	Turbulent flow	Mediumpermeability
1	BH-03	5.50 – 10.50	68	Turbulent flow	Highpermeability
2		19.25 – 23.70	67	Turbulent flow	Highpermeability
3		24.50 – 29.50	39	Turbulent flow	Medium permeability
4		29.05 – 34.05	32	Turbulent flow	Medium permeability
5		33.50 – 38.50	45	Turbulent flow	Medium permeability
6		37.80 – 42.80	38	Turbulent flow	Medium permeability
7		45.55 – 50.55	63	Turbulent flow	Highpermeability
8		49.10 – 53.10	36	Turbulent flow	Medium permeability
9		59.25 – 64.25	13	Turbulent flow	Moderate permeability
10		66.60 – 71.60	13	Turbulent flow	Moderate permeability
11		90.65 – 75.65	22	Turbulent flow	Medium permeability
12		74.60 – 79.60	19	Turbulent flow	Medium permeability
13		81.0 – 86.0	24	Turbulent flow	Medium permeability
14		87.15 – 92.15	5	Turbulent flow	Low permeability
15		92.80 – 97.80	5	Turbulent flow	Low permeability

Fig 6.14 shows the different zones of permeability in the dam foundation area. Accordingly, most of the foundation rocks fall in very low permeability zone (Lugeon values<5), few parts of the dam site on the left abutment falls in medium permeability zone (Lugeon value 5 – 15), and finally on the right side of the dam foundation the permeability values are very high (Lugeon15-65). This is possibly because of the weak zones that were encountered in borehole BH-3.

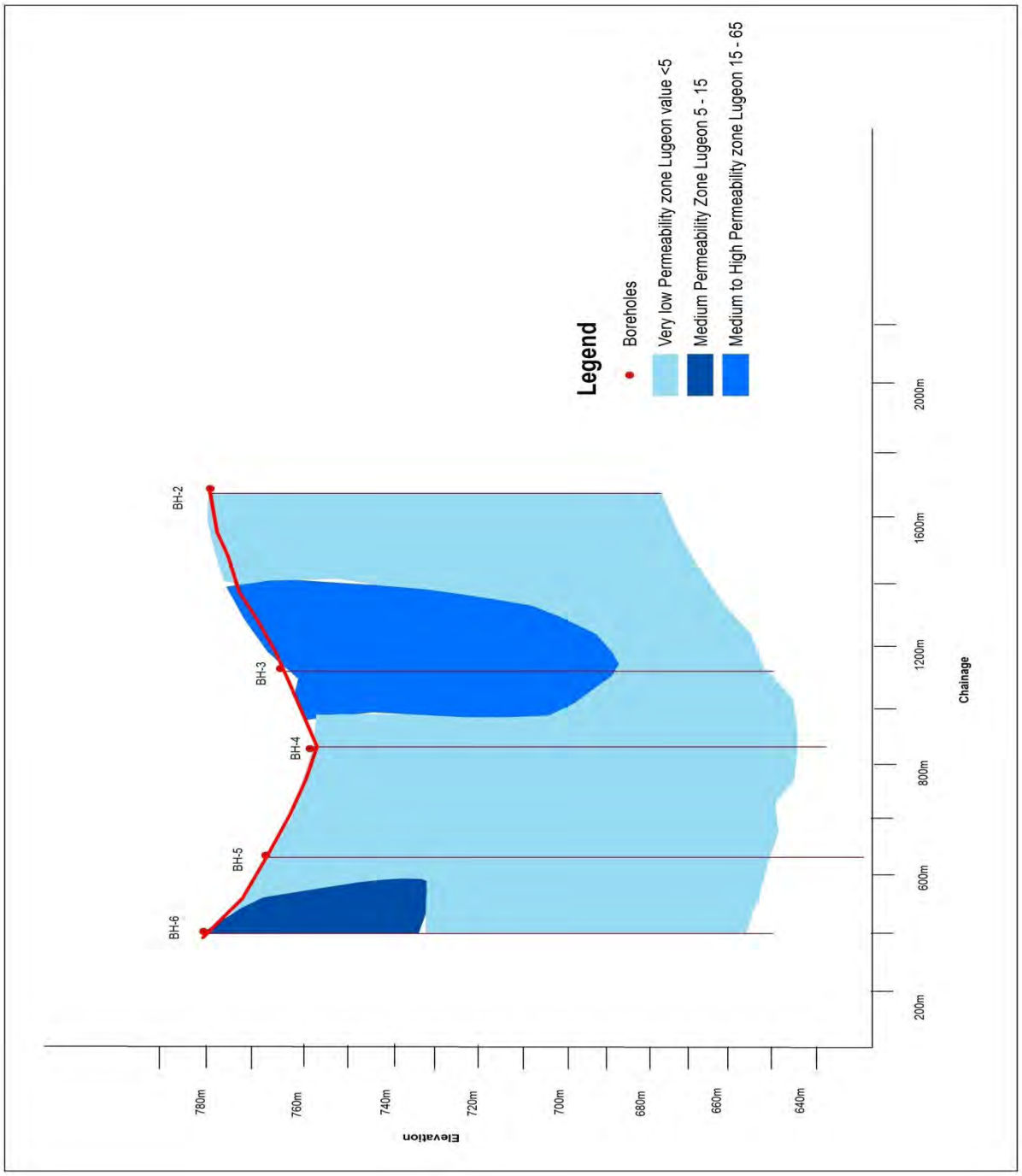

Fig. 6.14 Foundation permeability condition at the dam site.

6.7.2 Seepage and Leakage Conditions

Most of the seepage problems are related to the geological, hydrological and geotechnical conditions at the Dam foundation. Besides, the seepage problems are also associated with the main dam body also. Seepage through Dam foundation due to unfavorable geological conditions is an indicator of a risk of failure. Cendergern (1977) estimated 10% of Dam failures are associated with foundation seepage. TAMS Dam site is located in the western part of Ethiopia, which relatively represent stable systems. Most of the likely foundation problems at the dam site are in general associated with the geological structures.

From the surface observation and borehole data along the right abutment, unlike the left abutment, it is covered by rock blocks of schist of different type removed from the parent rock mass. The geology in general exposed on the right abutment slope is more or less similar to that of the left abutment, the geological sequence was observed from the surface geological traces and the borehole data. The rock mass is dissected by two major joint systems; which strike NNW-SSE with sub-vertical dips, and Strike NE-SW with sub vertical dip. However, in addition to these two more joint sets with comparatively less persistence are also present. Since the flow direction of the river is E – W, part of joint system is along the flow direction and rest are oriented across the flow direction. Such joint system may result into seepage problem if not treated adequately. The permeability test conducted by packer tests in borehole BH-3 and BH-8 indicate complete water loss from surface up to a depth of 25 – 60m. Within this section very high Lugeon values were observed (as high as 65 Lugeon).

Thus, the result indicates that there will be a serious seepage problem along the abutment if not treated adequately Based on the surface and subsurface explorations, on both the abutments variety of schist rocks are present, which are partly weathered and highly jointed. The permeability result indicates that in the top reaches the rocks are highly permeable on the abutments as there was total water loss during the water pressure tests conducted within this reach. The permeability in the intermediate reach on the right abutments is again high as the Lugeon value is more than 65.

6.8 . Assessment of Bearing Capacity of Foundation Rocks

The choice of a particular type of foundation depends on the magnitude of the loads, the nature of the subsurface strata, the type of the superstructure and its specific requirements (Bell, 1983). The allowable bearing pressure is the maximum net intensity of loading that can

be imposed on the soil or rock with no possibility of shear failure or the possibility of excessive settlement. It is hence the smaller of the net safe bearing capacity (shear failure criterion) and the safe bearing pressure (settlement criterion) that has to be considered (Bell, 1983).

The safe load bearing capacity of the foundation rock can be calculated based on UCS and RQD values and using a factor of safety of 3 as (Hoek and Bray, 1977):

$$Safe\ Load\ Bearing\ Capacity = \frac{UCS*(RQD)2}{Factor\ of\ Saftey} \text{.....} eq.\ 6.5, \text{ Given in Kpa}$$

Table 6.11 shows the safe load bearing capacity of the dam foundation in terms of Mega Pascal (Mpa) as computed from both surface and sub-surface data.

Table 6.11 Safe load bearing capacity of the TAMS dam foundation

ID	Point Source	Location	UCS (Mpa)	RQD	Factor of safety	Safe Load Bearing Capacity(Mpa)
LA1	Surface Points	Left Abutment	66.88	61	3	82.95
LA3			22.29	63	3	29.49
LA6			52.55	67	3	78.63
LA7			60.51	75	3	113.46
LA8			60.51	62	3	77.53
LA9			93.95	58	3	105.35
RA1		Right Abutment	85.99	69	3	136.47
RA3			100.32	67	3	150.11
RA4			93.95	77	3	185.68
RA6			66.88	67	3	100.07
RA7			81.21	63	3	107.44
RA8			81.21	62	3	104.06
BH-4	Borehole Points	Center of Dam axis	403	97	3	1263.94
BH-5			128	100	3	426.67
BH-7			122	89	3	322.12
BH-14			374	62	3	479.22

The calculated safe load bearing capacity of the foundation rocks with corresponding values of UCS and RQD ranges from 29 to 150 Mpa on average on surface data points, whereas the load bearing capacity increases with depth. Data from selected borehole points at the dam axis reveals that the safe load bearing capacity of the dam foundation at depth ranges from 322 – 1263 Mpa. Similarly load bearing capacity as discussed on section 6.5 is calculated by using Hoek-Brown Criterion, 2002. The calculated Rock mass compressive strength varies from 5- 45 Mpa at surface, and 54 – 230 Mpa at depth in selected boreholes, respectively.

6.9 Seismic Refraction Results and Discussions

6.9.1 Preamble

The Refraction Seismic survey has furnished useful information regarding the subsurface conditions at the proposed dam site. To facilitate interpretation a table of compressional wave velocities for various representative rock types of the project area, have been prepared (Table 6.12)on the basis of the refraction velocities in conjunction with the available borehole data along the line SL-03 with a maximum depth of 102m.

Table 6.12 Generalized Compressional wave velocities of various rock types of the survey area

No.	Rock Type	P-wave velocity (m/sec)
1	Alluvial deposit (Sandy silt, gravely sandy silt), loose partially moist moderately weathered and intensively fractured granite	< 1500
2	Intensively to moderately fractured and weathered groundwater saturated granite, weak to moderately foliated Diorite, or meta-volcanic rock	1500-2500
3	Moderately weathered and fractured meta volcanic rock or granite, moderately weathered and fractured to moderately foliated diorite, granodiorite or meta granite with higher degree of compaction towards the bottom	2500-4500
4	Massive, Slightly to very slightly fractured to fresh strong, meta granodiorite, meta granite, meta volcanic rock, High rock quality	4500-5500
5	Very strong, massive, fresh, unfractured granite, granodiorite, metagranite, very high rock quality	>5500

6.9.2 Line ST-06 (Dam axis)

The 2D P-wave tomography corresponding to Line ST-06 (Dam axis) is shown in Fig. 6.15. As indicated, the subsurface unit underlying the dam axis is mainly covered with granitic rock which is exposed to the surface in various parts of the area both on the left and right banks of Baro River. The compressional wave velocities are generally in the range of 1500-3000m/sec attributing intensively to moderately weathered and fractured granite, granitic gneiss, as observed on the left bank, and weakly to moderately foliated diorite.

The uppermost part is also covered with slope wash deposits comprising highly weathered and decomposed granitic materials and boulders, sandy silt and gravely silty sand especially close to the river banks and at relatively flatter/gentler parts of the dam axis as reflected from their p-wave velocity, which is generally below 1500m/sec. The maximum thickness of the later units seldom passes10m while the thickness of the former ones have a maximum thickness of 30m. The 2000m/sec unit is exposed only between stations 880 and945, in the left bank while it is shallow and exposed in several parts of the right bank.

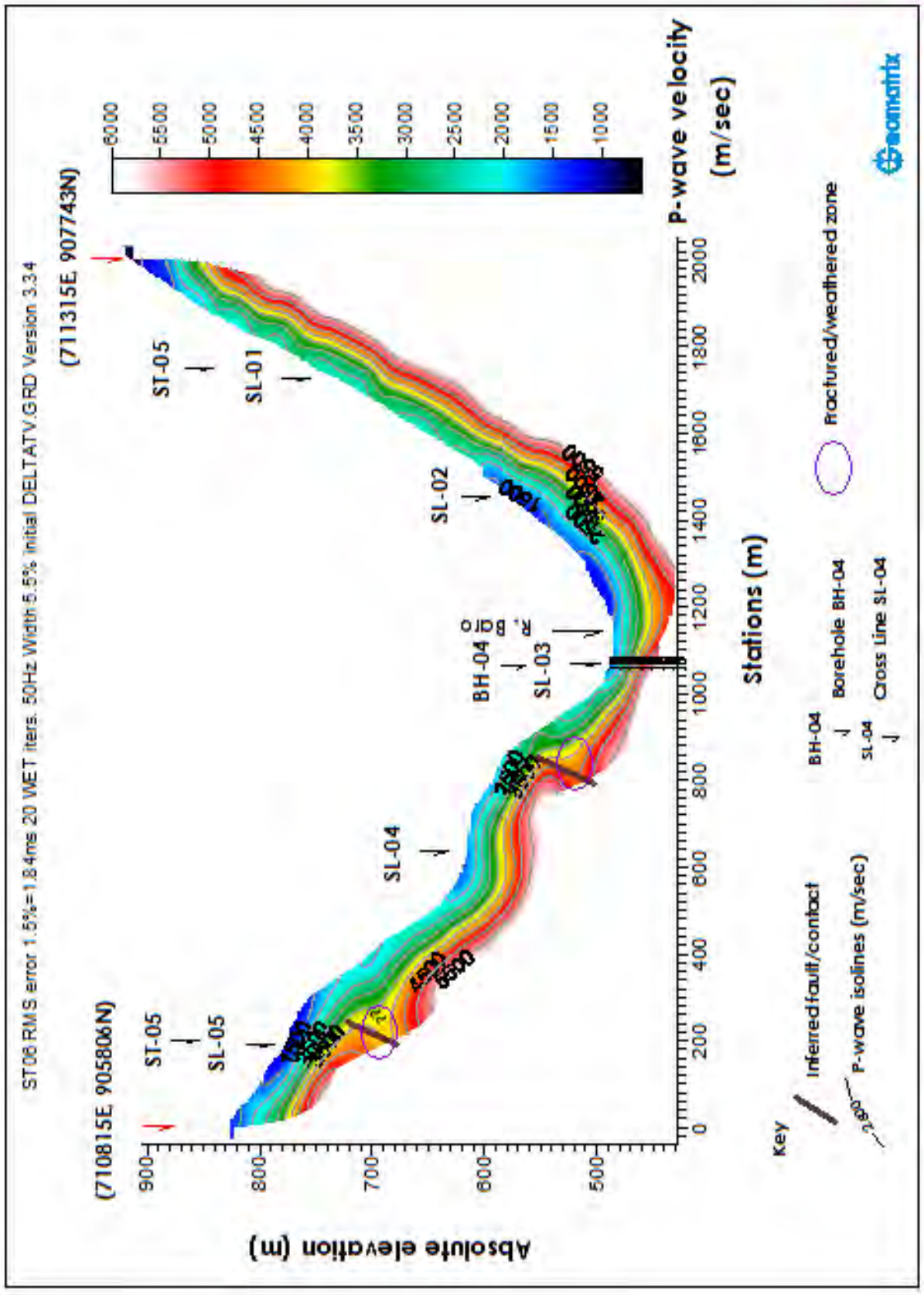

Fig. 6.15 2D P-wave Velocity Tomography, ST-06, Dam Axis, TAMS HPP (Geomatrix, 2016)

6.9.3 Line ST-05 (left of Dam axis)

According to the p-wave velocity tomography in Fig.6.16 and the available borehole log BH-07, the subsurface is represented by four main refractor velocity units. The top layer with p-wave velocities below 1500m/sec is associated with alluvial sediments comprising sandy silt and gravely sandy silt, close to the river banks (between stations 800-1800)and highly to moderately weathered and decomposed materials on the elevated and gently sloping parts of the line(Fig. 6.16).

The thickness of this unit is mostly in the range of 6-15m. The maximum thickness (about 15m) is noted in the right bank just to the right of station 1600 and between stations 160-400, on the elevated part of the left bank. The rest of the top unit is covered by intensively fractured and weathered granitic gneiss rocks.

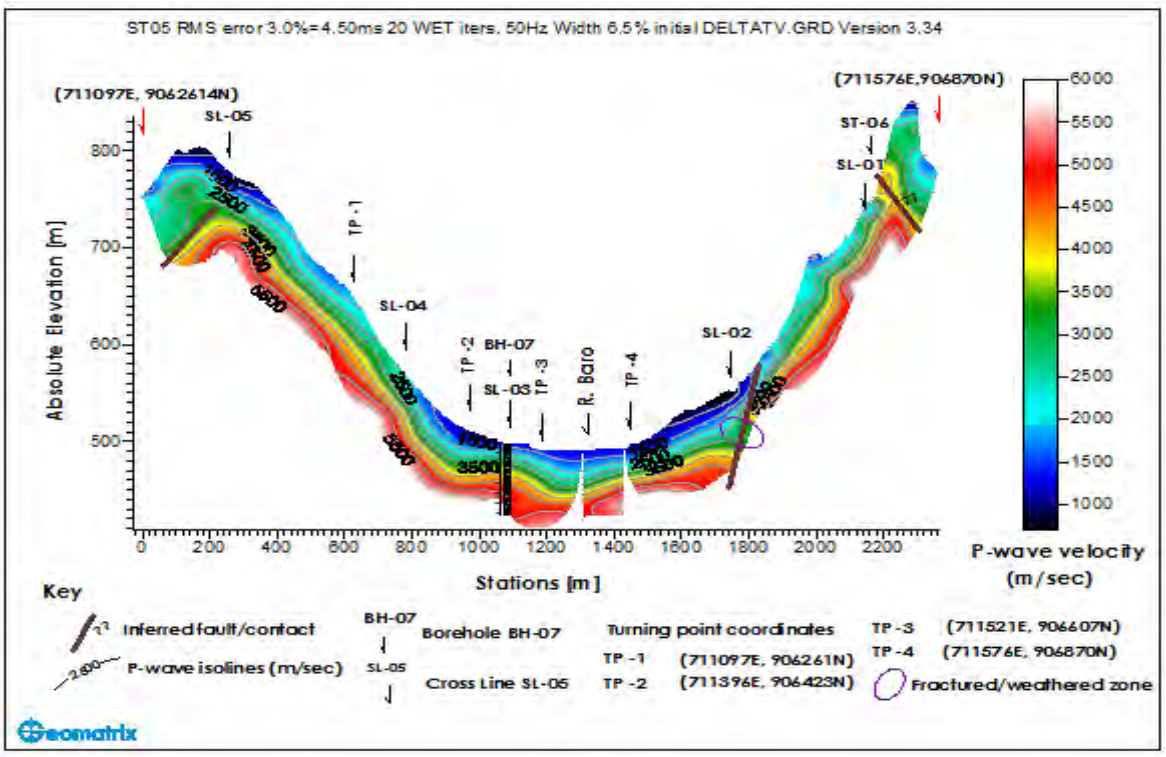

6.16 P-wave Velocity Tomography, ST-05, TAMS HP (Geomatrix, 2016)

6.9.4 Line ST-03 (upstream of dam axis)

On the 2D p-wave tomography (Fig. 6.17) the subsurface is clearly shown reflecting presence of five velocity layers. The first unit is characterized by compressional wave velocities below 1500m/sec which could be associated with alluvial deposit (sandy silt, gravely sandy silt), loose partially moist moderately weathered and intensively fractured granite. The thickness of this unit ranges from 6to 24m. It attains its maximum (about 24m) around station 740.

The second layer is represented by p-wave velocities in the range of 1500 – 2500m/sec probably attributed to intensively to moderately fractured and weathered groundwater saturated granite, weak to moderately foliated diorite. The thickness of this unit ranges from 6 to 15m.

The underlying higher velocity unit (3rd layer) with 2500m/sec-3500m/sec comprises moderately to slightly weathered and fractured granite and moderately weathered and fractured to moderately foliated diorite. The thickness of this unit undulates between 5m and 24m where the maximum thickness is obtained nearby station 210.

According to the 2D p-wave velocity tomography (Fig. 6.14) the fourth layer is characterized by velocities varying between 3500m/s and 4500m/s which could be attributed to moderately to slightly weathered, fragmented granodiorite and moderately weathered and slightly fractured granite. The thickness of this unit varies between 4m and 17m along the survey line except nearby the where its boundary is not defined.

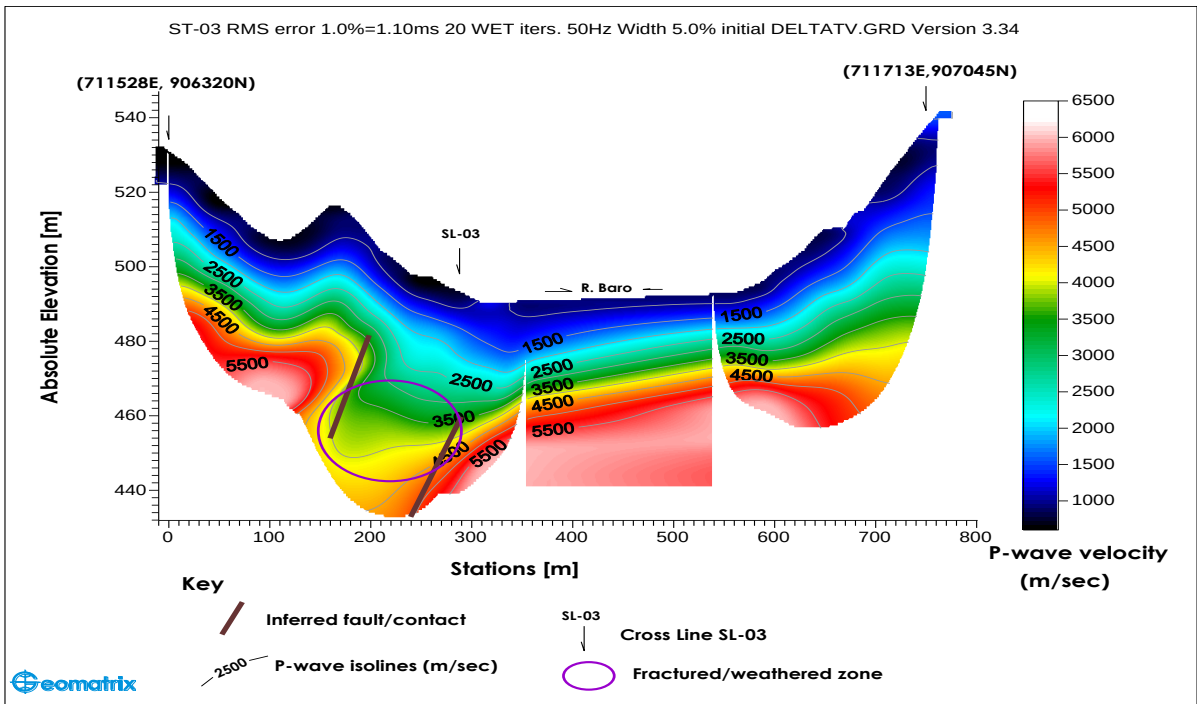

6.17 P-wave Velocity Tomography, ST-03, TAMS HP (Geomatrix, 2016)

6.9.5 Lithology

According to the geology of the area, available boreholes in the project site and the 2D P-wave velocity tomography, the study area comprises mainly metagranite, granodiorite, granitic gneiss and granite, etc. Depending on the degree of weathering and fracturing,

degree of compactness and mineralogic composition, moisture content and nature of fracture filling materials these are represented by widely varying p-wave velocities.

Consequently, the very fresh, massive, strong, unfractured, very high quality rocks, corresponding to the bedrock, are represented by very high velocities (above 5500m/sec). Massive slightly to very slightly fractured to fresh and strong, high quality foundation rocks corresponding to massive, slightly fractured to fresh strong metagranodiorite, metagranite and metabasic rocks are related with 4500 – 5500m/sec velocities. The substratum is characterized by high compressional wave velocities (>4500m/sec). The depth to the surface of this refractor in the entire project area ranges from 18m (north eastern part of the study area) to a maximum value of 132m (near the river). Regions of the bedrock with velocities above 4500m and depths above 60m are mapped in the southern and south western parts, relatively occupying a wider region in the left bank than the northern zone in the right bank where similar depth is observed, mainly in the northern central part of the area along the dam axis.

Intermediate units with velocities ranging generally between 2500 – 4000m/sec, are associated with moderately to slightly weathered fragmented granodiorite, moderately weathered and slightly fractured metabasic, moderately weathered, fractured granite with intercalation of thin layers of diorite and metagranite with higher degree of compaction at greater depths. The depth to this unit undulates widely and reaches about 75m.

Intensively to moderately fractured and weathered groundwater bearing or moist granite, granitic gneiss and weak to moderately foliated diorite are associated with lower compressional wave velocities (1500 – 2500m/sec) as indicated in the 2D p-wave velocity tomography (Fig.5.18). Maximum thickness (about 28m) is observed on the right bank along line ST-05 (around station 1980) on the steeply sloping zone.

Moreover, the least velocity range (below 1500m/sec) is associated with alluvial sediments (sandy silt, gravely sandy silt); loose partially moist moderately weathered and intensively fractured granite and highly weathered and decomposed slope wash deposits. The thickness of the later unit varies widely, generally from nullity to about 15m. However, it reaches 24m towards the extreme and of Line ST – 03and eastern part of line SL-02. These are dominantly seen at the left and right banks, close to Baro River and at the gently sloping and relatively flatter parts of the elevated areas as small patches elsewhere.

6.10 Interpretation based on geotechnical and geophysical methods

6.10.1 General

The 2D p-wave velocity tomography results and the results of the borehole logs indicate very good agreement especially for the uppermost and bottom units. It is known for long that geological structures (fault) affect the internal and adjacent properties of rocks to a widely varying degree of deformation by faulting from intra-grain micro cracking to severe alteration (Geomatrix , 2016).

Mildly fractured rocks do not exhibit a significant reduction in velocity, but, densely fractured rocks do show significant reduction in the velocities. The amount of reduction is generally proportional to the fracture density and thus to the velocity. Highly fractured rock and thick fault gouge along fault zones are identified by a pronounced seismic low-velocity, which is either very thin or absent along locked portions of the fault (Geomatrix, 2016).

In the present study, the inferred faults were interpreted on the basis of this background. Accordingly, fault zones are indicated either by the sudden dislocation of units often creating weak zones as a result of rock fracturing or gouge production resulting from shearing. The nature of the weak zones, degree of fracturing and fracture density depends on the shearing force and position (Geomatrix, 2016).

Therefore, the apparent variation in the interpreted compressional wave velocities and the borehole logs for the intermediate unit may be related just to this fact and not to lithologic change.

The seismic results at the junction between the cross lines and the lines traversing them are generally in good agreement. However, due to limited seismic data from the river side and the fact that saturated micro cracks and mildly fractured rocks do not exhibit a significant reduction in the velocity, the fresh bedrock and the slightly fractured bedrock indicated in BH-04 could not be differentiated on the p-wave velocity tomography (Fig. 6.19).

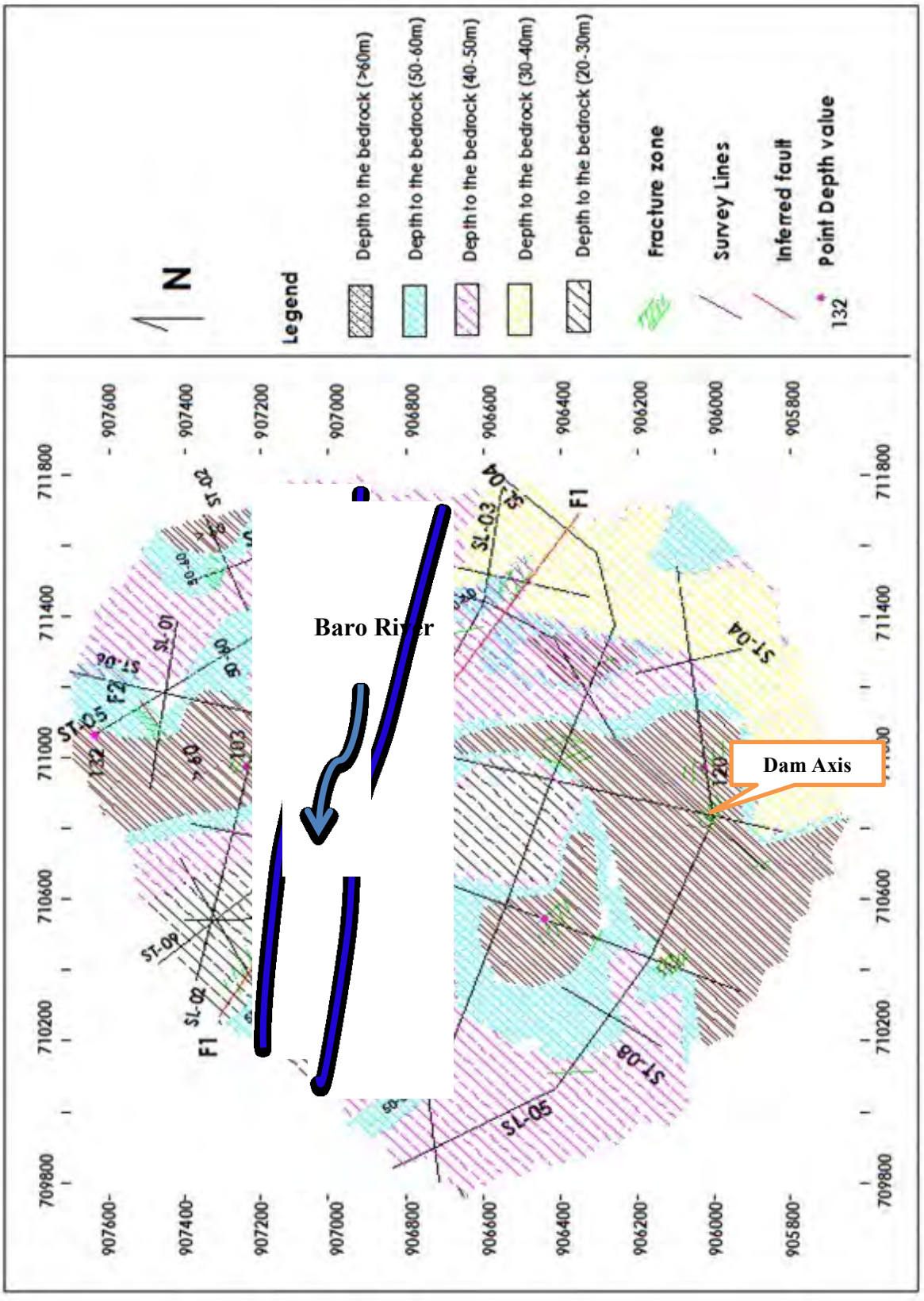

Fig. 6.18 Interpretation map based on Depth to the bedrock with P-wave Velocity above 4500m/sec

Furthermore, the target depth of investigation is met. Depths over 100m are investigated in most parts of the area excluding central, lower elevated zones, (for the cross lines ST's only), where the layout of refraction spreads along the river was not possible due to the high level of the river. Nevertheless, a good effort was made to conduct all possible shots inside the accessible parts of the river, which has enabled us to get a continuous image of the 2D sections across the river.

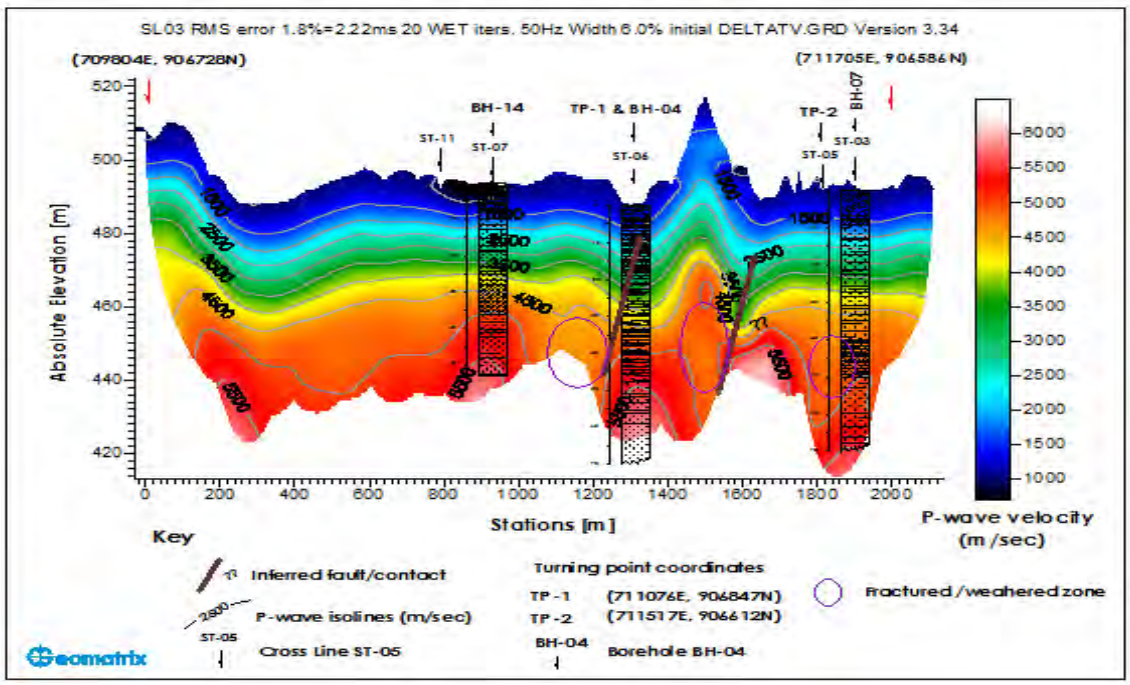

Fig. 6.19 2D P-wave Velocity Tomography with the boreholes

The 2D p-wave tomography corresponding to Line SL-03 (Fig 6.19) is correlated with three borehole drilled along the line (BH-07, BH-04 & BH-14). Since the line is located near the river, the subsurface is covered with alluvial sediments comprising sandy silt and gravely silty sand (BH-07 & BH-04) and highly weathered and decomposed granitic materials represented by compressional wave velocities generally below 1500m/sec excluding the area between stations 1420 and 1600 where higher velocities are noted. The average thickness of this unit is 9.0m.

The second velocity layer corresponds to intensively to moderately fractured and weathered groundwater bearing granite and weakly to moderately foliated diorite with an average thickness of 12m. This unit is represented by 1500 – 2500 m/sec. Its maximum thickness (over 20m) is situated around station 1500, where the unit is exposed to the surface.

6.10.2 Seismic velocity and RQD relation at selected boreholes

For correlation between rock quality and seismic velocity analysis two approaches were followed. The first approach was the velocity determination from the seismic refraction survey and the second approach was determination of RQD from the drilled boreholes. From the results good correlation was found in between the seismic velocity and the rock quality. Besides, the study also shows a significant correlation between seismic P-wave velocity changes due to their penetration strength.

6.10.2.1 Borehole 14

From the borehole data it is simple to work out the average RQD values. The seismic velocity is calculated from the 2D P-wave velocity tomography map. Because of its contour interval it was difficult to work out the seismic velocity at each target depth. The table below shows the calculated RQD values with the corresponding seismic velocity at selected target depths and Fig 6.20 shows the correlation between RQD and seismic velocity at borehole 14, which is drilled at the dam axis.

Depth	Average RQD	Average Seismic Velocity
10	54	1500
20	83	3200
30	94	3600
40	80	4500
50	52	4800
60	80	5200
70	71	5500

From the graph (Fig 6.20), it's clearly shown that the RQD value varies with different depth and it is difficult to produce a relation-ship between RQD and seismic velocity.

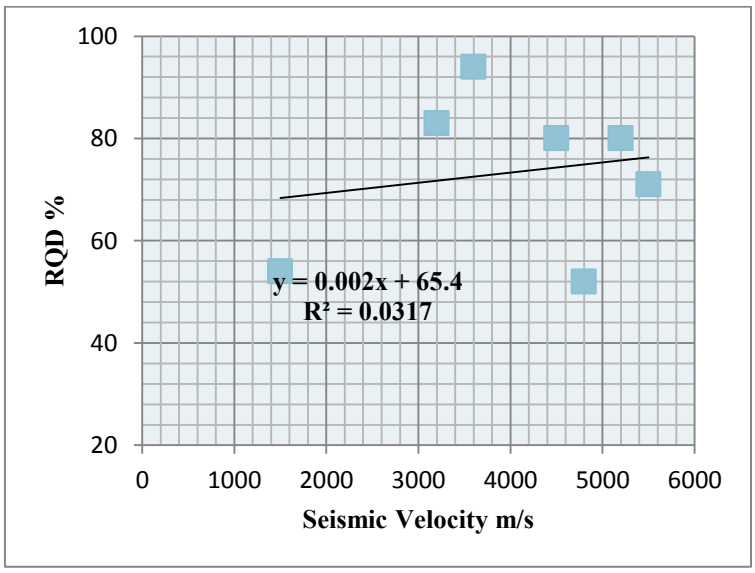

Fig. 6.20 RQD and seismic velocity relationship at BH-14

6.10.2.2 Borehole 04 and 07

Similarly an attempt was made to work out the relationship between RQD and the Seismic velocity at BH-04 and BH-07, located at the dam axis. Further, it is clear that the Seismic velocity and the RQD values have a linear relationship. Fig 6.21 and 6.22 shows the linear

relationship between the RQD and its seismic velocity at BH- 04 and BH- 07, located at the dam site. Finally, it is possible to make a general correlation between the seismic and borehole RQD values with respect to the degree of weathering of the rock mass. Table 6.13 describes the different degree of weathering with the corresponding P-wave velocity and RQD range.

Depth	Average RQD	Average Seismic Velocity
10	12	1400
20	52	1600
30	66	2400
40	68	3200
50	71	3500
60	80	4000
70	94	4400
80	96	4700
90	96	5000
100	97	5200
110	98	5600
120	99	6000

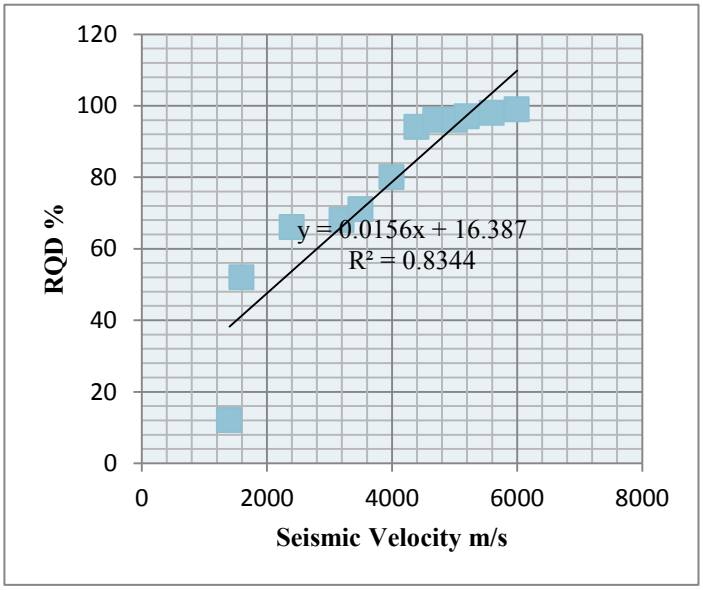

Fig. 6.21 RQD and seismic velocity relationship at BH-4

Depth	Average RQD	Average Seismic Velocity
10	96	1400
20	96	1600
30	98	2400
40	98	3200
50	89	3500
60	99	4000
70	99	4400
80	100	4700
90	100	5000
100	96	5200
105	100	5600

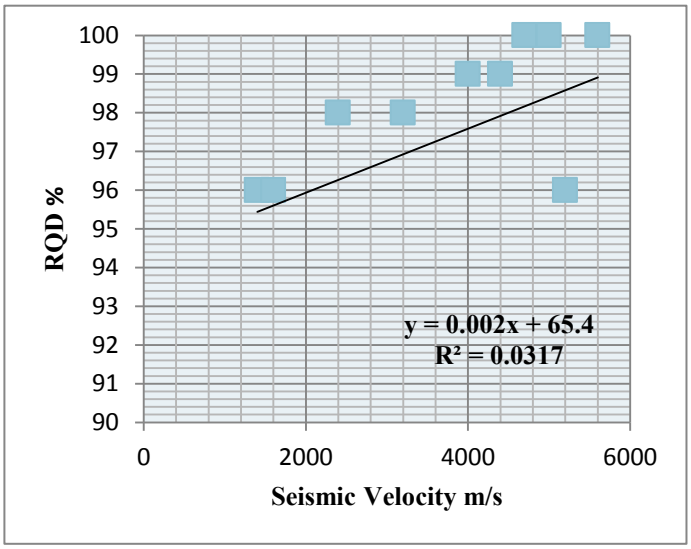

Fig. 6.22 RQD and seismic velocity relationship at BH-7

Table6.13 Correlation between P-wave velocity (infield) and RQD for medium depth investigation.

Description	P-wave velocity(m/s)	RDQ value
Residual Soils	<1500	-
Completely weathered material	1500 – 3000	Less than 50
Highly weathered material	3000 – 4500	50 – 70
Moderately weathered material	4500 - 5500	70 – 85
Fresh Material	>5500	Over 85

6.11 Discussion on overall characterization

For the present study, dam foundation characterization has been made by secondary data analysis and through field investigations. Besides, representative rock core samples were also collected from the dam foundation area. Thus, an overall dam foundation assessment has been done which is discussed in the following paragraphs.

The boreholes drilled at the dam site greatly enhanced better understanding of the subsurface configuration of geotechnical layers. General observations of the dam site include; visual observations of the drill core recovered from the boreholes, in situ tests, seismic refraction survey and laboratory tests conducted on representative samples. Finally, this enabled the determination of the geotechnical layers at the dam foundation.

Five engineering geological layers are identified across the full length of the profile, having different geometrical shapes, thickness and spatial distribution, which differ significantly in their geotechnical characteristics. Their thickness and shapes are highly variable; from very thin to thick and frequent change of lateral contact to the overlying and underlying layers. The rock mass exposed on the dam foundation falls into fair to good quality for the surface outcrops, whereas for boreholes it is of Good to Very Good quality, as per the Bieniawiski's (1989) RMR system.

According to the geological logs and geophysical results the bedrock underlying the dam site is generally represented by fresh granite, granodiorite and metagranite, which are characterized by fresh, massive, strong, very slightly fractured to unfractured rocks, of high quality represented by very high velocities (> 4500m/sec).

Some sections at the dam foundation are identified as zones of fracture porosity (secondary porosity) whose interstices are not effective to conduct water through and away from them. This is the case where there exist locally terminating fracture networks, which can be indicated by low RQD values, not connected to conductive fracture system. There are cases

also where effective fracture porosity may seem ineffective unless the section is tested by an applied pressure enough to resist the confinement pressure and its residual is sufficient to drive water through the fractures. On the contrary, some sections with high RQD values but highly conductive have been identified as there are few fractures connected to major conductive fracture system.

The water pressure test conducted at abutments indicates very low to medium permeability in most of the drilled boreholes. The permeability value at the right abutment specifically at BH-3 is high to very high (20 to 65 Lugeons) on top part of the dam foundation. Therefore, the most effective means of checking seepage through the abutments and the river section would be a provision of grout curtains.

From rock strength and bearing capacity point of view, rocks represented by compressional wave velocities over 4500 m/sec are of very good quality. However, rocks with over 5000m/sec velocities represents rocks of very high quality. These rocks can be characterized as stable, water tight and possess high bearing capacity thus, these rocks are very favorable for the foundations.

Founding conditions for rock-fill embankments are favourable except at the locations of weak and fractured zones identified on the right bank of the study area near Borehole -3.With regard to safe load bearing capacity of the Dam foundation rocks, various values have been obtained according to the type of rock, degrees of weathering and fracturing. The safe load bearing capacity of intrusive rocks (Granite and Granodiorite) are estimated to be in a range of 7 Mpa to 45Mpa from surface outcrops and 50Mpa to 130Mpa from drilled boreholes. The lower schist and gneiss layer which are present below the river bed on both banks possess high load bearing capacity (up to 230 Mpa). Based on the kinematic analysis and field observation it is identified toppling and circular failures are unlikely and are not potential instability problems on abutments but the kinematic analysis has indicated that wedge failure can occur.

6.12 Foundation Treatment

6.12.1 Grouting works

As indicated in section 6.7, the permeability result shows that Lugeon value varied from 1 to as high as 65 on the left abutment, which necessitate leakage treatment by means of cement grouting along the dam axis. Further, according to the core drilling results in the present

study area, the bed rocks that were encountered along the dam axis comprises of interconnected penetrating joint systems. The log of the boreholes has also revealed both open and filled joint sets in rock mass present in the dam foundation.

The representative Lugeon values of the rock mass in most of the boreholes in the dam foundation revealed very low to medium permeability conditions and high permeability at the right abutment especially in borehole BH-3, where there is a weak zone. Thus, seepage control at selected points is necessary to prevent excessive uplift pressures, instability of the downstream slope, piping through the foundation, and erosion of material by migration into open joints in the foundation and abutments.

Further, the correlation of the permeability and the depth in the foundation area indicated that it is necessary to design the depth of curtain grouting based on geologic condition of the dam site and on the engineering criteria. Therefore, considering the relevant factors such as permeability, discontinuities, and lithological properties of the rock foundation, it is proposed that a grout curtain with two rows needs to be provided in the dam foundation.

For the effective grouting it is required that consolidation grouting be completed first and later curtain grouting should be completed. The proposed consolidation grouting in the upper portion of the foundation rock may serves as a grout platform and prevents grout leakage during the curtain grouting at depth using high pressures (USACE, 1984).

6.12.1.1 Consolidation Grouting

Consolidation grouting in the dam base area is mainly done to improve the physical properties of the foundation rocks. Consolidation grouting makes the foundation rocks monolithic by fusing the dam foundation with the base of the dam. Consolidation grouting helps in closing all the openings fishers, joints in the foundation which not only weakens the foundation but also prevents the seepage through the opening, fishers and joints (USACE, 1984).

Hence, consolidation grouting is planned to reduce the seepage losses, seepage velocity and the likely hood of loss of embankment core material in to the foundation and in addition to seal the near surface rock against undue loss of grout during the high pressure curtain grouting. This grouting may be done to a depth of 10 m with holes spaced at 3 - 4.5 m to consolidate the rock in this zone so as to prevent piping of fines from the core into the rock

crevices in the vicinity of the critical core- rock contact and to seal the near surface rock against undue loss of grout during the high pressure curtain grouting to follow (USACE, 1984). Further, Mistry, 1983 proposed that consolidation grouting should be extended up to b/4 in the heel portion whereas; towards the toe it should be extended up to b/3, where `b' is the base width of the dam along the river section perpendicular to the dam axis. In the river bed section consolidation grouting may be done up to a depth of 10 - 15 m whereas, in the abutment section it may be don up to a depth of 5 - 15m. For the present study the maximum base width of the dam foundation is 500 m, hence the curtain grouting at the heel portion should extend up to 125 m, whereas towards the dam toe the consolidation grout length may reaches up to 166m.

6.12.1.2 Curtain Grouting

As indicated in section 6.5 and Table 6.4 the Lugeon values varies in dam foundation from 1 to 28 which indicates necessity for leakage treatment by means of cement grouting along the dam axis (USACE, 1984). Accordingly, the following recommendations are forwarded for the present project design;

- For the present dam foundation multiple grout lines are proposed. In multiple row curtain the outer row should be completed first (Houlsby, 1976). A spacing of 1.5 m between rows may be maintained, upstream row should be the tightest. The depth up to which this grout curtain be provided is obtained by formula given by Ewert (1985);

  $D = 1/3\ H + C$ …….*eq.6.6*

  Where, 'D'is the depth of grout curtain, 'H'is the height of dam and 'C' is the variable constant depending upon foundation condition and dam height 'C' ranges from 8 to 25. Accordingly, for the present study where the proposed dam height is 270 m, the depth of grout curtain is calculated based on the above formula, hence the depth of curtain grout should be a maximum of 100 m.

- Orientation of grout holes to be decided after test/ trial grouting.
- Single row grouting with primary, secondary and tertiary grout holes at 6, 3 and 1.5 m spacing to be conducted and quantity to be adjusted depending on the outcome of test/ trial grouting.

- Cement to be the main grouting material. In addition bentonite and fine sand shall be used in small percentage as appropriate.
- Final mix design shall be decided after trial grouting however for the beginning thinnest grout shall be 3:1 or 2:1 and thickest shall be 0.5:1.
- Maximum length of test/grouting stage shall be 5.0 m
- Grouting method shall be stage grouting either with descending or ascending.
- Grouting shall be executed after excavation to the bottom of the key trench.

Fig. 6.23 shows the proposed curtain grout layout at the dam foundation; clearly indicate primary, secondary and tertiary grout holes.

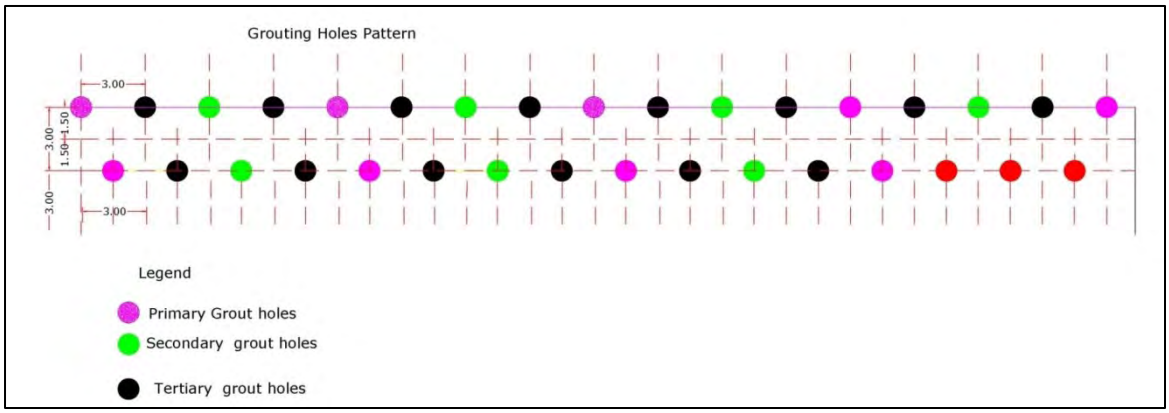

Fig. 6.23 Proposed grout hole pattern lay out (Red colors are Test Holes)

6.13 Foundation Excavation

Open excavation refers to the removal of material; within certain specified limits, for construction purposes. In order to accomplish this economically and without hazard, the character of the rocks and soils involved and their geological setting must be investigated. The method and the rate of progress are influenced very much by the geology on site. The inclination of discontinuities is always the most important parameter for slopes of medium and large height (USACE, 1994).

The lithological log of the borehole drilled at the dam site showed that the geology of the dam seat area is composed of fresh to slightly weathered, massive, hard granite rock overlain by about 5 m thick residual soil at places. As the excavation is huge the task should be properly planned and executed in order to excavate the material more efficiently, avoid dangerous slope faces and utilize the rock thus obtained. The top residual soil and loose rock can be stripped off using machineries only such as excavators and dozers. The slope face thus

created due to excavation of the residual soil should be provided with gabions or masonry work as well as drainage facility to protect it from erosion (USACE, 1994). Geological Strength Index chart is used to work out the excavatability of the rock mass at the dam foundation. Accordingly for the surface rocks it's calculated that the value zone is between 60 and 70, which corresponds to a very good quality of rock mass, which falls on the hammering and blasting zone. Similarly, the underneath rock mass falls on hard ripping to blasting, hence drilling and blasting is mandatory. Spacing of the blast holes is determined on the one hand in relation to the strength, density and fracture pattern within the rock and on the other hand in relation to the size of the charge. Fig. 6.24 shows GSI chart for estimation of excavatability of identified rock mass of the dam foundation area.

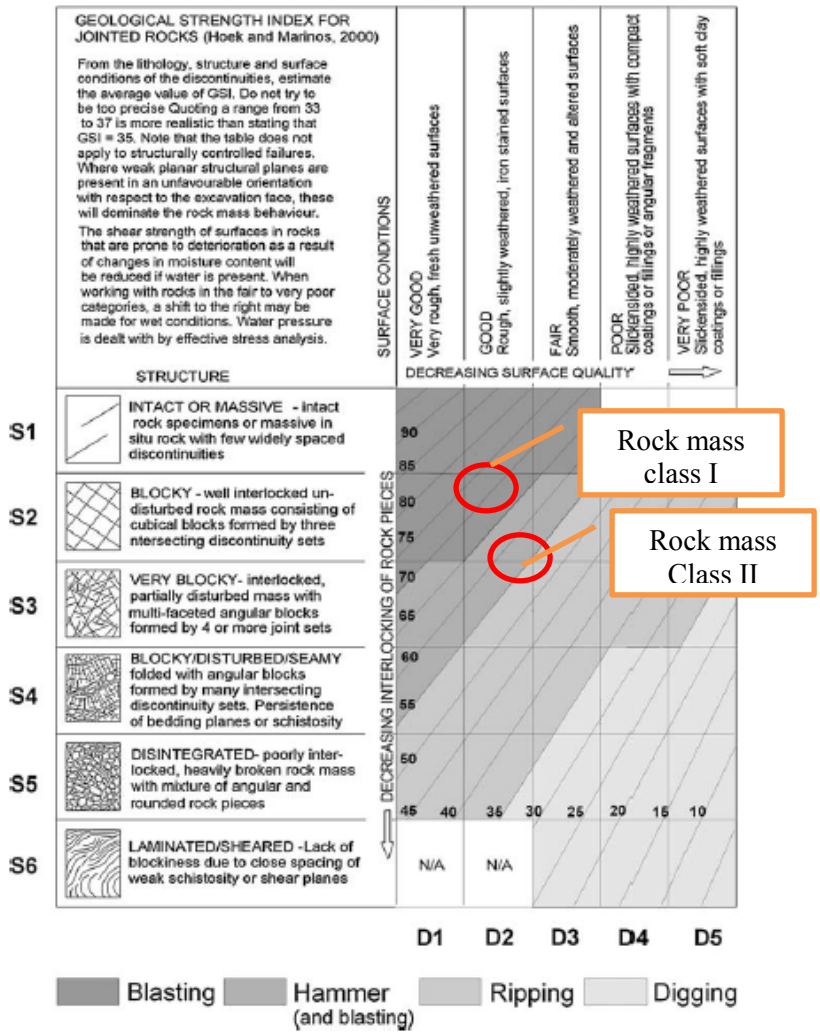

Fig. 6.24 GSI chart estimation of excavatability of identified rock masses of the foundation site

*****

Chapter VII CONCLUSIONS AND RECOMMENDATIONS

7.1 Conclusions

Surface rock mass classification at exposed rocks have been conducted to characterize the rock mass at the dam foundation, accordingly, 50% of the foundation rock mass falls in RMR class 66 – 70, 40% falls in 61 – 65 and the rest 10% falls in class 70 – 80. In general, surface mapping and results from boreholes revealed that the dam foundation on left bank side is relatively strong and possess competent rock, found at shallow depths. As the depth at the dam foundation increases, a subsequent closing of joint apertures and lowering of permeability values was observed. This can be probably due to closing of the discontinuities, as a result of increased confinement pressure. The rock mass exposed at the dam foundation falls into fair to good quality for the surface outcrops, whereas rock mass at depth, as observed from borehole logs, falls into good to very good quality as per the Bieniawiski's Rock mass classification rating system.

The data analysis from core logging and seismic refraction survey at the proposed dam site indicates that the bedrock in the dam foundation is fresh granite, granodiorite, metagranite and schist of different types. The rock mass in general can be characterized as fresh, massive, strong, slightly fractured to un-fractured rocks of high quality as represented by very high velocities (> 4500 m/sec) obtained from seismic refraction survey.

The depth to the surface of the seismic refraction survey in the entire project area ranges from 18m (North eastern part of the study area) to a maximum value of 132 m (at the river section).The results from seismic survey can be summarized as;

- The underlying rocks that showed velocities between 2000to 3000 m/sec are inferred as fractured weathered rocks and are also expected to be water bearing. The maximum thickness (over 50 m) of these rocks was observed in the north of station 40 along the dam axis. Since these rocks are fractured and weathered therefore they may not be suitable for the dam foundation. Further, rocks that showed velocities between 3000 to 4000 m/sec are inferred as relatively stronger rocks, however, for the expected height of the dam and volume of water to be impounded in the reservoir, the rock bearing capacity may not be adequate enough, and hence the quality of the rocks may

not be good enough for the dam foundation. The maximum thickness of this unit, estimated along the dam axis, was about 60 m which found in the right abutment.

- From rock strength and bearing capacity point of view, rocks that show compressional wave velocities over 4500m/sec are of very good quality. Regions of the bedrock with velocities above 4500 m/sec are mapped in the southern and south western parts, relatively occupying a wider region in the left bank than the northern zone in the right bank where similar depth is observed, mainly in the northern central part of the area along the dam axis and to the northwest of it. Further, the rocks with over 5000m/sec velocities represent very high quality rocks. Such rocks are stable, water tight and possess high bearing capacity thus, are very favorable for the dam foundations. Moreover, areas with relatively thick overburden materials: weak zones with highly decomposed and loosely cemented materials, silty sand, gravelly coarse sand and highly fractured and weathered rocks which showed velocities below 1500m/sec are unfavorable for the dam foundation. The maximum thickness of this overburden material was estimated to be about 20m on the right bank of the dam axis.

A false indication (low values) of RQD values were also noted in few sections, observed as highly broken rock pieces, originally formed by continuous and mildly foliated rocks with incipient and healed fractures. Mechanical breaking of the brittle rock during core retrieval may have resulted in the broken rock fragments. This could be indicated by fresh surfaces of the fragments. Some sections are also identified as zones of fracture porosity (secondary porosity) whose interstices are not effective to conduct water through and away from them. This is the case where there exist locally terminating fracture networks, which can be indicated by low RQD values, not connected to conductive fracture system. There are cases also where effective fracture porosity may seem ineffective unless the section is tested by an applied pressure enough to resist the confinement pressure and its residual is sufficient to drive water through the fractures. On the contrary, some sections with high RQD values but highly conductive have been identified as there are few fractures connected to major conductive fracture system. Founding conditions for rock-fill embankments are favorable except at the locations of weak and fractured zones identified on the right bank of the study area near Borehole -3.

Two approaches were followed to correlate the rock quality with its seismic velocity. The first approach was the velocity determination from the seismic refraction survey and the second approach was determination of RQD from the drilled boreholes. From the results

good correlation was found in between the seismic velocity and the rock quality except at the weakest portion of the dam foundation. Besides, the study also shows a significant correlation between seismic P-wave velocity changes due to their penetration strength.

The water pressure test conducted at abutments indicates very low to medium permeability in most of the boreholes. In general, based on the surface and subsurface explorations the seepage condition along the abutments may be summarized as; on both the abutments variety of rocks are present, which are partly weathered and highly jointed. The permeability result indicates that in the top reaches the rocks are highly permeable. The permeability value on right abutment, in BH-3 borehole, demonstrated high to very high permeability in the top part of the dam foundation. The right abutment showed total water loss during the water pressure tests conducted within this reach. The permeability in the intermediate reach on the right abutments is again high as the Lugeon value is more than 65.The rock mass in this reach is highly fractured, cracked and very weak in strength up to a depth of 61m. Excessive seepage may take place through this zone as it extends further downstream. In addition to this, the various contacts between different varieties of rocks are the potential areas for seepage. Therefore, it is necessary to provide adequate seepage measures in the abutment and river section of the dam foundation. The most effective means of checking seepage through the abutments and the river section would be a provision of a grout curtain.

Based on the results from the present study it may be concluded that the dam site is reasonably suitable for the proposed dam and have isolated problems mainly related to permeability and rock mass quality. Therefore, proposed site required adequate treatment to overcome said problems. Thus, on the basis of findings of the present research, recommendations are forwarded to be adopted as solutions against geotechnical problems identified at the proposed dam site.

7.2 Recommendations

From the results and findings of the present study, the following recommendations are forwarded to be considered in the design and construction of the dam and its appurtenant structures.

- All unconsolidated deposits (colluvial, residual and alluvial deposits) need to be removed from the dam foundation. Borehole data and seismic survey indicated that the upper parts of the rocks at the dam foundation are characterized by highly weathered material, with a low seismic velocity. Based on this data:

- ✓ The general foundation excavation level should be 35 m to 40 m on the river bed and island area. At the weakest portion of the dam foundation found in the right abutment the maximum depth of stripping is recommended to be about 40 –45 m from the original ground level. However, this depth could vary along the dam axis and excavation should continue until depths where groutable rock mass is encountered.

- ✓ The general stripping level recommended for the abutment, other than the weakest portion of the dam foundation, should be 26 m below the original ground level.

- Colluvial materials found at sloppy areas mainly in the right side of the dam foundation area are vulnerable for potential debris/ earth slides and thus shall be removed from the dam foundation area.
- There is a need to provide a curtain grouting up to a depth of about 100 m in the river section, where a maximum hydrostatic force is expected during the operational stage. However, this depth may be reduced on the abutment section as the seepage is a direct function of hydraulic head, especially at the left abutment where the permeability condition is relatively low.
- In order to improve the physical properties of the foundation rocks consolidation grouting is necessary. Consolidation grouting should be extended up to b/4 in the heel portion and b/3 towards the toe of the dam. i.e. for the dam foundation with maximum base width of the dam of 500 m, the curtain grouting at the heel portion should extend up to 125 m, whereas towards the dam toe the consolidation grout length reaches up to 166 m. Single row grouting with primary, secondary and tertiary grout holes at 6, 3 and 1.5 m spacing should be conducted and quantity to be adjusted depending on the outcome of test/ trial grouting.
- It has been found that the road slope cut at the left side slope sections satisfy the kinematics condition for wedge mode of failure defined by joints J2 and J3. However, no joint satisfies the kinematic condition for plane mode of failure. Thus, there is a possibility of wedge mode of failure in the left abutment slopes. This analysis is made with a limited point structural data because of lack of surface exposures at the dam abutments, therefore it is recommended to make a detailed slope stability analysis during excavation and construction period.
- During the site survey, a wide weathered dyke was observed on the side exposures at the left abutment of the dam site, near platform of BH-11 borehole. This dyke was found penetrating in the borehole section. This enabled the investigation to directly check the nature of the permeability of the dykes, and their contacts with the host rock, at the dam

site area. Accordingly, two (2) water pressure tests were conducted in the dyke during the feasibility study level. The results implied that the dykes in the foundation could be conductive channels for excessive leakage. Therefore, it is strongly suggested to deeply identify the presence, scale and frequency of unfavourable geologic structures (dykes, shear zones, faults, folds, etc.), their relative orientations/ attitudes with respect to the alignment of the dam (tunnel) axes, etc.

- Except that of schists, most of the drilled boreholes through geologic materials, for the engineering structure sites, where excavation is mandatory, seem to be appropriate for construction purposes and hence, consideration is recommended. Moreover, during site investigation survey it was observed that a ridge composed of massive granite intrusive is found also at a short distance on the left side of the Baro River. The site could be considered as potential source for construction material to construct the left part of the dam.
- The present research was focused only on the dam site, which is based on limited number of samples and small area coverage because of time and financial limitations. Therefore, it is recommended to make further analysis by making observations, using number of samples and in-situ tests, covering large area of the dam and appurtenant structures, to address the dam foundation, reservoir slope stability and water tightness for a more feasible and practicable result to come.

*****

REFERENCES

Agarwal, C.K., Mehrotra, V.K. and Mitra, Subhash, (1991). Need of Long Term Evaluation of Rock Parameters in the Himalayas Proc., 7th International Congress Rock Mech., Aachen, Germany.

Ajzebeokhai, P. (2010). 2D and 3D Geo-electrical resistivity imaging: Theory and field design. Sci. Res. Essays 5(23):3592-3605

Anbalagan, R., Sanjeev, S. and Tarun, K.R. (1995). An engineering geological appraisal of the Jamrani Dam Site, across the Gaula River in Kumaun Himalaya, India. Department of Earth Sciences, University of Roorkee, Roorkee, India

Andy, A. (2012). Correlation of Seismic P-Wave Velocities with Engineering Parameters (N Value and Rock Quality) for Tropical Environmental Study, Unpublished Ph.D. thesis, Geophysics Section, School of Physics, University of Saints Malaysia, Penang, Malaysia..

American Standard for Testing Material (ASTM) (2007).Book of Standards, Vol. 4, Section 08 and 09, Construction Materials: Soils & Rocks, Philadelphia, PA

Aydan, O., Ulusay, R., and Tokashiki, N. (2014). A new rock mass quality rating system: Rock Mass Quality Rating (RMQR) and its application to the estimation of geomechanical characteristics of rock masses: Rock Mechanics Rock Engineering journal. 47:1255-1276.

Barton, N.R. and Choubey, V. (1977). The shear strength of rock joints in theory and practice. Rock Mechanics. 10: 1-54.

Barton, N.R., Lien, R., and Lunde, J. (1974). Engineering classification of rock masses for the design of tunnel support: Rock Mechanics journal. 6:189-239

Barton, N.R., and Bandis, S.C. (1990).Review of predictive capability of JRC-JCS model in engineering practice, International symposium on Rock joints, Rotterdam: Balkema publisher, pp. 603-610.

Bell, F. G. (1983). Fundamentals of Engineering Geology. Butterworth and Co. Ltd., London, 648 pp.

Bieniawski, Z.T. (1976). The Geomechanics Classification in Rock Engineering Applications. proc.4th Inter.Cong. Rock.,Montreux.,2:36-48

Bieniawski, Z.T. (1989). Engineering Rock Mass Classifications. Wiley, New York, 251 pp.

Cai, M., Kaiser, P.K. and Uno, H. (2009). “Estimation of rock mass deformation modulus and strength of jointed hard rock masses using the GSI system” Geomechanics Research Centre, Mirarco Inc., Laurentian University, Sudbury, Ontario, Canada

Cecil, O.S. (1971). Correlation of seismic refraction velocities and rock support requirements in Swedish tunnels. StatensGeotekniskaInstitut, Sweden, pp. 58

Cendergern, H.R., (1977). Seepage, Drainage, and Flew nets John Wiley and sons, New York.

Cosar, S. (2004). Application of rock mass classification systems for future support design of the Dim Tunnel near Alanya. Published Ph.D. thesis, Middle East Technical University.

Deere, D. U. 1964. Technical description of rock cores for engineering purposes. Rock Mechanics Engineering Geology journal.1: 17-22.

Eldbor, C., (2004). Evaluation of Rock Mass Strength Criteria. Luela University of Technology, Department of Civil and Environmental Engineering, Division of Rock Mechanics. Published PhD Thesis, Lulea, Sweden. PP. 120

FAO (2006).Soil Map of Ethiopia

Geomatrix plc. (2016). Final Report on Seismic Refraction Investigation for the feasibility study of TAMS Hydropower Project on Baro River, Unpublished Report, Addis Ababa Ethiopia,111pp.

Goodman, R.E., (1989). Introduction to Rock Mechanics, John Wiley and Sons publishers. New York, 385pp.

Gouin, P. (1979).Earthquake History of Ethiopia and the Horn of Africa. Ottawa, Ontario, International Development Research Centre (IDRC), pp.258.

Hack, R. and Huisman, M. (2002). Estimating the intact rock strength of a rock mass by simple means. Proceedings of 9th congress of the Int. Ass. for Engineering Geology and the Environment, South Africa, 4:1971-1977.

Hoek, E. and Bray, J.W. (1989). Rock Slope Engineering, 3rd ed., Institute of Mining and Metallurgy, London, 358 pp.

https://www.google.nl/earth/ Accessed on: 6/3/2017

http://www.seimo.ethz.ch/static/GSHAP Accessed on: 19/5/2017

IAEG (1981). Rock and Soil Description and Classification for Engineering Geological Mapping: Report by IAEG Commission on Engineering Geological Mapping, Bull. Int. Assoc. Eng. Geol., 24:235-274.

ISRM (1981). Rock Characterization, Testing and Monitoring – ISRM Suggested methods, Pergamon Press, Oxford, E.T. Brown (ed), pp211.

Jaeger, A.J. and Ryder, J.A. (1960). A handbook on rock engineering practice for tabular hard rock mines, The Safety in Mines Research Advisory Committee (SIMRAC), Johannesburg, 256pp

Kebede Firew (1996).Seismic Hazard Assessment for the Horn of Africa. Proceedings of EASEE (the Ethiopian Association of Seismology and Earthquake Engineering) Workshop on Seismic Hazard Assessment and Design of Structures for Earthquake Resistance (EBCS-8: 1995), Addis Ababa, Ethiopia, February 21, 1996, pp. 25-38.

Laubsher, D. (1990). A geomechanics classification system for the rating of rock mass in mine design. African Institute of Minerals and Metal, Johannesburg, South Africa. pp257.

Mengesh Tefera, Seife Berhe and Kazmin (1987). Geological Report and of Gore Map Sheet. Ethiopian Institute of Geological Surveys, scale 1:250,000. Regional Mapping Department of the Ethiopian Geological Survey.

Midzil, V., Hlatywayod, D. J., Chapola, L. S., Kebede, F., Atakan, K., Lombe, D. K., Turyomurugyendo, G. & Tugume, F. A. (1999). Seismic hazard assessment in Eastern and Southern Africa. Annali di Geofisica.

Mostyn, G and Douglas, K.J. (2000). The shear strength of intact rock and rock masses. An International Conference on Geotechnical and Geological Engineering, Melbourne, Australia. 3:19-24.

MoWIE (2014). Pre-Feasibility and Feasibility Study for the TAMS HYDROPOWER PROJECT, Pre-Feasibility Study Geological Report, Vol 3.Unpublished Report, Addis Ababa Ethiopia.

MoWIE (2016). Draft factual report of the TAMS HYDROPOWER PROJECT Geotechnical investigation, Unpublished Report, Addis Ababa Ethiopia.

Nigatu Fikadu (2006). Engineering Geological Studies for Suitability of Construction Material and Foundation Condition Evaluation- with special emphasis on seepage studies, Tendaho Dam, Afar Region, Ethiopia, Unpublished MSc Thesis, Addis Ababa University, and Addis Ababa Ethiopia.122pp.

Ocepec, D. (2006). New Trends in Rock Mass Characterization for Designing Geotechnical Structures published Ph.D. thesis Geoinženiringd.o.o.Ljubljana, Slovenia.

Palmstrom, A. (1982). The volumetric joint count – a useful and simple measure of the degree of jointing. In proceedings of the 4th Int. Cong, pp. 221–228. IAEG, New Delhi, India.

Palmstrom, A. (1996): Classification as a tool in rock engineering, Tunneling and Underground Space Technology, *Proceedings of the 4th Int. Cong*, pp. 221–228. IAEG, New Delhi, India.

Palmstrom, A. (2009). Combining the RMR, Q, and RMi Classification Systems. Oslo, Norway, pp. 400.

Robin, F., Patric, M., David, S and Graeme B. (2005). Geotechnical Engineering of Dams. A.A Balkema Publisher Lienden, Netherlands.

Scott, S. (2000). Rock Mass Strength and Deformability of Unweathered Closely Jointed Newzeland Grey wakey. published Ph.D. Thesis, University of Canterbury, Christchurch Newzeland.

Serafim, J.L., Pereira, J.P., (1983). Considerations of the geomechanics classification of Bieniawski. In: Proceedings of the international symposium on engineering geology and underground construction, Lisbon, Portugal, LNEC, 1:33–44.

Sjögren, B. (1984). Shallow refraction seismic. Chapman and Hall publishers, London, 270 PP.

Sjögren, B., Malthus, A. and Sandberg, L. (1979). Seismic classification of rock mass qualities. Geophysical Prospecting journal, Sandvika Norway 27: 409 - 442.

Singh, M., Rao, K. S. and Ramamurthy, T. (2002). Strength and Deformational Behavior of a Jointed Rock Mass. Rock Mechanics and Rock Engineering Journal.3: 35-39

Syed, A. (2015). Rock Mass Classification Systems. Geotechnical Institute and National Centre of Excellence in Geology publishers, University of Peshawar, Freiberg Germany, pp. 286.

Teklewolde Ayalew & Moore J. M. (1989). The Gore-Gambela Geo-traverse, Western Ethiopia. Internal Report by Addis Ababa University - Ethiopian Institute of Geological Survey - Ottawa-Carleton Geoscience Centre, Canada. pp.153.

U.S. Army corps of Engineers, (U.S. ACE, 1994). Earth and Rock fill Dams-General Design and construction Considerations. EM 1110-2-2300 Washington, DC 20314-1000.

U.S. Army Corps of Engineers (1984). Engineering and Design GROUTING TECHNOLOGY, Engineer Manual, 1110-2-3506, Washington, DC 20314-1000.

Wickham, G.E., Tiedemann, H. R. and Skinner, E. H. (1972). Support determination based on geologic predictions, In: Lane, K.S.a.G., L. A., ed., North American Rapid Excavation and Tunneling Conference: Chicago, New York: Society of Mining Engineers of the American Institute of Mining, Metallurgical and Petroleum Engineers, pp. 43-64.

*****

ANNEXES

Annex I Borehole Core log at BH-4

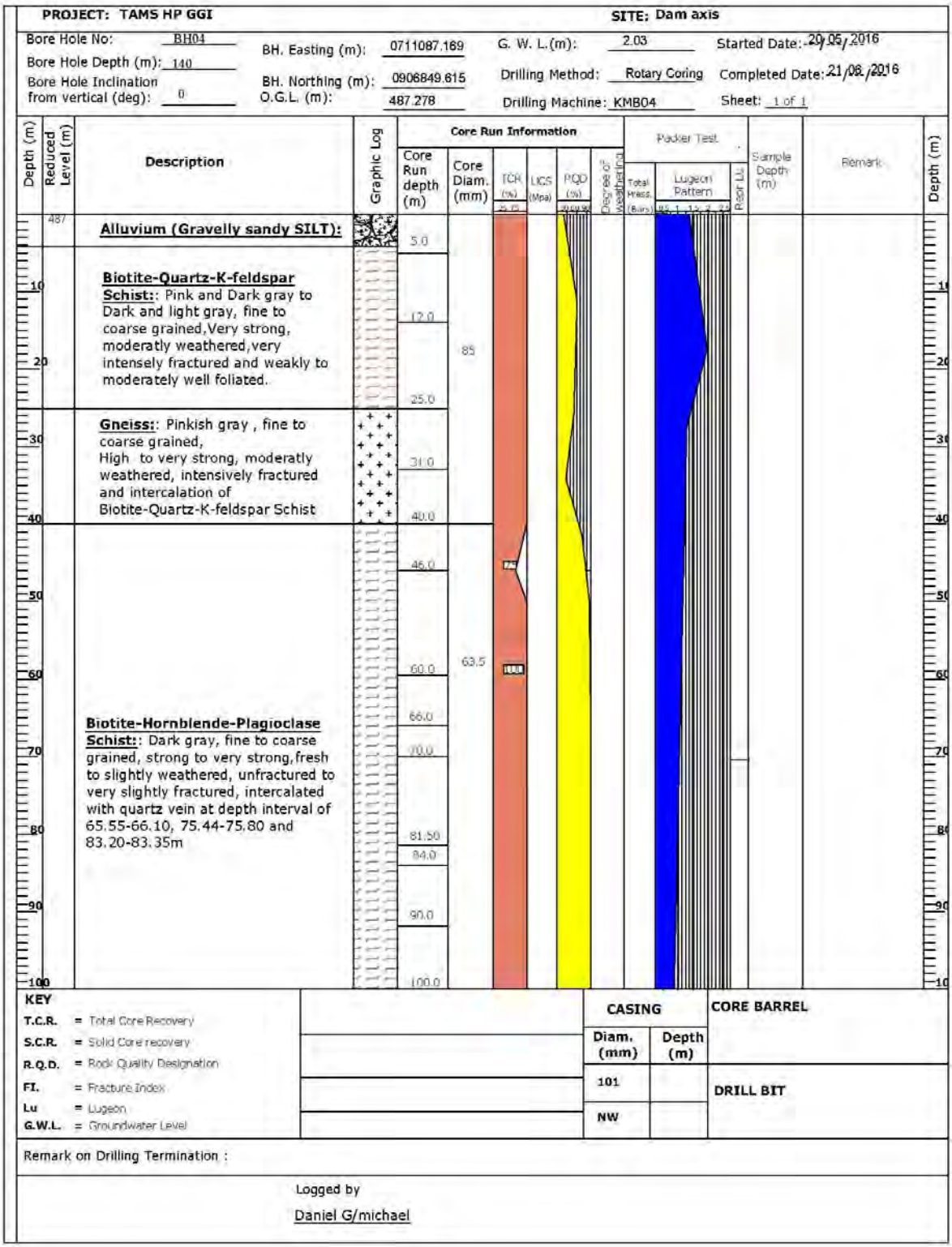

Annex II Laboratory Test Results

TAMS Hydropower Geological and Geotechnical Investigation Project
Summary of Test Result of soils
Date: 4/11/2016

Lab No	BH ID	Location	Lithological Field Description	Sampling Depth(m)	Parameters			
					Unit Weight	Point Load (MPa)	UCS(MPa)	Alkali Silika reaction
263/09	BH-10RS-1	Diversion Intake Structure	Meta Diorite	13.10-13.40	2.71	-	-	-
264/09	BH-10RS-2			8.05-8.49	-	-	348.75	-
266/09	BH-10RS-6			21.77-22.03	-	8.22	-	-
267/09	BH-10RS-9		Ortho Gneiss	26.60-26.83	2.57	-	-	-
268/09	BH-10RS-10			27.59-27.82	-	5.31	309.45	-
269/09	BH-04RS-2	Center of Dam Axis	Meta Granodiorite	10.77-11.00	2.95	-	-	-
270/09	BH-04RS-5		Meta Granite	25.75-26.05		9.98	-	-
271/09	BH-04RS-6			32.40-32.60	2.64	-	-	-
272/09	BH-04RS-9			91.68-92.10	-	-	403.59	-
273/09	BH-04RS-10		Meta Volcanic	62.75-63	-	8.12	178.72	-
274/09	BH-07RS-1	Upstream of Dam Axis	Meta Granite	38.75-38.95	-	2.52	124.70	-
275/09	BH-07RS-2			41.70-42.02	2.57	-	-	-
276/09	BH-07RS-4		Syenite	89.45-89.75	2.56	-	-	-
277/09	BH-07RS-5		Meta Granite	91.65-91.90	-	5.08	-	-
278/09	BH-07RS-6			45.10-45.45	-	-	369.98	-
279/09	BH-14RS-3	Downstream of Dam Axis	Meta Volcanic	34.95-35.30	2.89	6.26	360.02	-
280/09	BH-14RS-4		Meta Granodiorite	39.30-39.45	-	-	374.77	-
281/09	BH-14RS-7		Meta Granite	75.08-75.35	2.68	9.94	-	-
283/09	BH-05RS-3	Center of Dam Axis	Meta Volcanic	61.15-61.75	2.91	-	363.00	-
284/09	BH-05RS-5			99.00-99.76	-	5.33	-	-
285/09	BH-05RS-7		Meta Tonalite	130.00-130.60	2.69	3.57	198.09	-

Checked by: _____ Approved by: _____

Cont'd

TAMS Hydropower Geological and Geotechnical Investigation Project
Summary of Test Result of soils
Date: 4/11/2016

Lab No	BH ID	Location	Lithological Field Description	Sampling Depth(m)	Parameters			
					Unit Weight	Point Load (MPa)	UCS(MPa)	Alkali Silika reaction (mmol/L)
286/09	BH-06RS-3	Spillway and Dam Axis	Meta Diorite	29.40-30.00	2.79	4.69	-	-
287/09	BH-06RS-5		Granite Pegmatite	82.85-83.40	-	13.49	-	-
288/09	BH-06RS-6		Ortho Gneiss	85.85-86.45	-	-	324.55	-
290/09	BH-06RS-7		Ortho Gneiss Intercalated with meta volcanic	132.35-132.7	2.59	-	276.51	-
291/09	BH-11RS-2	Spillway	Meta Volcanic	28.85-29.45	2.82	-	-	-
292/09	BH-11RS-3		Meta Granite	46.50-46.70	-	-	433.51	-
293/09	BH-11RS-4		Meta Volcanic	54.34-54.90	-	4.51	-	-
294/09	BH-11RS-6		Meta Volcanic	75.00-75.50	-	-	224.34	-
295/09	BH-11RS-7		Meta Granite	79.70-80.15	2.73	4.78	-	-
296/09	BH-12RS-3		Meta Volcanic	42.45-42.9	-	6.79	231.39	-
297/09	BH-12RS-6	Spillway	Meta Syanite and Meta Tonalite	99-99.75	2.75	-	-	-
298/09	BH-12RS-7		Meta Diorite	106.4-107	-	5.63	338.48	-
299/09	BH-12RS-8		Ortho Gneis	121.75-122	2.91	6.88	290.67	75.00
300/09	BH-13RS-1	Setting Basin structure	Meta Volcanic	21.35-21.54	-	2.39	-	-
301/09	BH-13RS-2			20.83-20.97	-	-	-	-
302/09	BH-13RS-3			39.55-39.75	3.04	2.30	-	-
303/09	BH-13RS-4			39.75-40.00	-	-	181.31	-
304/09	BH-13RS-5		Meta Granite	43.50-43.65	2.05	-	-	20.00
305/09	BH-13RS-6			43.65-43.90	-	6.37	140.14	-

Remark: For Rock Samples of Lab No 292/09 & 272/09 UCS test results are repeated results.

Checked by: _____ Approved by: _____

Annex III Input Parameters used in the Bieniawski RMR_{89} classification system

A. Classification parameters and their ratings in the RMR system

PARAMETER			Range of values // RATINGS						
1	Strength of intact rock material	Point-load strength index	> 10 MPa	4 - 10 MPa	2 - 4 MPa	1 - 2 MPa	For this low range, uniaxial compr. strength is preferred		
		Uniaxial compressive strength	> 250 MPa	100 - 250 MPa	50 - 100 MPa	25 - 50 MPa	5 - 25 MPa	1 - 5 MPa	< 1 MPa
	RATING		15	12	7	4	2	1	0
2	Drill core quality RQD		90 - 100%	75 - 90%	50 - 75%	25 - 50%	< 25%		
	RATING		20	17	13	8	5		
3	Spacing of discontinuities		> 2 m	0.6 - 2 m	200 - 600 mm	60 - 200 mm	< 60 mm		
	RATING		20	15	10	8	5		
4	Condition of discon-tinuities	a. Length, persistence	< 1 m	1 - 3 m	3 - 10 m	10 - 20 m	> 20 m		
		Rating	6	4	2	1	0		
		b. Separation	none	< 0.1 mm	0.1 - 1 mm	1 - 5 mm	> 5 mm		
		Rating	6	5	4	1	0		
		c. Roughness	very rough	rough	slightly rough	smooth	slickensided		
		Rating	6	5	3	1	0		
		d. Infilling (gouge)	none	Hard filling		Soft filling			
			-	< 5 mm	> 5 mm	< 5 mm	> 5 mm		
		Rating	6	4	2	2	0		
		e. Weathering	unweathered	slightly w.	moderately w.	highly w.	decomposed		
		Rating	6	5	3	1	0		
5	Ground water	Inflow per 10 m tunnel length	none	< 10 litres/min	10 - 25 litres/min	25 - 125 litres/min	> 125 litres /min		
		p_w / $\sigma 1$	0	0 - 0.1	0.1 - 0.2	0.2 - 0.5	> 0.5		
		General conditions	completely dry	damp	wet	dripping	flowing		
	RATING		15	10	7	4	0		

p_w = joint water pressure; $\sigma 1$ = major principal stress

B. RMR rating adjustment for discontinuity orientations

		Very favourable	Favourable	Fair	Unfavourable	Very unfavourable
RATINGS	Tunnels	0	-2	-5	-10	-12
	Foundations	0	-2	-7	-15	-25
	Slopes	0	-5	-25	-50	-60

C. Rock mass classes determined from total RMR ratings

Rating	100 - 81	80 - 61	60 - 41	40 - 21	< 20
Class No.	I	II	III	IV	V
Description	VERY GOOD	GOOD	FAIR	POOR	VERY POOR

D. Meaning of ground classes

Class No.	I	II	III	IV	V
Average stand-up time	10 years for 15 m span	6 months for 8 m span	1 week for 5 m span	10 hours for 2.5 m span	30 minutes for 1 m span
Cohesion of the rock mass	> 400 kPa	300 - 400 kPa	200 - 300 kPa	100 - 200 kPa	< 100 kPa
Friction angle of the rock mass	< 45°	35 - 45°	25 - 35°	15 - 25°	< 15°